Consortium for Small-Scale Modelling

Newsletter

February 2001

No. 1

Deutscher Wetterdienst

MeteoSwiss

Ufficio Generale per la Meteorologia

Hellenic National Meteorological Service

Amt für Wehrgeophysik

Il Servicio Meteorologico Regionale di ARPA

www.cosmo-model.org

Editors: G. Doms and U. Schättler, Deutscher Wetterdienst, P.O. Box 100465, 63004 Offenbach, Germany
Printed at Deutscher Wetterdienst, Offenbach am Main

Table of Contents

1 Introduction

This is the first Newsletter of the Consortium for Small-Scale Modelling (COSMO). At the recent SRNWP meeting of European weather services in October 2000, we were strongly encouraged to initiate an annual report series for our group as already exists for the other NWP groups (HIRLAM, Aladin/Aladnet and UKMO). At their meeting in November 2000, the Work Package Coordinators decided to publish a *COSMO Newsletter* series and G. Doms and U. Schättler committed to do the editorial work. It is planned to prepare the Newsletter once a year in January, with the opportunity to add special issues at irregular intervals if required.

The basic purpose of the Newsletter is threefold:

- to review the present state of the model system and its operational application and to give information on recent changes;
- to present the principal events concerning COSMO during the last year and to summarize recent research and development work as well as results from the model verification and diagnostic evaluation;
- to provide the meteorological community and especially all external users of the model system with information on COSMO's activities and with new information on the model system and its current forecast quality.

The present Newsletter is organized as follows. Section 2 gives a general overview of the current organizational structure of the COSMO consortium. The present state of the model system, i.e. the LM-package, is summarized in Section 3, including a short description of the model and its data assimilation system, information on the preprocessor programs to provide initial and boundary conditions, and finally remarks on postprocessing utilities and hints on the available model documentation. Section 4 gives you an overview of the six COSMO Working Groups and their recent research and development activities.

Operational and pre-operational applications of the LM-system at the COSMO meteorological centres are described in Section 5. Information about the recent changes to the model system as well as changes in the model set-up at the meteorological centres are outlined in Section 6.

Section 7 provides short information on the main COSMO meetings and events during the last year. Other activities such as internal visits and guest scientist programs are also included. Finally, some forthcoming events planned for this year are announced.

Recent results of the model verification as well as reports concerning the development of new verification and diagnostic tools are summarized in Section 8. At the end of this Section, the experiences related to the general model performance and conclusion about model deficiencies are summarized.

Section 9 is dedicated to scientific reports on research topics and on model development. Finally, all COSMO activities related to the LM-system within international and national projects of the member meteorological services are listed in Section 10. This list will be updated in the forthcoming issues.

The Appendices concern the use of the GRIB binary data format for the output and input analyses and forecast fields. These lists will also be updated, and we hope they will be helpful, especially for new users of the LM and its forecast products.

The present organization of the Newsletter is only a first guess. Please contact the editors for any comments and suggestions as well as proposals for items to be included or excluded in the next issue. The editors recognize that typographical and other errors or inconsistencies may be present. We apologize for this, and your assistance in correcting them will be welcome.

We would also like to encourage all the scientists in the COSMO Working Groups to document their work, e.g. in form of a short progress summary or a longer report, to be included in the next Newsletter. Special thanks to all who provided contributions and graphical material for the present issue:

R. Amorati (ADGB, Bologna)
Heinz-Werner Bitzer (DWD)
Carlo Cacciamani (ARPA-SMR)
M. Cervino (ISAO-CNR, Bologna)
G. Contri (CMIRL, Genova)
Ulrich Damrath (DWD)
Stefano Gallino (CMIRL, Genova)
Almut Gassman (DWD)
Thomas Hanisch (DWD)
Erdmann Heise (DWD)
Reinhold Hess (DWD)
Vincenzo Levizzani (ISAO-CNR, Bologna)
Laura Mannozzi (OSGM)
Enrico Minguzzi (CSI, Torino)
M. Lazzeri (OGSM)
Tiziana Paccagnella (ARPA-SMR)
Ulrich Pflüger (DWD)
Matthias Raschendorfer (DWD)
Laura Sandri (ARPA-SMR)
Ronaldo Rizzi (ADGB, Bologna)
Christoph Schraff (DWD)
Jürgen Steppeler (DWD)
Francis Schubiger (MeteoSwiss)
Elisabetta Trovatore (CMIRL, Genova)
Emanuele Zala (MeteoSwiss)

To run a complex NWP system at a COSMO meteorological centre requires the continuous effort of many people. Thanks to all of them, especially to those implementing new model versions, maintaining the operations, and organizing the data transfer between the centres:

- Michael Gertz and Thomas Hanisch at DWD,
- Jean-Marie Bettems and Emanuele Zala at MeteoSwiss,
- Matthew Manoussakis at HNMS and
- Davide Cesari and Paolo Patruno at ARPA-SMR.

Finally, thanks to all who supported us concerning technical problems during the editorial work, especially to Andreas Anlauf and Yvonne Reiter at DWD.

For any comments, suggestions and questions please contact the

Editors:

Günther Doms
guenther.doms@dwd.de

Ulrich Schättler
ulrich.schaettler@dwd.de

2 Organizational Structure of COSMO

2.1 General

The ***Consortium for Small-Scale Modelling*** (COSMO) was formed in October 1998 at the regular annual DWD/MeteoSwiss meeting. At present, the following national, regional and military meteorological services are participating:

HNMS	Hellenic National Meteorological Service, Athens, Greece
DWD	Deutscher Wetterdienst, Offenbach, Germany
MeteoSwiss	MeteoSchweiz, Zürich, Switzerland
UGM	Ufficio Generale per la Meteorologia, Roma, Italy
ARPA-SMR	Il Servizio Meteorologico Regionale di ARPA, Bologna, Italy
AWGeophys	Amt für Wehrgeophysik, Traben-Trarbach, Germany

The general goal of COSMO is to develop, improve and maintain a non-hydrostatic limited-area modelling system to be used both for operational and for research applications by the members of COSMO. The emphasis is on high-resolution numerical weather prediction by small-scale modelling. COSMO is initially based on the "Lokal-Modell" (LM) of DWD with its corresponding data assimilation system.

A Memorandum of Understanding (MoU) on the scientific collaboration in the field of non-hydrostatic modelling was signed by the Directors of MeteoSwiss, UGM, HNMS and DWD in March/April 1999. The MoU shall be replaced by an Agreement between the four national meteorological services where the structure of the cooperation is further detailed.

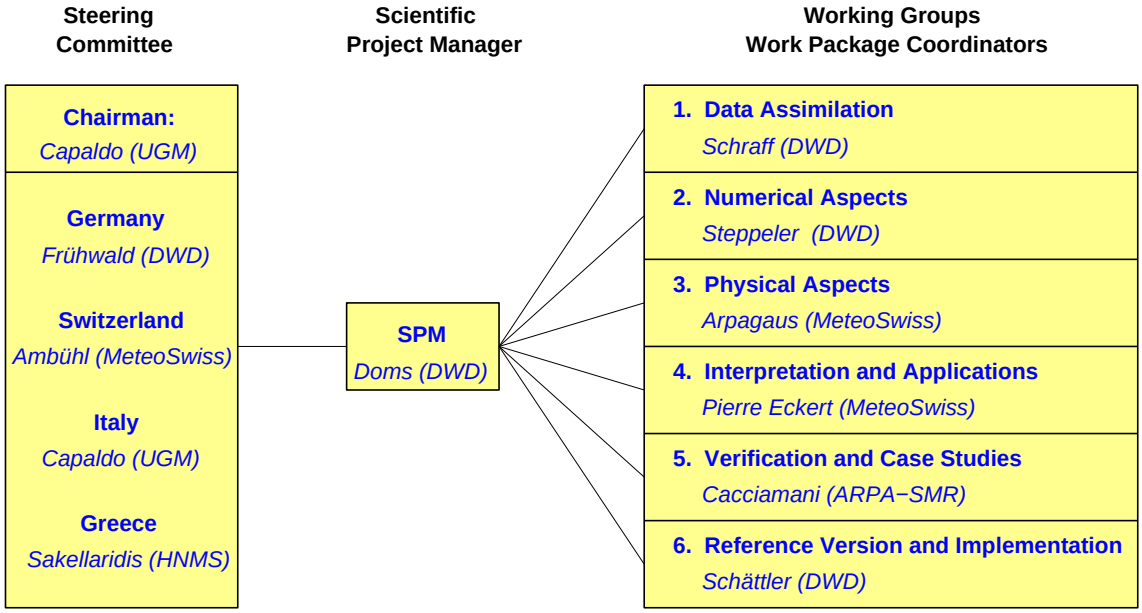

Figure 1: *Structure of COSMO*

2.2 Organizational Structure

COSMO's organization, as sketched in Fig. 1, consists of a steering committee (composed of one representative from each national weather service), a scientific project manager, work-package coordinators and scientists from the member institutes performing research and development activities in the COSMO working groups. At present, six working groups cov-

ering the following areas are active: Data assimilation, numerical aspects, physical aspects, interpretation and applications, verification and case studies, reference version and implementation.

COSMO's activities are developed through extensive and continuous contacts among scientists, work-package coordinators, scientific project manager and steering committee members via electronic mail, special meetings and internal workshops. Once a year there is a General Meeting of the COSMO group in order to present results, deliverables and progress reports of the working groups and to elaborate a research plan with new projects for the next annual period. Following this meeting, a final work plan for each working group is set up. The recent COSMO General Meeting was held on 28-30 September 2000 in Zürich.

2.3 Agreement

All internal and external relationships of COSMO are defined in a draft agreement between the national weather services of the participating countries (DWD, HNMS, MeteoSwiss and UGM). The final version of the agreement is expected to be signed in spring 2001.

There is no direct financial funding from or to either member. However, the partners have the responsibility to contribute actively to the model development by providing staff resources, by making use of research cooperations and by seeking for national funding whenever possible. A minimum of 2 scientists working in COSMO research and development areas is required from each member.

In general, the group is open for collaboration with other NWP groups, research institutes and universities as well as for new members. In September 2000, the national weather service IMGW of Poland (Institute of Meteorology and Water Management, Warsaw, Poland) has formally applied for membership.

3 Model System Overview

The limited-area model LM is designed as a flexible tool for numerical weather prediction on the meso-β and on the meso-γ scale as well as for various scientific applications using grid spacings from 50 km down to about 50 m. Besides the forecast model itself, a number of additional components such as data assimilation, interpolation of boundary conditions from a driving host model and postprocessing is required to run a NWP-system at a meteorological service. In the following sections, the components of the LM-package - as available to the COSMO group - are shortly described.

3.1 Lokal-Modell (LM)

The regional model LM is based on the primitive hydro-thermodynamical equations describing compressible nonhydrostatic flow in a moist atmosphere without any scale approximations. A basic state is subtracted from the equations to reduce numerical errors associated with the calculation of the pressure gradient force in case of sloping coordinate surfaces. The basic state represents a time-independent dry atmosphere at rest which is prescribed to be horizontally homogeneous, vertically stratified and in hydrostatic balance. The basic equations are written in advection form and the continuity equation is replaced by a prognostic equation for the perturbation pressure (i.e. the deviation of pressure from the reference state). The model equations are solved numerically using the traditional finite difference method. Table 1 summarizes the dynamical and numerical key features of the LM.

Table 1: ***LM Model Formulation: Dynamics and Numerics***

Model Equations:	Basic hydro-thermodynamical equations in advection form, no scale approximations (i.e. non-hydrostatic, fully compressible); subtraction of horizontally homogeneous basic state at rest.
Prognostic Variables:	Horizontal and vertical wind components, temperature, pressure perturbation, specific humidity, cloud water content.
Diagnostic Variables:	Total air density, precipitation fluxes of rain and snow.
Coordinate System:	Rotated geographical (lat/lon) coordinate system horizontally; generalized terrain-following height-coordinate vertically
Grid structure:	Arakawa C-grid, Lorenz vertical grid staggering.
Spatial discretization:	Second order horizontal and vertical differencing.
Time integration:	Leapfrog HE-VI (horizontally explicit, vertically implicit) time-split integration scheme by default; includes extensions proposed by Skamarock and Klemp (1992). Additional options for: - a two time-level 2nd order Runge-Kutta split-explicit scheme (Wicker and Skamarock(1998)), - a three time-level 3-d semi-implicit scheme (Thomas et al., 2000).
Numerical Smoothing:	4th order linear horizontal diffusion; Rayleigh-damping in upper layers; 3-d divergence damping and off-centering in split steps
Lateral Boundaries:	1-way nesting using the lateral boundary formulation according to Davies (1976). Option for periodic boundary conditions.

Table 2: ***LM Model Formulation: Physical Parameterizations***

Grid-scale clouds and precipitation:	Cloud water condensation/evaporation by saturation adjustment; precipitation formation by a bulk parameterization including water vapour, cloud water, rain and snow (scheme HYDOR); rain and snow are treated diagnostically by assuming column equilibrium. Optional: cloud ice scheme.
Subgrid-scale clouds:	Subgrid-scale cloudiness is interpreted by an empirical function depending on relative humidity and height. A corresponding cloud water content is also interpreted.
Moist convection:	Mass-flux convection scheme (Tiedtke, 1989) with closure based on moisture convergence. optional: modified closure based on CAPE.
Radiation:	δ-two stream radiation scheme after Ritter and Geleyn (1992) for short and longwave fluxes; full cloud-radiation feedback.
Vertical diffusion:	Diagnostic K-closure at hierarchy level 2. Optional: a new level 2.5 scheme with prognostic treatment of turbulent kinetic energy; effects of subgrid-scale condensation and evaporation are included.
Surface layer:	Constant flux layer parameterization based on the Louis (1979) scheme. Optional: a new surface scheme including a laminar boundary layer and effects from subgrid-scale thermal circulations.
Soil processes:	Soil model after Jacobsen and Heise (1982) with 2 soil moisture layers and Penman-Monteith transpiration; snow and interception storage are included. Climate values changing monthly (but fixed during forecast) in third layer.

For real data simulations, LM can be driven by the former operational regional models EM or DM or by the new global model GME of DWD using the traditional boundary relaxation technique (see Section 3.3). To reduce noise and spin-up resulting from non-balanced interpolated data, a diabatic digital filtering initialization scheme (Lynch et al., 1997) has been implemented. Four-dimensional data assimilation for LM is based on a nudging analysis scheme (see Section 3.2). Additionally, LM provides a capability to handle idealized cases using user-defined artificial initial and/or boundary data. For these types of application, periodic lateral boundary conditions can be specified optionally. Also, a 2-dimensional model configuration can be used.

A variety of subgrid-scale physical processes are taken into account by parameterization schemes. A large part of the present physics package of LM is adapted from the former operational hydrostatic models EM/DM. Current activities of the COSMO physics group concentrate on an upgrade of the physics routines for the operational application. Table 2 gives a short overview on the parameterization schemes used operationally and on additional options implemented so far.

The parameterization of physical processes, but also the adiabatic model part requires some parameters which are not derived by data assimilation or by interpolation from a driving model. These so-called external parameters are defined in additional data sets. The LM requires the following external parameters: mean topographical height, roughness length, soil type, vegetation cover, land fraction, root depth and leaf area index. The sources for these data are indicated below.

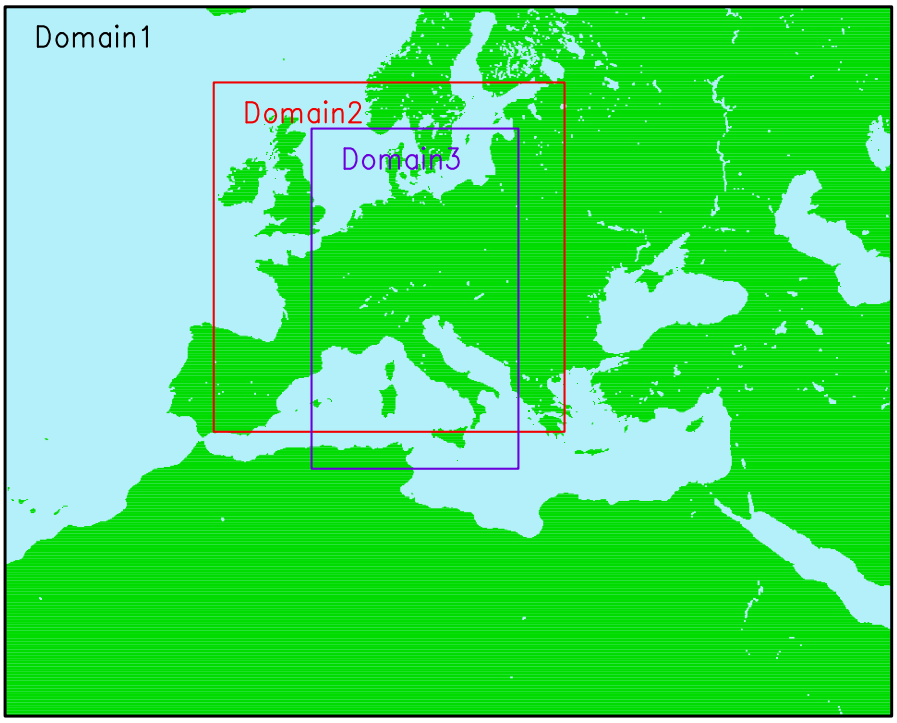

Figure 2: *Domains of external parameter datasets used by COSMO partners*

- Mean orography
  derived from the GTOPO30 data set (30"x30") from USGS.
- Prevailing soil type
  derived from the DSM data set (5'x5') of FAO.
- Land fraction, vegetation cover, root depth and leaf area index
  derived from the CORINE data set of ETC/LC.
- Roughness length
  derived from the GTOPO30 and CORINE datasets.

External parameters for LM can be derived by a preprocessor program for any domain on the globe at any required spatial resolution. However, this is very time consuming because of the size of the high-resolution global data sets. Within the COSMO group, we thus have prepared some predefined data sets with external parameters on three different domains (see Fig. 2).

Domain 1 covers Europe and surrounding countries; data sets for this domain are available at 28 km, 21 km, 14 km and 7 km grid spacing. The smaller Domain 2 covers Germany and surrounding countries; the corresponding data set gives the external parameters at 7 km resolution. Domain 2 is only used at DWD. Finally, Domain 3 covers central and southern parts of Europe. For this domain, the external parameters are given at 2.8 km resolution. The LM can then be very easily positioned anywhere within these domains.

Details on the location of the three domains, the resolution and the corresponding file names (these are required for the interpolation programs to generate initial and boundary data from a host model) are given below. The specifications refer to a rotated lat-lon grid of LM with the north-pole at geographical latitude 32.5° (N) and longitude -170.9° (W); longitude (λ)

and latitude (ϕ) of the rotated coordinates and those of the geographical lat-lon grid (λ_g, ϕ_g) are in degree.

(a) Domain 1

Location of the domain

upper left:	$\lambda = -26.75$	$\phi = 9.25$	upper right:	$\lambda = 33.25$	$\phi = 9.25$
	$\lambda_g = -42.74$	$\phi_g = 56.07$		$\lambda_g = 70.36$	$\phi_g = 51.49$
lower left:	$\lambda = -26.75$	$\phi = -38.75$	lower right:	$\lambda = 33.25$	$\phi = -38.75$
	$\lambda_g = -11.26$	$\phi_g = 14.54$		$\lambda_g = 35.96$	$\phi_g = 12.34$

Resolution and file name of datasets

$\Delta\lambda, \Delta\phi$ (°)	Δs (m)	no. of grid points	Filename
0.2500	28000	241 x 193	lm_d1_28000_241x193.g1
0.1875	21000	321 x 257	lm_d1_21000_321x257.g1
0.1250	14000	481 x 385	lm_d1_14000_481x385.g1
0.0625	07000	961 x 769	lm_d1_07000_961x769.g1

(b) Domain 2

Location of the domain

upper left:	$\lambda = -12.625$	$\phi = 4.125$	upper right:	$\lambda = 11.125$	$\phi = 4.125$
	$\lambda_g = -15.25$	$\phi_g = 59.26$		$\lambda_g = 32.48$	$\phi_g = 59.77$
lower left:	$\lambda = -12.625$	$\phi = -19.50$	lower right:	$\lambda = 11.125$	$\phi = -19.50$
	$\lambda_g = -4.87$	$\phi_g = 36.62$		$\lambda_g = 23.15$	$\phi_g = 36.92$

Resolution and file name of dataset

$\Delta\lambda, \Delta\phi$ (°)	Δs (m)	no. of grid points	Filename
0.0625	07000	381 x 379	lm_d2_07000_381x379.g1

(c) Domain 3

Location of the domain

upper left:	$\lambda = -6.00$	$\phi = 1.00$	upper right:	$\lambda = 8.00$	$\phi = 1.00$
	$\lambda_g = -1.37$	$\phi_g = 58.00$		$\lambda_g = 25.06$	$\phi_g = 57.61$
lower left:	$\lambda = -6.00$	$\phi = -22.00$	lower right:	$\lambda = 8.00$	$\phi = -22.00$
	$\lambda_g = 3.19$	$\phi_g = 35.20$		$\lambda_g = 19.06$	$\phi_g = 34.97$

Resolution and file name of dataset

$\Delta\lambda, \Delta\phi$ (°)	Δs (m)	no. of grid points	Filename
0.0250	02800	561 x 921	lm_d3_02800_561x921.g1

To meet the computational requirement of the model, the program has been coded in Standard Fortran 90 and parallelized using the MPI library for message passing on distributed memory machines. Thus it is portable and can run on any parallel machine providing MPI. Also it can still be executed on conventional scalar and vector computers where MPI is not available.

The parallelization strategy is the two dimensional domain decomposition which is well suited for grid point models using finite differences (see Fig. 3). Each processor gets an appropriate part of the data to solve the model equations on its own subdomain. This

subdomain is surrounded by halo gridlines which belong to the neighboring processors. At present, we use 2 gridlines for the halo. However, as the number of halo gridlines is softcoded, this can be easily changed whenever necessary (e.g., in case of high order advection schemes). During the integration step each processor updates the values of its local subdomain; grid points belonging to the halo are exchanged using explicit message passing. The number of processors in longitudinal and latitudinal direction can be specified by the user to fit optimal to the hardware architecture.

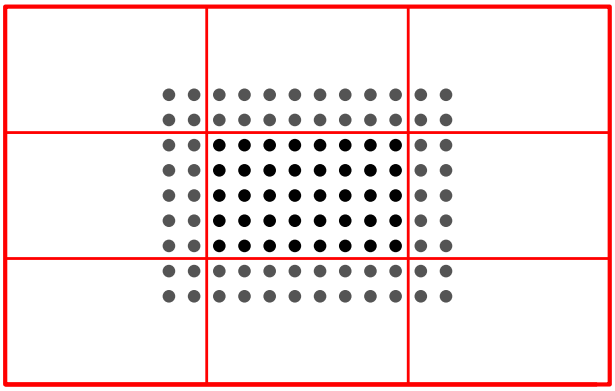

Figure 3: *2-D domain decomposition with a 2 gridline halo*

Figure 4 shows timings for one hour of forecast from full-physics test runs with different domain sizes on a SGI/Cray T3E. The parallel speedup is illustrated on the log-log-scale, showing that the model scales well to hundreds of processors for appropriate domain sizes.

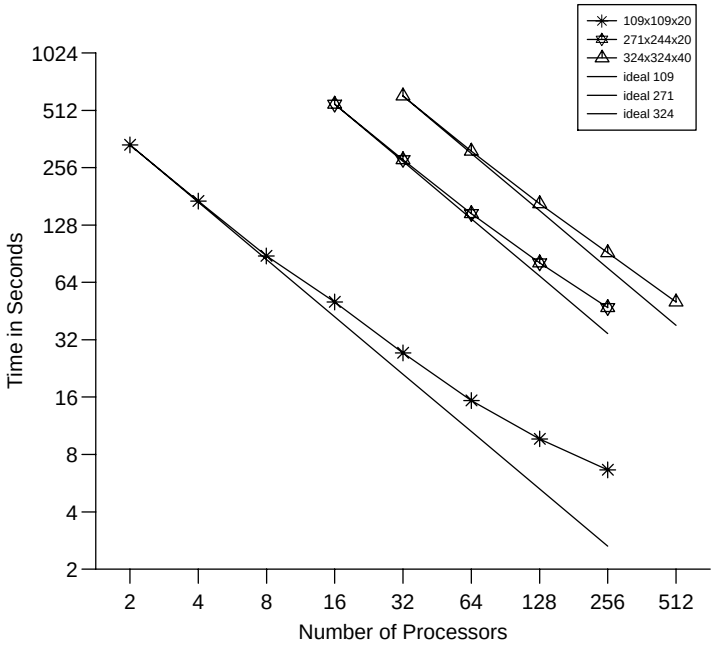

Figure 4: *Timings for different model sizes; the straight lines show perfect scalability*

3.2 Data Assimilation

The LM data assimilation system is based on the observational nudging technique. The scheme has been derived from an experimental nudging analysis scheme which has been developed for DM and the Swiss model version SM (Schraff, 1996; 1997) and which compared favorably with the operational OI-analysis of the DM in various case studies. The new LM-scheme, however, runs on distributed memory machines and uses the domain decomposition of the model to compute the analysis increments locally for the grid points of each sub-domain, using the previously distributed observational information of the total domain.

Table 3: *Data Assimilation for LM*

Method	Nudging towards observations
Implementation	continuous cycle of 3-hour assimilation runs
Realization	identical analysis increments used during 6 advection time steps
Balance	1. hydrostatic temperature increments (up to 400 hPa) balancing 'near-surface' pressure analysis increments 2. geostrophic wind increments balancing 'near-surface' pressure analysis increments 3. upper-air pressure increments balancing total analysis increments hydrostatically
Nudging coefficient	$6 \cdot 10^{-4} s^{-1}$ for all analyzed variables
Analyzed variables	horizontal wind vector, potential temperature,relative humidity 'near-surface' pressure (i.e. at the lowest model level)
Spatial analysis	Data are analyzed vertically first, and then spread laterally along horizontal surfaces. vertical weighting: approximately Gaussian in log(p) horizontal weighting: isotropic as function of distance
Temporal weighting	1.0 at observation time, decreasing linearly to 0.0 at 3 hours (upper air) resp. 1.5 hours (surface-level data) before and 1.0 resp. 0.5 hours after observation time; linear temporal interpolation of frequent data.
Observations	SYNOP, SHIP, DRIBU: - station pressure, wind (stations below 100 m above msl) - humidity TEMP, PILOT: - wind, temperature: all standard levels, significant levels up to 150 hPa - humidity: all levels up to 300 hPa - geopotential used for one 'near-surface' pressure increment
Quality control	Comparison with the model fields from assimilation run itself

The variables being nudged are horizontal wind, temperature, and humidity at all levels, and pressure at the lowest model level. The lateral spreading of the observational information is horizontal, or optionally along model levels or isentropic surfaces. A temperature correction is applied, so that the mass field will not change above a certain height when only the pressure at the lowest model level is nudged. This correction is designed to be largest in the lower troposphere and to preserve the stability in the boundary layer approximately, and

it helps to sustain the impact of the surface pressure data. The mass field change imposed by the pressure nudging including the temperature correction is then partly balanced by a geostrophic wind correction.

Pressure increments at upper levels are computed from the pressure analysis increments at the lowest model level and the temperature and humidity increments (including the temperature correction, and the effect of evaporation and condensation due to the nudging) at all levels by integrating the hydrostatic equation from the lowest level upwards. Balancing the total analysis increments hydrostatically in this way avoids uncontrolled sources in the vertical velocity equation during a nudging integration.

At present, the scheme uses only conventional data of type TEMP, PILOT, SYNOP, SHIP and DRIBU. Table 3 summarizes the features of the LM nudging scheme.

As an external component of the LM-analysis, a new 2-d variational soil moisture analysis scheme has also been developed (see Section 9.2). The soil moisture content is determined by assuming a unique dependence of 2-m temperature on the soil moisture content in the uppermost two soil layers and minimizing a functional measuring the distance between predicted and observed temperature. In order to suppress too large variations for advection dominated situations, a background soil moisture is included in the cost function. The scheme has been successfully tested in various case studies and it is operated at DWD since March 2000.

Two additional external analyses complete the LM data assimilation: a sea surface temperature (SST) analysis based on the correction method using SST data from ships and buoys and a snow depth analysis using SYNOP observations.

3.3 Boundary Conditions from Driving Models

The LM can be nested in the new global model GME (Majewski, 1998) or the former hydrostatic regional models EM or DM of DWD. The lateral boundary formulation is by the Davies (1976) relaxation technique, where the internal model solution is nudged against an externally specified solution within a narrow boundary zone by adding a relaxation forcing term to the equations.

The external solution is obtained by interpolation from the driving host model at discrete time intervals. The interpolated fields are hydrostatically balanced, i.e. a hydrostatic pressure is prescribed for the nonhydrostatic pressure variable in LM at the lateral boundaries. Within these specified time intervals, the boundary data are interpolated linearly in time (which is done inside the model). Normally the boundary update interval is chosen to be one hour for meso-β scale applications of the LM. The boundary values (and initial values, if no data assimilation suite is operated) are obtained by a preprocessing program from the host model:

- ***GME2LM***
  interpolation from the new triangular mesh global model GME of DWD
- ***HM2LM***
  interpolation from the hydrostatic regional models EM or DM of DWD

A documentation of the GME2LM preprocessor program is available at the COSMO Website. Additional interpolation programs IFS2LM (to nest LM into the ECMWF model) and LM2LM (for 1-way self-nesting of LM) are in preparation.

3.4 Postprocessing

Postprocessing includes all applications that use the direct model output of LM runs. In general, there is a wide range of such application at each meteorological service, ranging from simple graphical display of weather charts or meteograms for single grid points, over statistical correction of near surface weather elements by Kalman filtering, to more complex derived products supplying information on environment and health, transportation, agriculture and media presentation. Most of these postprocessing tools are very specific to the computer platform, data base system and visualization software of each service and thus cannot be shared within the COSMO group. There is, however, a number of postprocessing programs available within COSMO.

(a) Graphics

Work on two common plotting packages has been completed. The first has been developed at MeteoSwiss and uses Metview with an interface to the GRIB1 LM output data; the other one has been developed at ARPA-SMR and is based on the public domain VIS5D packages; a special routine converts the GRIB1 binary format to the VIS5D data format.

(b) Models

A *Lagrangian Particle Dispersion Model* (LPDM) may be used operationally in case of radioactive accidental releases to predict long-range transport, dispersion, and wet and dry deposition of radioactive material. The calculation of about $10^5 - 10^6$ trajectories of tracer particles is based on wind fields from LM (at hourly intervals) and superimposed turbulent fluctuations (TKE, Monte Carlo method). Radioactive decay and convective mixing are included. The concentration is calculated by counting the particle masses in arbitrary grids.

A *Trajectory Model* may provide guidance on transport routes. The meteorological input is derived from LM at hourly intervals.

An integral part of the NWP-system at DWD is a *Wave Prediction Suite* comprising two models, namely the global model GSM (global sea state model), and a local one (LSM) which covers the Baltic Sea, the North Sea and the Adriatic Sea with a high-resolution mesh. GSM and LSM have been developed by research institute GKSS in Geesthacht (Germany).

(c) Interpretation

An objective weather interpretation scheme (developed at DWD) derives the forecasted 'weather', i.e. the WMO weather code, based on LM output fields. Pressure, temperature, dew point temperature, liquid water content, cloud cover, precipitation and wind speed values are used as input parameters to define the present weather.

3.5 Documentation

The following parts of the model system documentation are available on the COSMO website.

(a) The Nonhydrostatic Limited-Area Model LM of DWD

Part I: *Scientific Documentation*
Part II: *Implementation Documentation*
Part III: *User's Guide*
Part X: *Soil Moisture Analysis*

(b) The Interpolation Program GME2LM

4 Working Groups

COSMO's scientific and technical activities are organized in *Working Groups* (WG) which cover the main research areas related to a NWP-system. Each Working Group is headed by a *Work Package Coordinator* (WPC), who is responsible for the consistency of the execution of the work packages and for the coordination, planning, and supervision of the scientific and technical activities related to the work packages in his group.

This section gives an overview on the current personnel composition of the WGs. All scientists contributing actively to the work packages are included in the lists, also those from outside COSMO member institutions. For each WG, the main research activities from the recent COSMO period (Oct 1999 - Oct 2000) are briefly summarized and a short note on the planned activities for the present period (Oct 2000 - Sept 2001) is given. The detailed work plans, i.e. the description of the work packages of WGs, are available at the member area of our web-site.

4.1 Working Group 1: Data Assimilation

The WG on data assimilation is headed by Christoph Schraff (DWD) as WPC. The following scientists are members of this group.

Contributing Scientists	Institution	email
Jean-Marie Bettems	MeteoSwiss	jmb@sma.ch
Michael Buchhold	DWD	michael.buchhold@dwd.de
Davide Cesari	ARPA-SMR	dinamici@smr.arpa.emr.it
Massimo Ferri	UGM	m.ferri@ecmwf.int
Guergana Guerova	University of Bern (CH)	guergana.guerova@mw.iap.unibe.ch
Christian Häberli	MeteoSwiss	christian.haeberli@meteoschweiz.ch
Reinhold Hess	DWD	reinhold.hess@dwd.de
Andrea Rossa	MeteoSwiss	rossa@sma.ch
Georgio Sakellaridis	HNMS	nwpapa@hnms.gr
Christoph Schraff	DWD	christoph.schraff@dwd.de
Panageotis Skrimizeas	HNMS	mans@hnms.gr
Maria Tomassini	DWD	maria.tomassini@dwd.de
Helmut Walter	AWGeophys	hwalter@amg.dwd.de

The main research activities of WG 1 for the period Oct 1999 - Oct 2000 covered the following points.

- Work on the nudging assimilation scheme has been continued. The following items have been considered in detail.
  - The explicit vertical influence of surface-level humidity observations was reduced from about 700 m to the lowest model level. This nearly eliminated a tendency to overestimate precipitation in the assimilation cycle, which was also related to the current surface layer parameterization diagnosing the 2-m relative humidity to be equal to that at the lowest model level (about 30 m above the ground).
  - The observed 3-hourly pressure tendency was included in the threshold for quality control of surface pressure data. This results in a better acceptance of surface pressure data in case of fast moving storm cyclones.
  - An additional height and thickness check for multi-level temperature observations was introduced.
  - A multi-level check for wind, temperature and humidity was implemented.

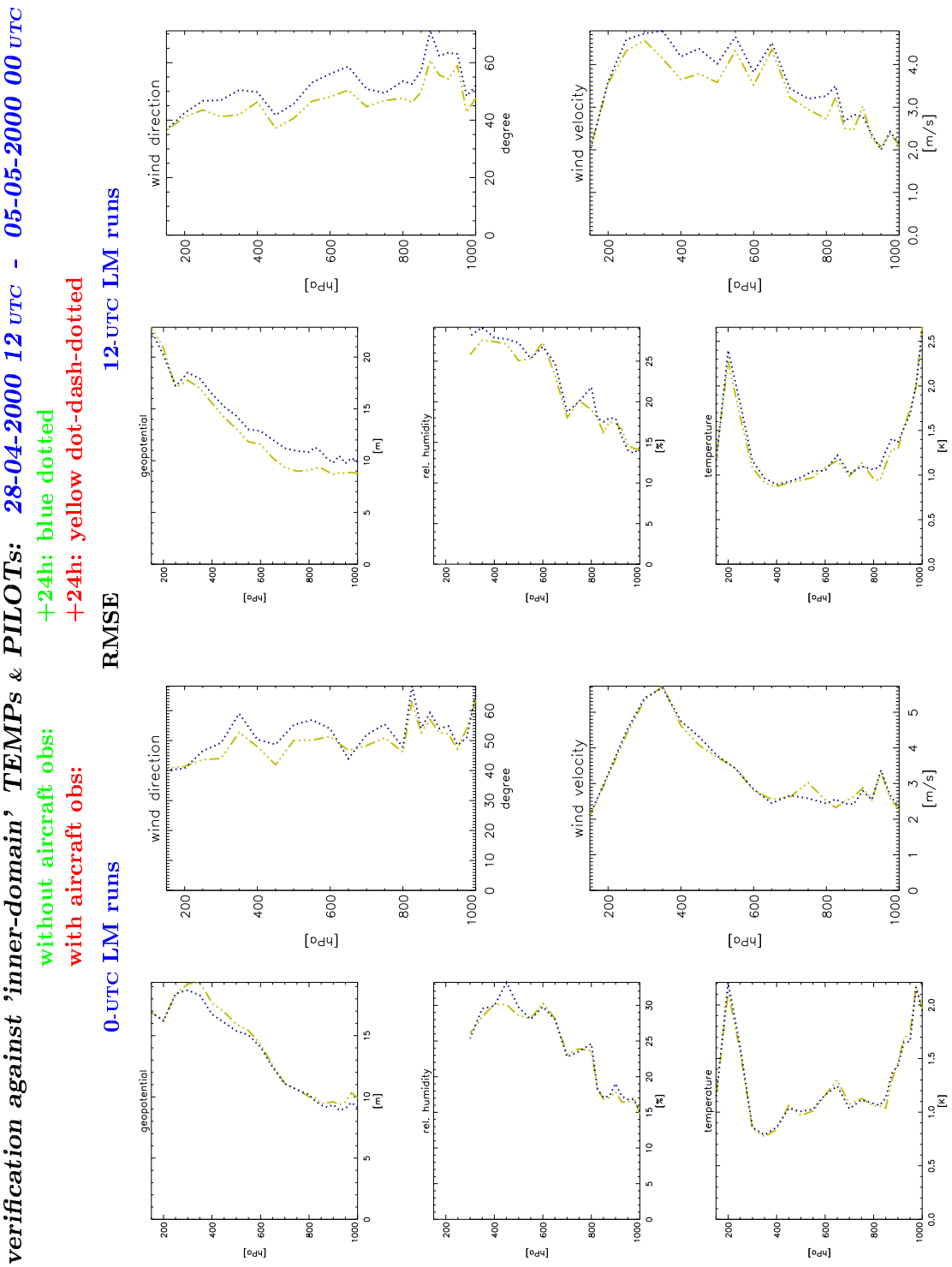

Figure 5: *Verification (RMSE) against TEMPs and PILOTs of an experiment (28 April 2000 - 5 May 2000) with aircraft data and without aircraft data (routine). Left: 00 UTC runs. Right: 12 UTC runs.*

  - Work on the assimilation of aircraft data has been started. At present, a thorough test in a parallel assimilation cycle is conducted. First results show a significant positive impact on predicted vertical profiles of wind, temperature and geopotential for 12 UTC runs (see Fig. 5).

- The development and evaluation of a new variational (two-layer) soil moisture analysis (Hess, 2000) has been completed. The scheme is in operation at DWD since March 2000 and it has a significant positive impact on the predicted 2m-temperature.

- An experimental model version for the assimilation of radar data by latent heat nudging has been developed and tested in some case studies. However, the work on it had to be ceased since the responsible scientist left DWD.

The major work packages for 2001 include further evaluation and tuning of the nudging scheme. Especially, the tuning and evaluation work on the assimilation of aircraft data will be continued aiming at an operational use of aircraft data in the LM assimilation cycle. Furthermore, observing system experiments are planned to be conducted as a contribution to the EUCOS (EUMETNET Composite Observing System) project. Also, the work on the latent heat nudging will be resumed in two work packages, one of it taking the approach to derive vertical profiles of latent heating from 3-d radar reflectivities.

4.2 Working Group 2: Numerical Aspects

The WG on numerical methods and basic model dynamics is headed by Jürgen Steppeler (DWD) as WPC. Currently, the following scientists are members of this group.

Contributing Scientists	Institution	email
Heinz-Werner Bitzer	AWGeophys	heinz-werner.bitzer@dwd.de
Luca Bonaventura	Universita' di Trento	bonavent@ing.unitn.it
Günther Doms	DWD	guenther.doms@dwd.de
Almut Gassmann	DWD	almut.gassmann@dwd.de
Annemarie Link	DWD	annemarie.link@dwd.de
Yannis Papageorgiou	HNMS	nwpapa@hnms.gr
Maria Refene	HNMS	diso@hnms.gr
Georgio Sakellaridis	HNMS	nwpapa@hnms.gr
Ulrich Schättler	DWD	ulrich.schättler@dwd.de
Reinhold Schrodin	DWD	reinhold.schrodin@dwd.de
Jürgen Steppeler	DWD	juergen.steppeler@dwd.de

The main research activities of WG 2 for the period Oct 1999 - Oct 2000 covered the following points.

- The present terrain-following coordinate system will result in large and presumably not acceptable numerical errors in case of steep topography. Thus, work on a z-coordinate system version of LM for high-resolution applications has been started. The following items have been considered so far:

  - basic studies related to a shaved element finite volume discretization,
  - formulation and test of lower boundary conditions,
  - set-up of a 2-D test version of the model.

- The evaluation of the 2-time-level RK split-explicit integration scheme has been continued. The scheme works well for real data cases, however, for some idealized cases (linear mountain waves) larger deviations from the analytical solution have been noticed.

- For applications on the meso-γ scale the full 3-D transport of rain and snow has to be considered instead of the present column-equilibrium approximation. A test version using positive definite transport and a time-splitting approach for the fallout of precipitation has been developed. Test integrations at 7-km grid spacing show a much smoother structure of the precipitation pattern (see Fig. 6), where peaks over mountain tops are significantly reduced.

- The representation of two-grid-interval (2dx) waves is hopelessly inaccurate in numerical models, but this type of noise is constantly forced by using a mean topography. Thus, filtering of orography, i.e. removing all 2dx and 3dx components from the orography, is necessary for a more correct interaction of the dynamics with the surface. Tests with the Raymond (1988) filter using different filter parameters have shown that the forecast quality can be improved if the orography is weakly filtered.

- The current leapfrog scheme with centered differencing for humidity advection is not very accurate. Thus, work on a positive definite leapfrog advection scheme based on flux correction has been started.

- Artificial horizontal diffusion is required to control small-scale noise on the 2dx interval. The current linear 4th-order scheme, however, introduces new errors on the resolvable scales via the Gibbs phenomena. A monotonic version of the scheme, which lacks over- and under-shootings but retains the filter characteristics, has been implemented and is in test.

- The simple addition of tendencies from horizontal diffusion and advection in the Leapfrog integration scheme results in an instability when the wind velocity is close to the advective CFL limit (as happened for the December 99 storms). A reformulation of the time integration scheme by applying Marchuk-splitting for horizontal diffusion could cure this problem.

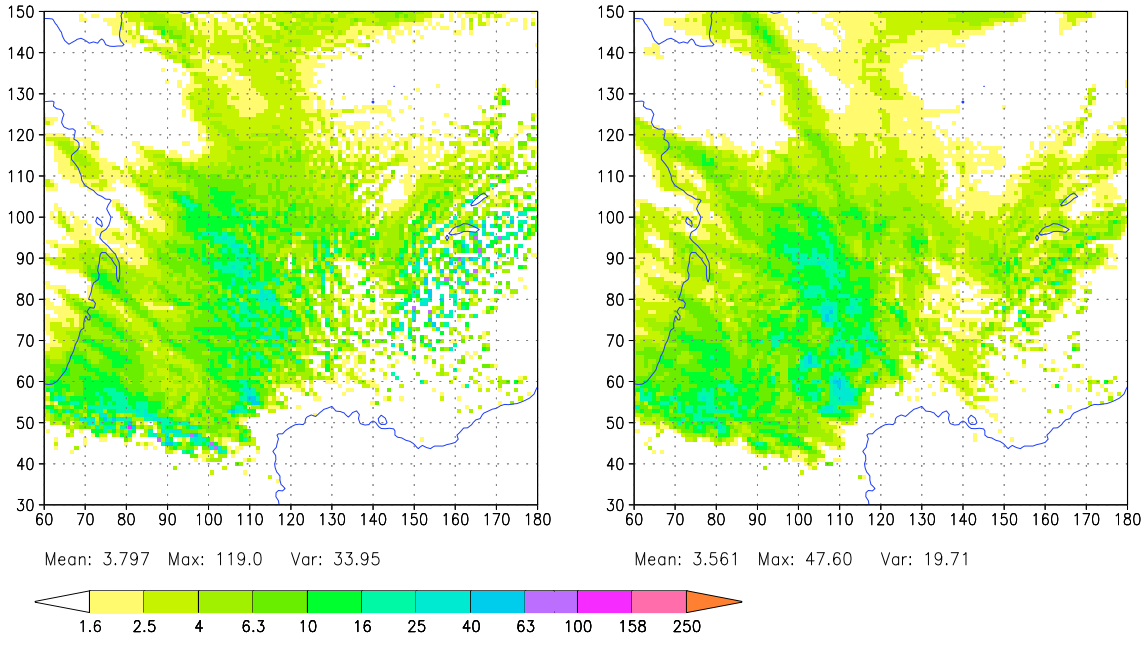

Figure 6: *12-hr accumulated precipitation (mm) from an LM-simulation of 2 February 2000 06 - 18 UTC. Left: reference version. Right: experimental version with the prognostic precipitation scheme.*

The major work packages for 2001 include further development work for the new z-coordinate, which is considered to be essential for NWP on the meso-γ scale. This work package aims at the derivation of a full 3-D model version including physics in late autumn this year. Other points of interest are horizontal diffusion, orographic filtering and further evaluation of the 2 time-level integration scheme.

4.3 Working Group 3: Physical Aspects

The WG on physical processes and their parameterization is headed by Marco Arpagaus (MeteoSwiss) as WPC. The following scientists are members of this group.

Contributing Scientists	Institution	email
Marco Arpagaus	MeteoSwiss	marco.arpagaus@meteoschweiz.ch
Claudio Cassardo	Universita' del Piemonte Orientale (UNIPMN)	cassardo@al.unipmn.it
Günther Doms	DWD	guenther.doms@dwd.de
Erdmann Heise	DWD	erdmann.heise@dwd.de
Nicola Loglisci	Universita' di Torino (UNITO)	loglisci@ph.unito.it
Dmitrii Mironov	DWD	dmitrii.mironov@dwd.de
Renata Pelosini	CSI Servizio Meteorologico Regione Piemonte	Renata.Pelosini@csi.it
Matthias Raschendorfer	DWD	matthias.raschendorfer@dwd.de
Bodo Ritter	DWD	bodo.ritter@dwd.de
Reinhold Schrodin	DWD	reinhold.schrodin@dwd.de

During the recent COSMO period, the main effort of this group focused on the development of a new physics package for future operational applications. Activities concentrated on the following items.

- A new turbulence scheme (level 2.5) based on a prognostic treatment of turbulent kinetic energy has been implemented for optional use. Effects from subgrid-scale condensation are also considered by this parameterization. The new scheme is evaluated and tuned in a parallel experimental suite including data assimilation.
- Also, a new surface layer scheme which is based on the TKE approach and includes effects from a laminar boundary layer as well as from subgrid-scale thermal circulations has been implemented for optional use. Currently, this scheme is tested in combination with the new turbulence scheme.
- A new multi-layer version of the soil model TERRA has been developed. The new version includes freezing and melting of soil layers and a revised formulation of the snow model. Fig. 7 shows the current vertical layer structure and the processes considered in the water and energy budget of the soil.
- An alternative closure for the Tiedtke (1989) mass-flux scheme has been formulated. It is based on CAPE and replaces the current moisture convergence approach for deep and shallow convection. First tests indicate a much better representation of the daily cycle of convective activity.
- A Penman-Monteith-type formulation of transpiration has been implemented into the soil model TERRA. This modification is in operation.
- A horizontal averaging of the convective forcing functions has been introduced for optional use (not yet operational). This averaging has a beneficial impact on the spatial structure of convective precipitation over mountainous areas.

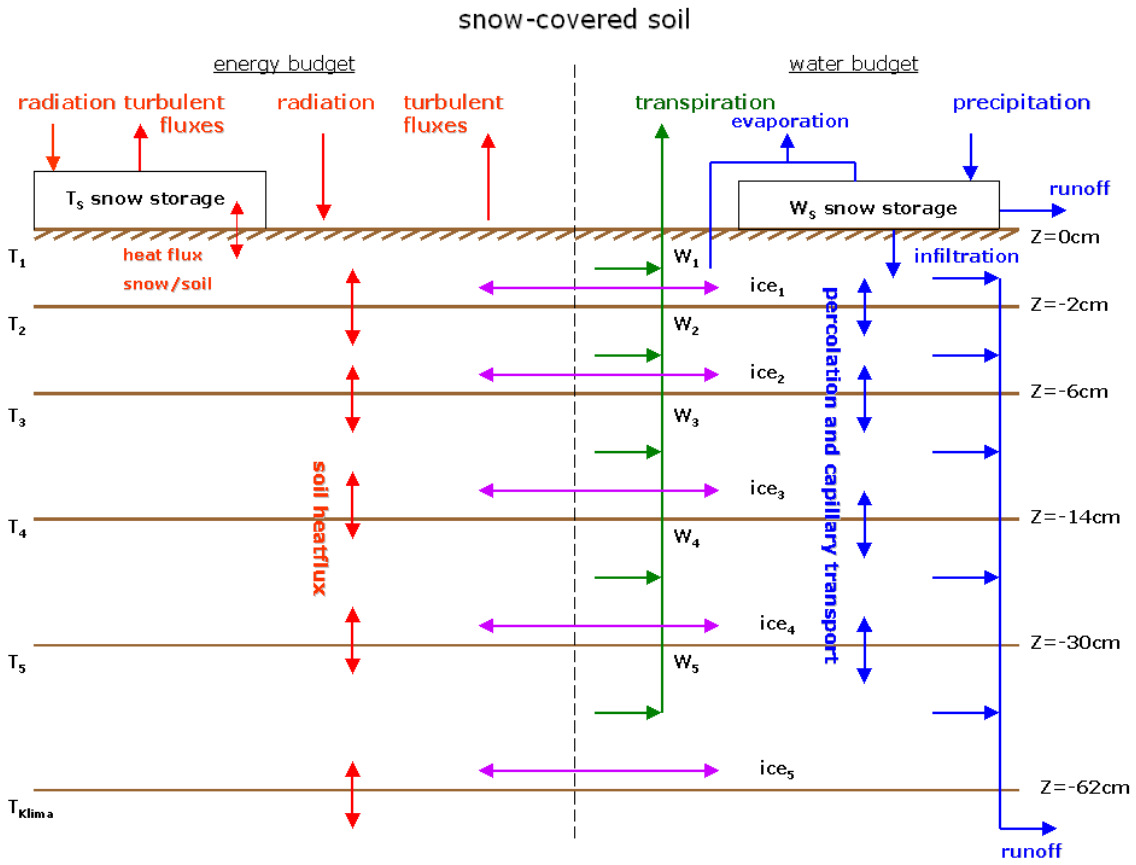

Figure 7: *The new multi-layer version of the soil model TERRA: General structure and physical processes considered (in case of snow-covered soil).*

The major work packages for 2001 include further evaluation and tuning work for the TKE-based turbulence parameterization and for the new multi-layer soil model. The aim is to have these new schemes operationally within the current COSMO period. Other work packages consider a tuning of the cloud-radiation interaction and the implementation of the Kain-Fritsch convection scheme. Also, the development and evaluation of a new grid-scale cloud and precipitation scheme including cloud ice as an additional prognostic variable besides cloud water will be continued. The scheme will also be implemented in the global model GME.

4.4 Working Group 4: Interpretation and Applications

This WG has not yet been active during the recent COSMO period. At the annual meeting, it was decided to open this group. The Steering Committee assigned Pierre Eckert from MeteoSwiss to take the responsibility as work package coordinator for WG 4. Currently, the following scientists are members of this group.

Contributing Scientists	Institution	email
Pierre Eckert	MeteoSwiss	pierre.eckert.@meteoschweiz.ch
Massimo Ferri	UGM	m.ferri@ecmwf.int
Andrea Montani	ARPA-SMR	a.montani@smr.arpa.emr.it
Tiziana Paccagnella	ARPA-SMR	t.paccagnella@smr.arpa.emr.it
Volker Renner	DWD	volker.renner@dwd.de

To start this group, three work packages have been defined so far. They include the following items

- COSMO-LAMEPS: Implementation and testing of a limited area ensemble prediction system based on LM.
- Statistical postprocessing of weather parameters from deterministic high-resolution forecasts using (a) the neighborhood method and (b) the wavelet method.
- Review and comparison of Kalman filtering methods for LM surface weather parameters at various COSMO centres.

4.5 Working Group 5: Verification and Case Studies

The WG on verification and case studies is headed by Carlo Cacciamani (ARPA-SMR) as WPC. The following scientists are members of this group.

Contributing Scientists	Institution	email
Marco Arpagaus	MeteoSwiss	marco.arpagaus@meteoschweiz.ch
Jean-Marie Bettems	MeteoSwiss	jean-marie.bettems@meteoswiss.ch
Carlo Cacciamani	ARPA-SMR	c.cacciamani@smr.arpa.emr.it
Ulrich Damrath	DWD	ulrich.damrath@dwd.de
Massimo Ferri	UGM	m.ferri@ecmwf.int
Stefano Gallino	CMIRL (Genova)	stefano@cmirl1.ge.infn.it
Pirmin Kaufmann	MeteoSwiss	pirmin.kaufmann@meteoswiss.ch
Enrico Minguzzi	SMR Piedmont	enrico.minguzzi@csi.it
Tiziana Paccagnella	ARPA-SMR	t.paccagnella@smr.arpa.emr.it
Ulrich Pflüger	DWD	ulrich.pflueger@dwd.de
Andrea Rossa	MeteoSwiss	andrea.rossa@meteoswiss.ch
Georgio Sakellaridis	HNMS	nwpapa@hnms.gr
Francis Schubiger	MeteoSwiss	francis.schubiger@meteoswiss.ch

The main activities of WG 5 for the period Oct 1999 - Oct 2000 covered the following points.

- The operational verification of predicted surface weather parameters is done at each COSMO site for its own LM application and for LM results from other centres. The observational basis are SYNOP stations and regional high-resolution networks. Results are summarized in verification reports which are distributed on a quarterly basis.
- An internal Mini-Workshop on the verification of LM was held on 14-15 February in Bologna. The participants addressed the following items.
  - discussion of methods and techniques (types of scores, standard and new ones)
  - agreement on a common method for the verification of surface parameters
- Work on the development of a common TEMP-verification package has been started.
- Verification of precipitation using high-resolution precipitation analyses from ARPA-SMR for the Emilia Romagna region. The analyses are available every hour and are obtained by using surface raingauges and calibrated radar data.
- A cloud classification and cloud indexing scheme using high-resolution calibrated data of IR and VIS METEOSAT channels has been developed. The procedure takes into account spectral as well as statistical properties of the clouds detected. The scheme will be used to verify LM cloud coverage (low, middle, high and total) at hourly intervals.

The major work packages for 2001 include a continuation of the current operational verification of surface parameters using both GTS and special observational data from regional networks. Also, work on the verification of vertical profiles at TEMP stations and the verification of LM cloudiness using Meteosat VIS and IR data will be continued. A central aspect will be the definition of a common verification system to be used for a new parallel test suite at ECMWF.

4.6 Working Group 6: Reference Version and Implementation

The WG on code maintenance, reference version, documentation and implementation is headed by Ulrich Schättler (DWD) as WPC. The following scientists are members of this group.

Contributing Scientists	Institution	email
Theodore Andreadis	HNMS	andrea@hnms.gr
Jean-Marie Bettems	MeteoSwiss	jean-marie.bettems@meteoswiss.ch
Davide Cesari	ARPA-SMR	dinamici@srm.arpa.emr.it
Almut Gassmann	DWD	almut.gassmann@dwd.de
Guy de Morsier	MeteoSwiss	guy.de.morsier@meteoswiss.ch
Manoussakis Matthew	HNMS	mans@hnms.gr
Paolo Patruno	ARPA-SMR	p.patruno@smr.arpa.emr.it
Ulrich Schättler	DWD	ulrich.schaettler@dwd.de
Friedrich Theunert	AWGeophys	-
Lucio Torrisi	UGM	torrisi@ecmwf.int

The main activities of WG 6 for the period Oct 1999 - Oct 2000 covered the following points.

- All external parameters have been recalculated for specific COSMO domains at various resolutions (24, 14, 7, and 2.8 km). The new external parameters are based on the GTOPO30 and the CORINE data sets.
- Work on the interpolation programs to provide initial and boundary conditions from a driving host model has been continued.
  - the GME2LM preprocessor program has been parallelized, installed and is running at all COSMO member sites.
  - Work on the IFS2LM and LM2LM interpolation programs to nest LM in the ECMWF model and for one-way self-nesting, respectively, has been started.
- The reference version of LM is maintained at DWD using a source code and version control system based on SCCS. The LM is installed and running at all COSMO member sites and at ECMWF. All members apply the latest release of the model. A common update procedure has not been defined yet.
- Work on common plotting packages with interfaces to Metview and Vis5d has been completed. The packages are available for all COSMO members.

The major work packages for 2001 include further work on the interpolation programs to generate initial and boundary conditions. A central aspect is the definition of an update procedure for the LM-package. This includes the installation of test suites for single cases and fixed time periods and corresponding verification packages at ECMWF. A *Quick Reference for the LM-Package* is also planned. Finally, the COSMO web-site (www.cosmo-model.org) will be designed and installed at HNMS.

5 Operational Applications

The LM is operated in four centres of the COSMO members. Following a 1-year preoperational trial from October 1998 to November 1999, the model became operational at DWD in December 1999. At MeteoSwiss the LM is integrated in a preoperational mode two times a day since July 2000. In Italy the model runs preoperational once a day at ARPA-SMR. Also, the HNMS in Greece integrates the LM once a day in parallel to their old operational system. Switzerland plans to replace the current operational SM by the LM in March 2001.

All four centres use interpolated boundary conditions from forecasts of the global model GME of DWD. Only a subset of GME data covering the respective LM-domain of a COSMO meteorological centre are transmitted from DWD via the Internet. MeteoSwiss, ARPA-SMR and HNMS start the LM from interpolated GME analyses, followed by an initialization using the digital filtering scheme of Lynch et al. (1997). At DWD, a comprehensive data assimilation system for LM has been installed. MeteoSwiss plans to introduce this LM data assimilation system in spring 2001.

The following sections give a brief overview on the configurations of the operational LM system in the COSMO meteorological centres.

5.1 ARPA-SMR (Bologna)

The regional meteorological service ARPA-SMR in Bologna operates the LM in a preoperational mode at 7 km grid spacing. The rotated lat-lon coordinates of the lower left and of the upper right corner of the integration domain are $(\lambda = -5°, \phi = -24.0°)$ and $(\lambda = 9.5625°, \phi = -7.0625°)$, respectively. Figure 8 shows the orography of this model domain. The main features of the model set-up are summarized in Figure 9.

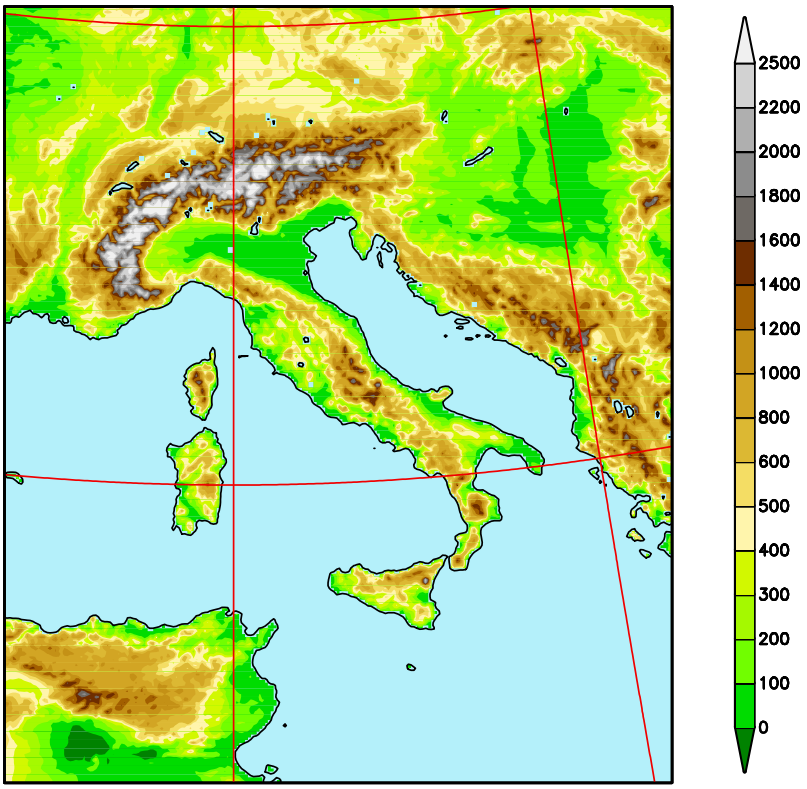

Figure 8: *Orography of the LM integration domain used at ARPA-SMR*

Domain Size	234 x 272 gridpoints
Grid Spacing (horizontal)	0.0625° (7 km)
Number of Layers	32
Time Step and Integration Scheme	40 sec, 3 timelevel split–explicit
Forecast Range	48 hrs
Initial Time of Model Runs	00 UTC
Lateral Boundary Conditions	Interpolated from GME at 1 hour intervals
Initial State	Interpolated from GME, initialization by DFI scheme
External Analyses	None
Status	Preoperational since 1 Feb 2000
Hardware	CRAY T3E (using 64 of 256 processors)

Figure 9: *Configuration of the LM at ARPA-SMR*

5.2 DWD (Offenbach)

Basic set-up of LM

The LM is run operationally at DWD using a 7 km grid spacing and 35 vertical levels. The rotated lat-lon coordinates of the lower left and of the upper right corner of the integration domain are $(\lambda = -12.5°, \phi = -17.0°)$ and $(\lambda = 7.75°, \phi = 3.25°)$, respectively. Figure 10 shows the orography of this model domain. The main features of the model set-up are summarized in Figure 11.

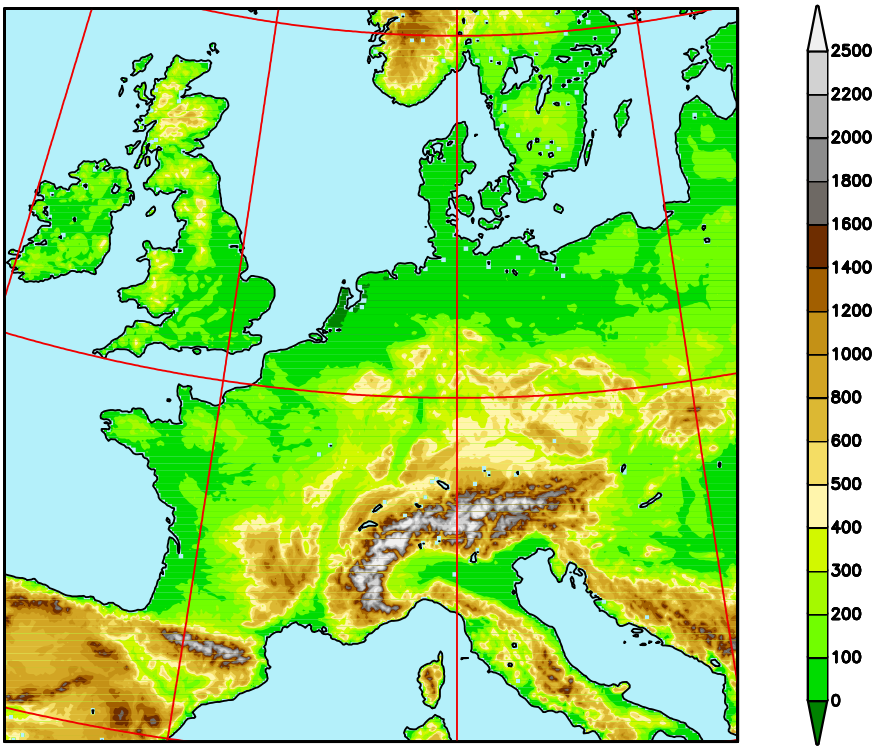

Figure 10: *Orography of the LM integration domain used at DWD*

Domain Size	325 x 325 gridpoints
Grid Spacing (horizontal)	0.0625° (7 km)
Number of Layers	35
Time Step and Integration Scheme	40 sec, 3 timelevel split−explicit
Forecast Range	48 hrs
Initial Time of Model Runs	00 UTC, 12 UTC, 18 UTC
Lateral Boundary Conditions	Interpolated from GME at 1 hour intervals
Initial State	Nudging data assimilation cycle, no initialization
External Analyses	SST (00 UTC), snow depth (00, 06, 12, 18 UTC) variational soil moisture analysis (12 UTC)
Status	Operational since 1 Dec 1999
Hardware	CRAY T3E (using 400 of 812 processors)

Figure 11: *Configuration of the LM at DWD*

Data Assimilation

At DWD, a comprehensive data assimilation system for LM has been installed. Besides the analysis by observational nudging, three external analyses are run: a sea surface temperature (SST) analysis (00 UTC), a snow depth analysis (00, 06, 12 and 18 UTC) and a variational soil moisture analysis (00 UTC), which was brought into operations in March 2000.

The data assimilations for the models GME and LM proceed as parallel streams which are coupled only via the boundary data: the GME forecasts from the global data assimilation to generate a first guess for the intermittent GME OI analysis scheme are used to generate LM boundary data for the continuous nudging assimilation stream of LM (see Fig. 12).

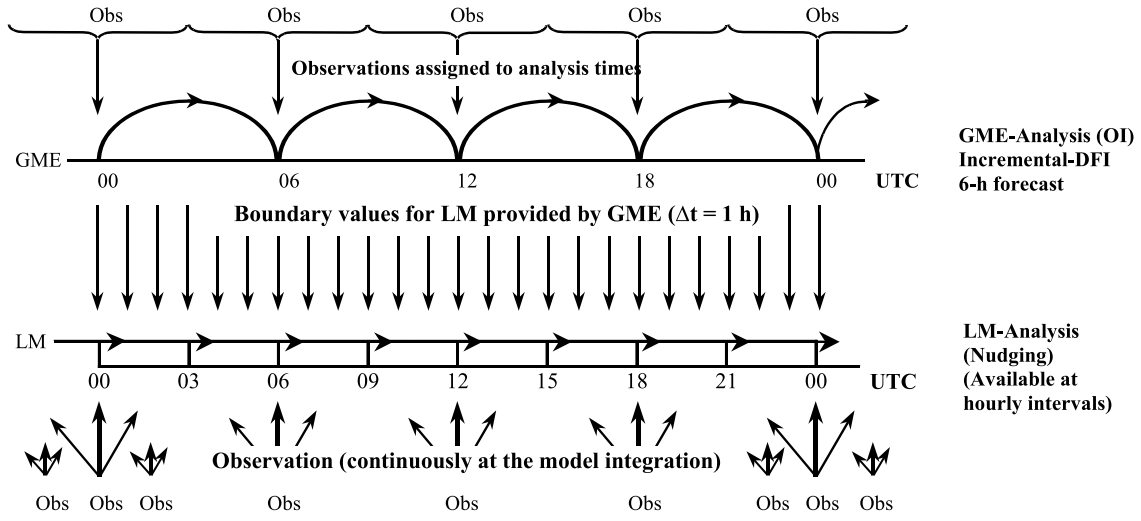

Figure 12: *4-D data assimilation for GME and LM*

Operational schedule

The operational schedule is structured by data assimilation for GME every six hours, i.e. for 00, 06, 12 and 18 UTC. However, the LM data assimilation is implemented with a continuous cycle of 3-hour assimilation runs. GME is first started with a short data cut-off time of 2 h 14 min to run a 78 hours prediction (early run) both for 00 UTC and 12 UTC. The forecast from this early run offers boundary values for the LM forecast. When the LM forecast has completed, the main runs of GME are started with 3h 40 min data cut-off time to achieve a 174 h forecast. Another 48 h prediction of both models is performed at 18 UTC with a data cut-off time of four hours. Besides the forecast models, a wave prediction suite comprising a global and a local sea state model (GSM and LSM) is run operationally. Figure 13 gives an overview of the operational schedule.

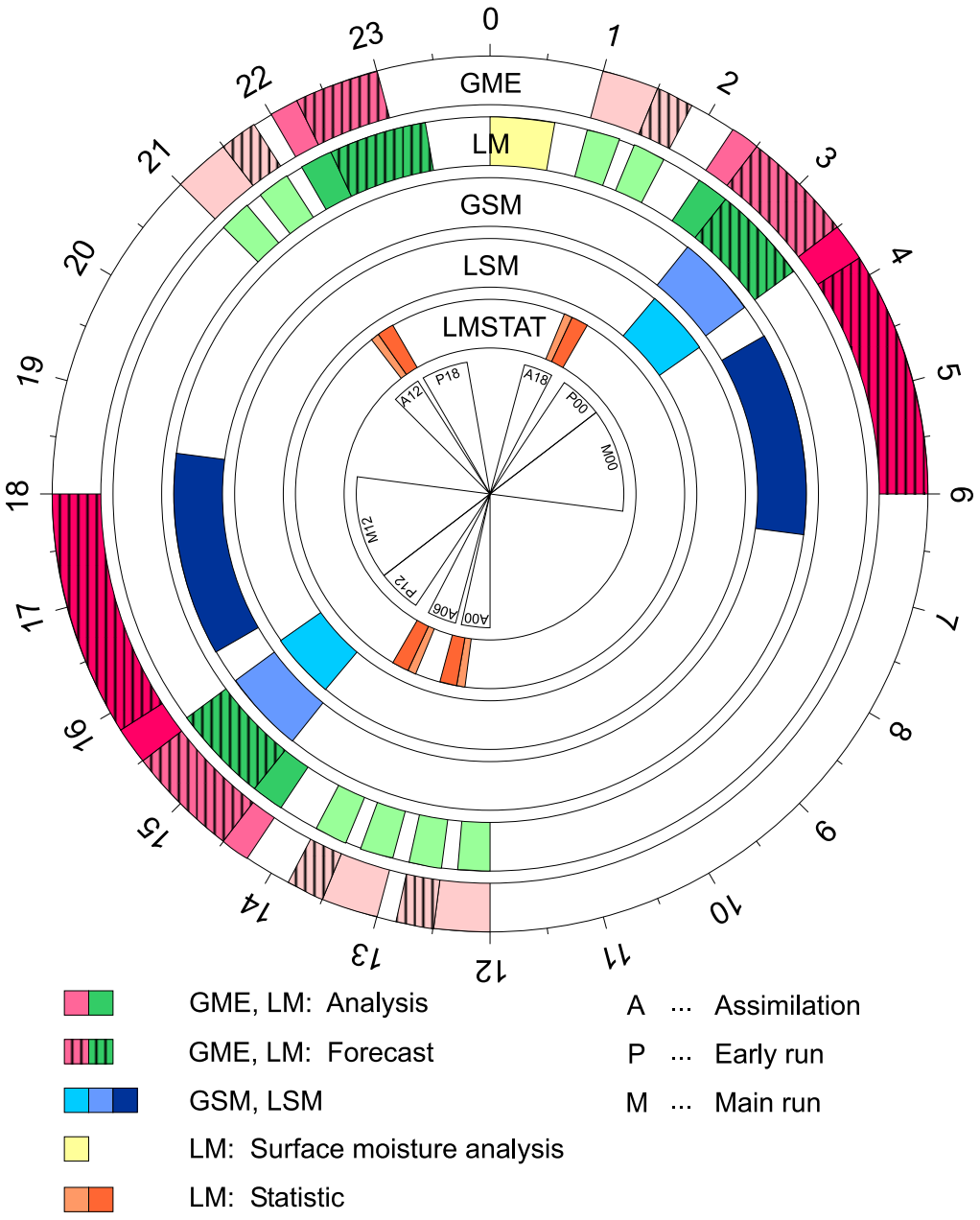

Figure 13: *Operational timetable of the forecast models GME, LM, GSM and LSM at DWD*

Computer System

A powerful *Cray T3E 1200* distributed memory MPP (massively parallel processors) system is the main number cruncher at DWD. This computer consists of 792 application PEs (processing elements, 20 with 0.5 GByte, 772 with 128 MByte of memory), 12 command PEs, and 12 operation PEs. Each PE has a nominal peak performance of 1.2 GFlop/s (floating point operations per second); for typical NWP programs a sustained speed of nearly 64 GFlop/s has been realized using all application PEs. Programmes running on the Cray T3E use standard MPI (message passing interface) routines to exchange data between the processors.

A *SGI Origin 2000* system with 2 x 16 processors, 16.4 GByte memory and 2337 GByte disk space (configured as fail-save RAID system) is used as data server. All observations (BUFR code) and model results (GRIB1 code) are stored in huge *ORACLE* data bases. For example, one GME forecast run up to 174 h produces more than 12 GByte of data, and one LM forecast up to 48 h about 5 GByte. The daily NWP production exceeds 40 GByte of data. Archiving of the NWP data is based on *AMASS* (Archival Management and Storage System) with about 75 TByte of data on REDWOOD cassettes. Most pre- and post-processing, like observation decoding and graphics, is performed on so-called 'operational servers', a *SGI Origin 2000* system with 8 + 14 processors and 6.1 + 7.9 GByte of memory. Figure 14 gives an overview of the hardware configuration at DWD.

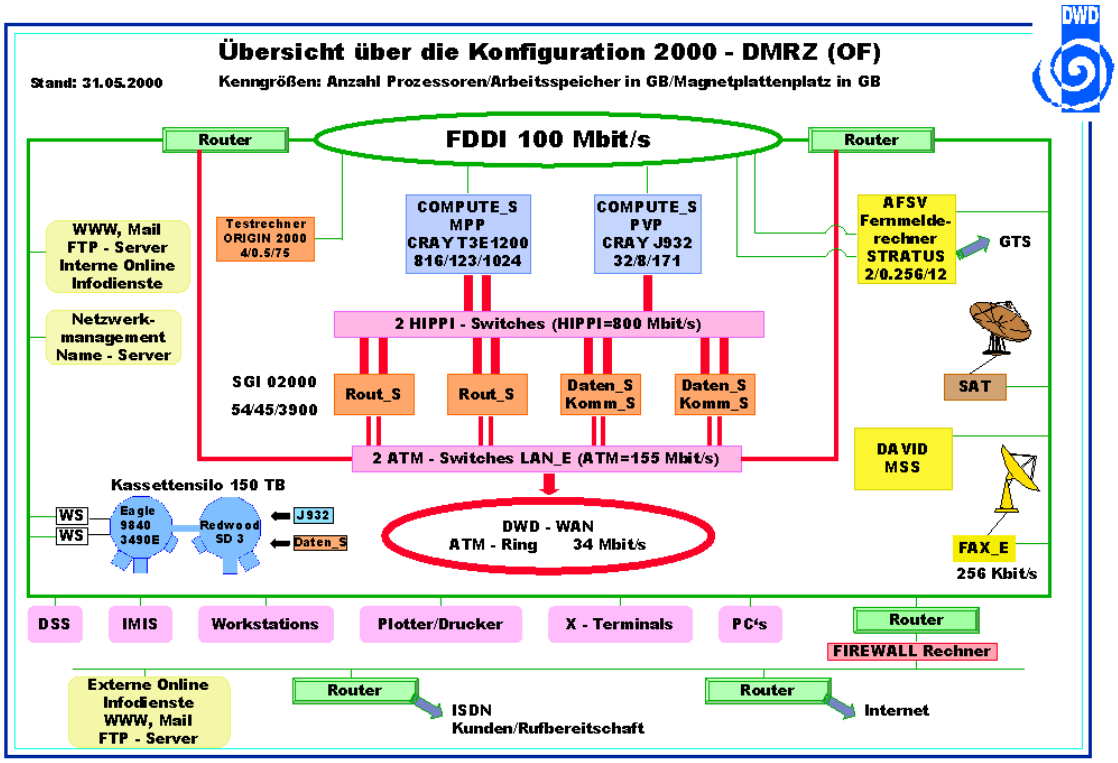

Figure 14: *Present configuration of hardware at DWD*

5.3 HNMS (Athens)

The national meteorological service of Greece, HNMS in Athens, operates the LM in a pre-operational mode at 14 km grid spacing. The rotated lat-lon coordinates of the lower left and of the upper right corner of the integration domain are $(\lambda = 4.5°, \phi = -24.0°)$ and $(\lambda = 16.25°, \phi = -10.0°)$, respectively. Figure 15 shows the orography of this model domain. The main features of the model set-up are summarized in Figure 16.

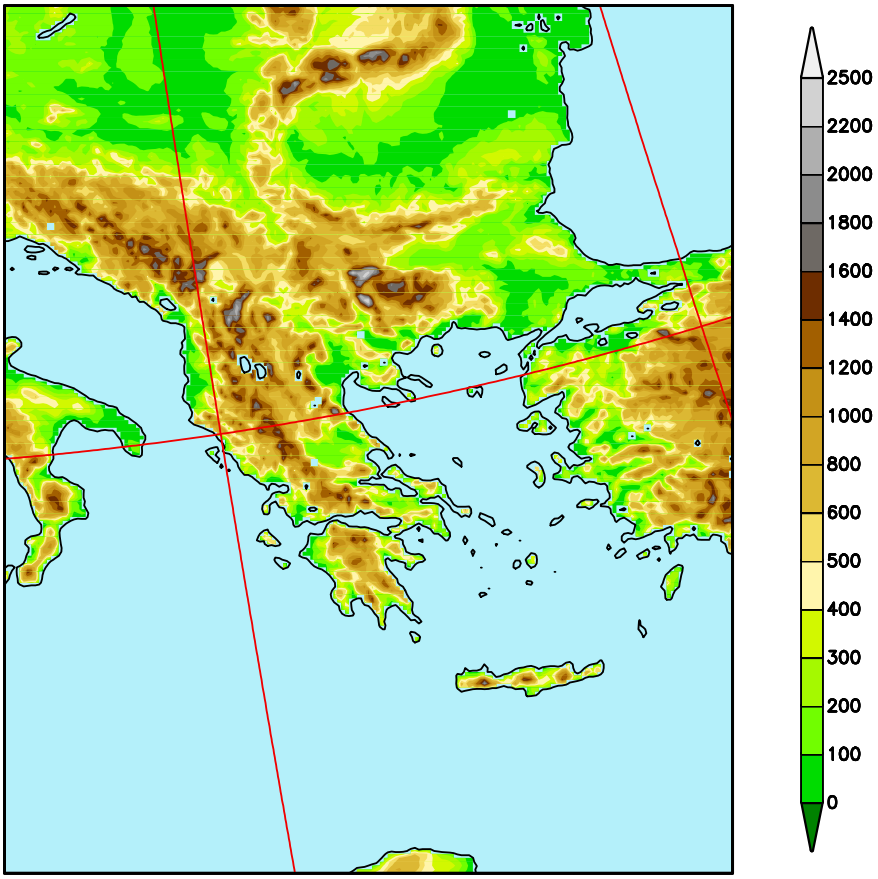

Figure 15: *Orography of the LM integration domain used at HNMS*

Domain Size	**95 x 113 gridpoints**
Grid Spacing (horizontal)	**0.125° (14 km)**
Number of Layers	**35**
Time Step and Integration Scheme	**80 sec, 3 timelevel split−explicit**
Forecast Range	**48 hrs**
Initial Time of Model Runs	**00 UTC**
Lateral Boundary Conditions	**Interpolated from GME at 1 hour intervals**
Initial State	**Interpolated from GME, initialization by DFI scheme**
External Analyses	**None**
Status	**Preoperational since 1 Feb 2000**
Hardware	**CONVEX (using 14 of 16 processors)**

Figure 16: *Configuration of the LM at HNMS*

5.4 MeteoSwiss (Zürich)

(E. Zala, MeteoSwiss)

The Lokal-Modell runs on a NEC SX5 placed at the Swiss Centre for Scientific Computing (CSCS) in Manno. During the operational forecasting slots the SX5 enters dedicated mode: 6 CPUs are then reserved for the model integration, 1 for the interpolation of the initial and lateral boundary fields provided by DWD. The operational suite is steered by the LM Package. This is a set of scripts running on SUN workstations.

Operational integration domain of LM

The domain extends from 35.11 N -9.33 E (lower left) to 57.03 N 23.41 E (upper right). This domain is covered by a grid of 385x325 points with a horizontal resolution of 7 km (see Figure 17). The borders are placed prevalently over sea in order to reduce negative interferences generated at the transition zone of the orographies of the driving model (GME) and LM.

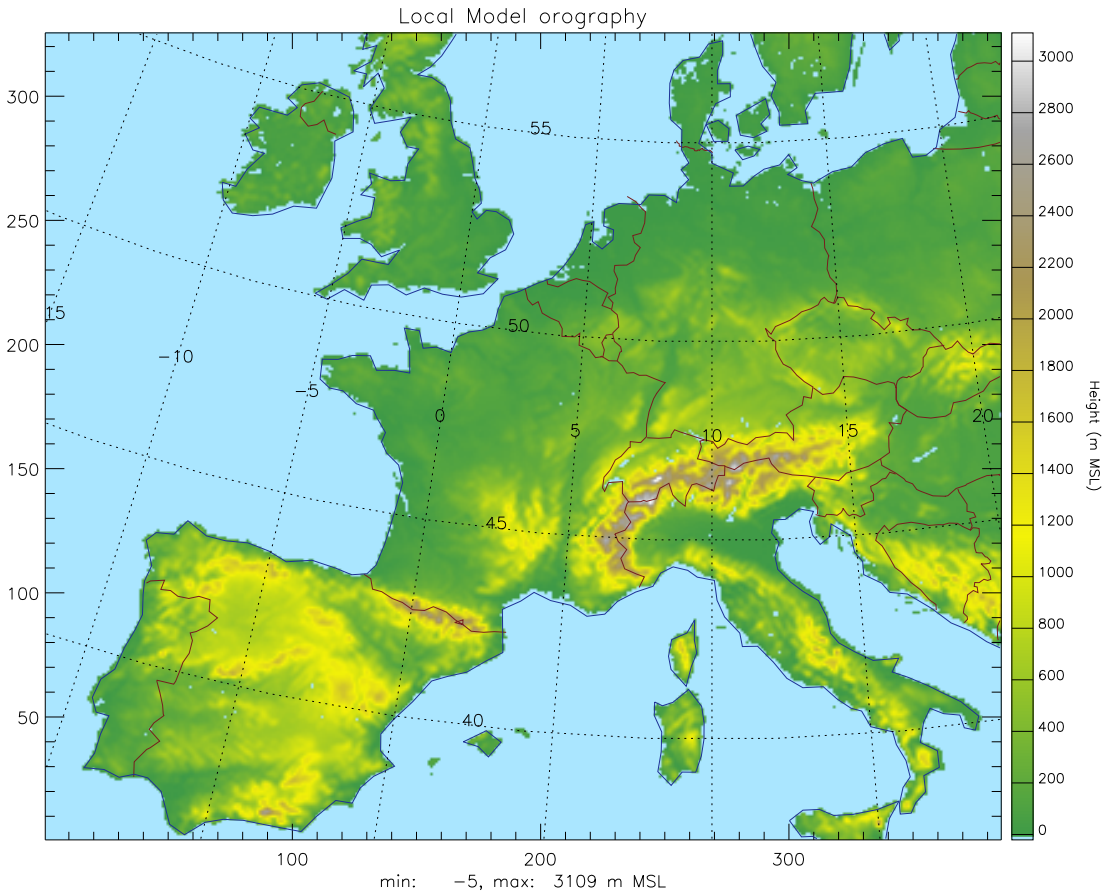

Figure 17: *LM integration domain used at MeteoSwiss*

Vertical coordinates

In operational mode the model runs with 45 levels vertically distributed as shown in Figure 18.

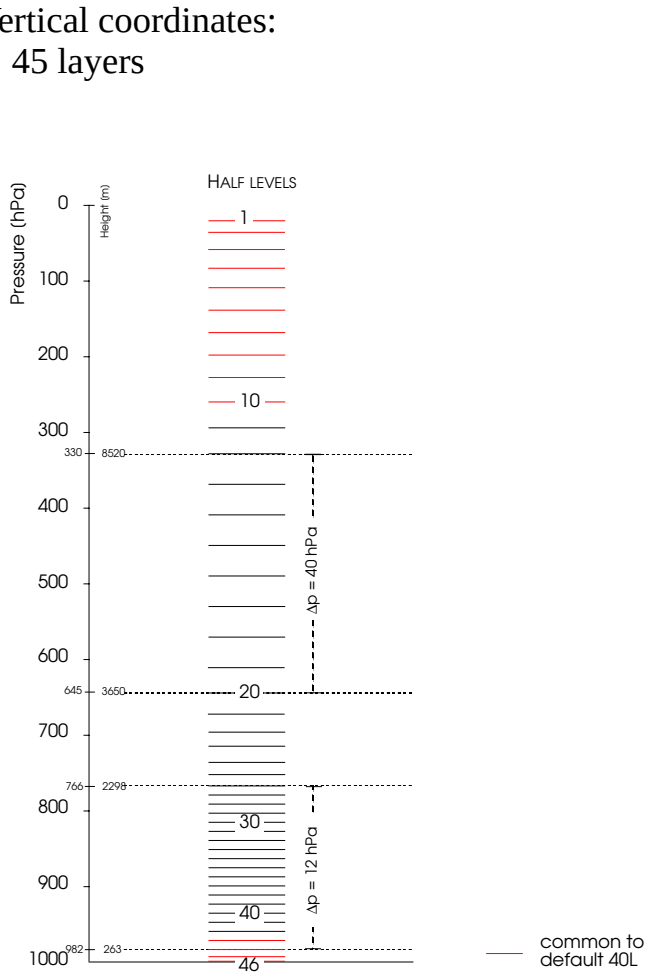

Figure 18: *Vertical distribution of levels used at MeteoSwiss*

Hardware and communications
The computational work of the LM suite is managed by 3 systems:

- SUN E3000 at Meteo Swiss (conduct, dissemination)
- SUN E6000 at CSCS (postprocessing)
- NEC SX5 at CSCS (GME2LM, LM, LPDM)

Figure 19 shows the present configuration of hardware and communication used for the operational application of LM.

Data flow
Figure 20 sketches the dataflow of the operational system.

LM package
The operational suite is driven by "LM Package", a software developed at Meteo Swiss. It has a modular structure and is composed by 50 C-shell scripts. It can be executed in three different modes: operational, test and personal mode. In operational mode preprocessing, LM and postprocessing are running concurrently; warnings and exits are transmitted to operating which has the possibility of manual intervention.

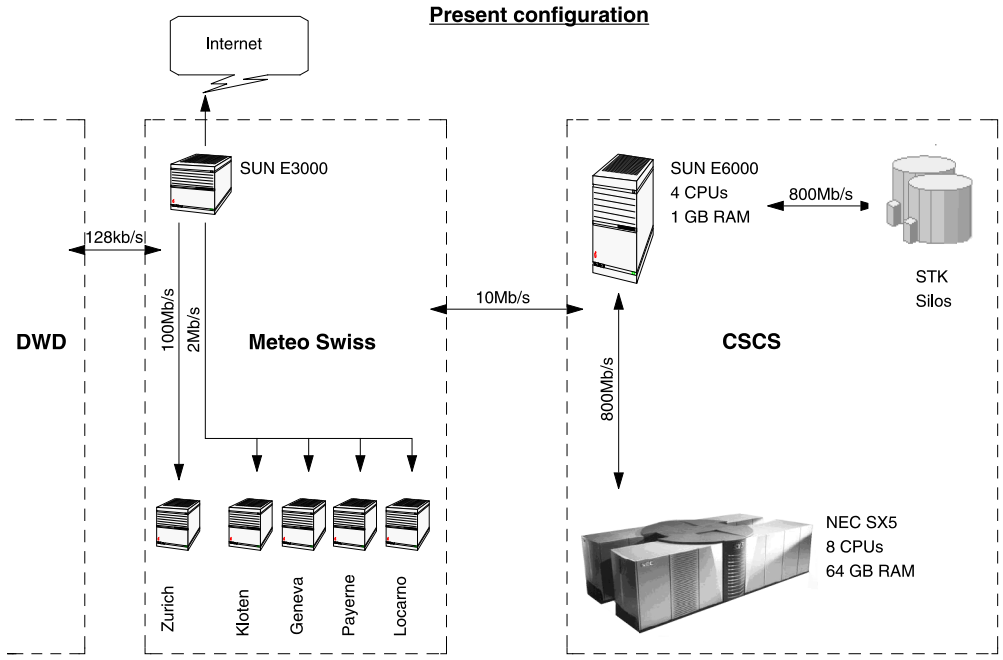

Figure 19: *Present configuration of hardware and communications at MeteoSwiss*

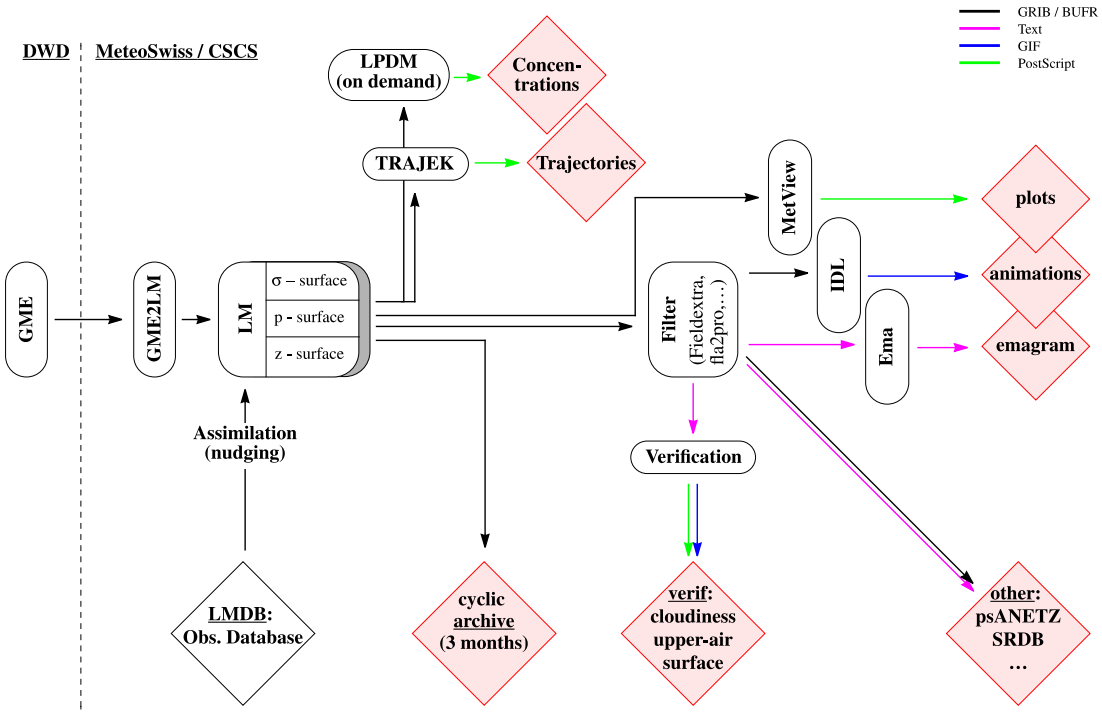

Figure 20: *Dataflow of the current operational system at MeteoSwiss*

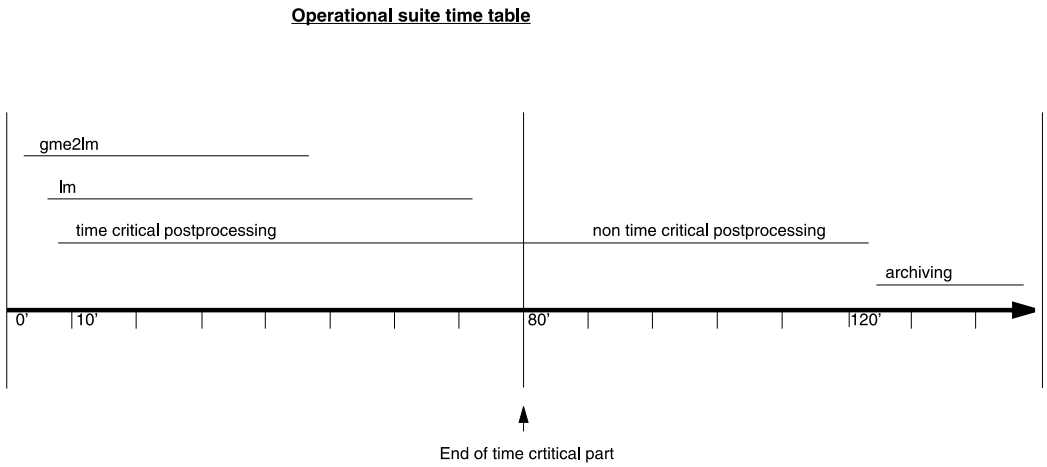

Figure 21: *Time table of the operational suite at MeteoSwiss*

Products
- 2-D plots: produced by MetView every 6 hours
- Animations: Hourly loops produced with IDL
- Tables, extracts of the model output in different formats
- Trajectories
- Concentrations from LPDM module

Time table
The postprocessing is divided into a time critical and a non time critical part (see Figure 21). During the first part the crucial products for Meteo Swiss internal clients (mainly forecasters) are generated and disseminated. During the second part the remaining products for internal and external clients are created. Archiving and statistics take place at the very end of the task.

Verification
The output of the Model undergoes three different types of verification:

- Surface verification: The surface parameters are compared to measurements taken by synoptical and automatic stations.
- Upper air verification: verification of the model against measured radiosonde ascents
- Cloud verification: verification of the model cloudiness based on METEOSAT visible images

6 Changes to the Model System

In this section, important changes to the LM-system which have been introduced during the last year are briefly described, and the possible impact on the forecast products are summarized. Of course, changes in the host model GME can also have a significant impact on the LM forecasts. For changes to GME and its data assimilation, please refer to the *Quarterly Report of the Operational NWP-Models of the Deutscher Wetterdienst, No. 22-25* (available at www.dwd.de).

6.1 Major Changes to LM

During 2000, there have been a number of correction updates of LM. But also a few more significant changes to the model code have been introduced.

The operational model integration for the Lothar storm on Christmas 1999 resulted in a crash due to a numerical instability. A rerun of the model with a reduced time step of 30 sec (instead of 40 sec) proved to be stable. This time step, however, is much smaller than that estimated from the advective CFL criterion, i.e. $\Delta t < \Delta x/v_m$, where Δx is the horizontal grid spacing and v_m is the maximum horizontal wind velocity in the domain. The standard 40 sec time step at 7 km grid spacing is estimated by assuming a maximum velocity of about 125 m/s. For the Lothar case, the wind velocities increased up to about 12 m/s and the standard time step should had guaranteed a stable integration, but failed.

A large number of possible reasons for this instability have been investigated and finally the simultaneous treatment of horizontal diffusion and advection was shown to be responsible. The simultaneous time integration of the diffusion and advection terms results - in combination with the Asselin time filtering - in a modified CFL criterion with a significantly reduced stable time step at high wind velocities. In order to run the model close to the advective stability limit, the time integration scheme has been changed: Horizontal diffusion is now treated by Marchuk time-splitting at the end of the time step. The prognostic equations are integrated in time as before except that the tendency from horizontal diffusion is omitted from the total tendencies. This results in provisional values of the variables at time $t + \Delta t$.These are then used as starting values to integrate the time tendency of diffusion separately over the time interval to give the final values of the prognostic variables at time $t + \Delta t$.

Such a time split integration proves to be stable if each of the sub-steps is stable for a given time step. Since the diffusion coefficient is chosen to guarantee stability (this is done automatically during model set-up), the stability depends now only on the first integration step. And for this sub-step, the stable time step is given by the advective CFL-criterion. Thus, by splitting horizontal diffusion in the time integration, the model can now be run close to the advective stability limit: the Lothar case could be integrated with no problems at all using a 40 sec time step.

Much work was invested in a basic redesign of the code. The new version has a strongly increased modularity. This allows for faster compilation of the code. Also, due to the reduced interdependency of the modules, the simultaneous work on the code by different groups has become much more easy. Within the nudging module, a large number of both technical and scientific changes have been introduced.

The standard mass-flux convection scheme has been modified to enable a horizontal averaging of the forcing functions of convection (i.e. surface moisture flux, moisture convergence and vertical velocity). This results in a slightly smoother spatial distribution of convective precipitation over mountainous regions with strongly reduced peaks in the precipitation

amount. The area mean total precipitation, however, is nearly unaffected.

Table 4: *Software changes to LM*

Date	Changes	Version
01.07.1999	More complete use of multi-level observations.	1.31
10.12.1999	Changes in the organization of the program (Part I).	1.34
24.02.2000	Adaptations of observation processing to comply to the new 32-bit AOF file format; introduction of ACAR reports, a new type of aircraft observations, in the nudging observation processing.	1.36
24.03.2000	Changes in the time integration scheme to allow larger time steps for wind speeds close to the CFL stability limit; modification of the CAPE-type closure condition in the convection scheme and correction of CAPE calculation.	1.37
06.04.2000	Extended quality control of observations; adaptions to the new surface layer parameterization; modifications to VOF (verification observation file) output.	1.38
03.05.2000	Changes in the organization of the program (Part II); introduction of the possibility to use asynchronous I/O.	1.39
04.08.2000	Switch to cycle 2	2.1
18.08.2000	Update of the new turbulence and surface layer scheme; introduction of a switch to use horizontally averaged forcing functions for the convection scheme.	2.2

6.2 Major Changes to GME2LM

The interpolation program GME2LM has been rewritten in large parts and is now fully parallelized using MPI. Table 5 summarizes the changes to the GME2LM code.

Table 5: *Software changes to GME2LM*

Date	Changes	Version
02.12.1999	Normalization of the climatological water content with the pore volume.	1.4
15.12.1999	Significant correction update.	1.6
30.11.2000	Introduction of possibility for parallel asynchronous IO; introduction of possibility to filter the orography; optimizations for vector processing.	1.7

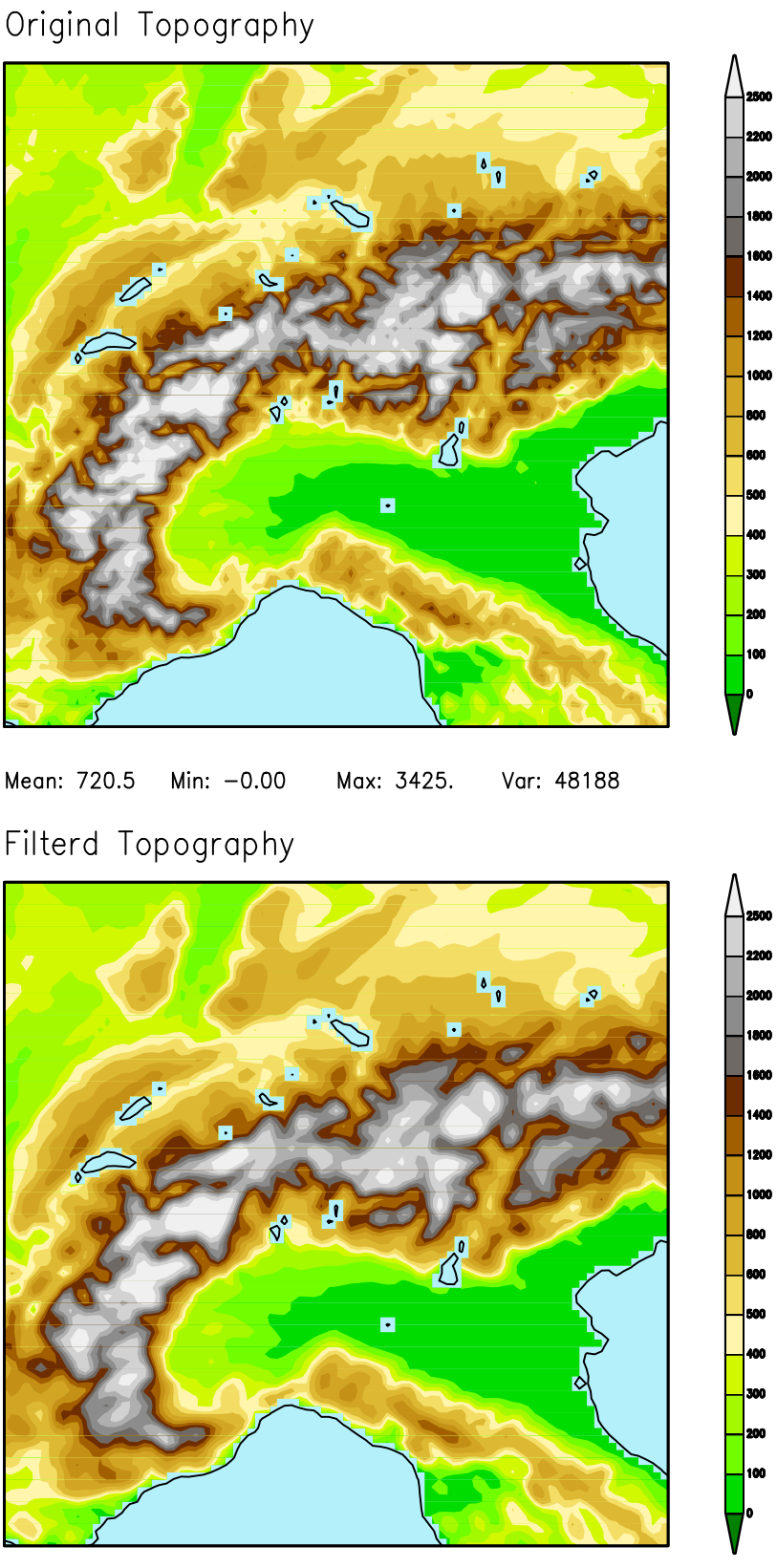

Figure 22: *LM topography for the Alps at 7 km resolution. Top: original topography; bottom: filtered topography*

6.3 Changes to Model Configurations at COSMO Centres

During early spring 2000, all meteorological centres running the LM have switched to the new files of external parameters which are now based on the CORINE and GTOPO30 datasets. Other changes to the operational model configurations are indicated below.

December 1999
Reduction of the integration time step from 40 sec to 30 sec at DWD because of a model instability for the Lothar Christmas storm.

January 2000
Eastward extension of the LM-integration domain at HNMS to include the island of Rhodos.

April 2000
Increase of the integration time step from 30 sec to the former 40 sec at DWD. A change in the model time integration (use of additive splitting for horizontal diffusion) now guarantees stability at high wind speeds.

July 2000
Start of the quasi-operational integration of LM in parallel to the old hydrostatic model SM at MeteoSwiss.

November 2000
Use of a weakly filtered orography in the preoperational suite at MeteoSwiss. The 10th order Raymond filter with filter parameter $\epsilon = 0.1$ is used; $2dx$ and $3dx$ wavelength components are removed by this filter, whereas $4dx$ components are almost untouched. Fig. 22 compares the orography in a subdomain including the Alps for both cases. Also, the optional horizontal averaging of convective forcings has been switched on.

December 2000
Use of a weakly filtered orography (as at MeteoSwiss, the 10th order Raymond filter with filter parameter $\epsilon = 0.1$ is used) in the operational production at DWD. A cold start of the LM (i.e. a start from an interpolated GME analysis) was necessary to get the new orography into the continuous data assimilation cycle.

7 COSMO Meetings and Events

This section summarizes the main meetings, workshops and seminars as well as management decisions from the previous year. Other COSMO activities such as guest scientists and internal visits are also considered. Finally, an overview of the forthcoming activities in the present COSMO working period is given.

7.1 Meetings in 2000

(1) Meeting of the COSMO Steering Committee

The COSMO Steering Committee (M. Capaldo, D. Frühwald, G. Sakellaridis, headed by J. Ambühl) and the Scientific Project Manager (SPM, G. Doms) met at MeteoSwiss in Zürich at 24 January 2000. The proposed work plan for Oct.1999 - Oct.2000 - as prepared by the work package coordinators - was assessed and revised. The final work plan was then formulated by the SPM and has been distributed. Besides a number of other business issues, the discussion of the draft COSMO agreement was a central point of the meeting. Minutes of the meeting have been formulated and circulated by J. Ambühl.

(2) COSMO Workshop on Verification

The members of the working group for verification met at 14-15 February 2000 in Bologna at ARPA-SMR for the first internal COSMO workshop on verification.

During the first part of the workshop the verification scores of the different LM forecasted parameters and the activities performed so far have been shown. Seventeen WPs are present in the 'WG5 Verification' and most of them have been found to be in a good status of advancement. Some others have just been started. The different WPs and the main results obtained so far have been presented and discussed.

After the first part, a detailed discussion of the techniques and methods used to achieve the LM verification has followed. The group believed that it is necessary to define a minimum common agreement for the verification of some surface parameters (precipitation, 2m-temperature, cloud coverage) within the COSMO community. This common agreement will allow to compare results of the verification performed in the different geographical areas. During the meeting the group also stressed the importance to evaluate skill scores (against persistence forecast, for example) and not only 'absolute' indices for the different parameters simulated by the model.

Finally the group stressed the importance to achieve a stratification for 'weather regimes' in order to discriminate the scores of LM forecast for each regime. These weather regimes can be different for each region and differently defined using subjective or objective classification criteria.

A detailed workshop report has been prepared by C. Cacciamani. It includes the minutes of the meeting, the common agreement on the methods for the verification of surface weather elements and result reports of the various work packages. The report has been distributed and will also be available on our web-site.

(3) COSMO Seminar on Step-mountain Type Vertical Coordinates

A seminar on various z-coordinate approaches for high-resolution modelling was held at DWD (G) in Offenbach, 7 March 2000. The participants (J. Steppeler, H.W. Bitzer, L.

Bonaventura, M. Minotte, D. Cesari, E. Minguzzi, M. Refene, G. Doms and U. Schättler) discussed problems of different methods. A work plan for the implementation of the z-coordinate in a simplified 2-D version of LM was elaborated.

(4) Meeting of the Work Package Coordinators

The work package coordinators (WPCs, i.e. C. Schraff, J. Steppeler, M. Arpagaus, C. Cacciamani and U. Schättler), the scientific project manager (SPM, G. Doms) and the head of the Steering Committee (J. Ambühl) met at DWD on the 15th of June. The purpose of this meeting was to discuss the progress in the work packages, to identify problems in specific aspects and to elaborate remedies.

Most of the work packages (WP) with top priority were found to be in good progress. For time-critical WPs as well as for severe technical problems, a short-term plan of action was formulated. WPs that had a significant delay were identified and put on the list for the next working period. Also, some basic model deficiencies, as seen from verification results, were identified and proposals for corresponding new WPs were made. Finally, the basic goals for the next COSMO period have been discussed. The minutes of this meeting have been distributed by email.

(5) Seminar on Scientific Application of the LM

This seminar was held at DWD in Langen, 26-28 June 2000. It was dedicated to research activities with the LM at various universities and had a more educational purpose. Proceedings of the seminar will be published by DWD (in German language). For questions about the program and the proceedings, please contact Jürgen Steppeler.

(6) COSMO Workshop on Numerical Methods

The COSMO numerics group met at 27 September 2000 in Zürich (CH). The participants (J. Steppeler, J. Quiby, H.W. Bitzer, G. Doms, A. Gassmann and U. Schättler) discussed the current state of dynamics and numerics in European NWP models. J. Quiby gave an introduction on numerical activities within SRNWP and J. Steppeler reported on current numerical activities in COSMO. Crucial questions, such as the efficiency of semi-Lagrangian schemes for nonhydrostatic modelling and problems in very high resolution simulation of mountain flow systems have been addressed. Also, problems of a more long-term interest, such as conservation form of the equations, adaptive meshes and global nonhydrostatic modelling have been discussed. The minutes of this internal workshop are available on the COSMO web-site (member area).

(7) Annual Scientific Meeting of the COSMO Consortium

The recent COSMO general meeting was held in Zürich (CH), 28-30 September 2000. In the first (scientific) part, the work package coordinators gave an overview on progress in the various research and development activities of the working groups and talks on selected issues were given by the responsible scientists. Summaries of the talks including the slides are currently selected to be presented on our web-site.

The second (internal part) of the meeting was dedicated to formulate the research plan for the next period (Oct 2000 - Oct 2001). Proposals for the work packages have been elaborated in parallel workshops and thereafter discussed in the plenum. The participants agreed on the three basic goals for the next working period (Oct 2000 - Oct 2001).

- ***Consolidation and upgrade of the LM operational systems***
  - tuning and optimization for both model and data assimilation components
  - operational use of the new physics package
  - experimental work on the meso-γ scale
  - continue work on the z-coordinate model version
  - resume development work on 2-way interactive self-nesting

- ***Application and Interpretation as a new Working Group***
  - interpretation of high-resolution forecasts using statistical methods
  - installation of a LAM ensemble prediction system based on LM
  - common postprocessing tools

- ***Improvement of the internal and external communication***
  - installation of a COSMO web-site (www.cosmo-model.org) for external presentation and internal exchange and documentation
  - publications and participation in international projects
  - publishing COSMO Newsletters and Technical Notes

Provisional work plans have been set-up along these guidelines by the working groups. The last part of the meeting was dedicated to a general strategic discussion. Minutes of this discussion are also available on our web-site.

(8) Meeting of the COSMO Work Package Coordinators

The WPCs (C. Schraff, J. Steppeler, M. Arpagaus, C. Cacciamani and U. Schättler) and the SPM (G. Doms) met at DWD in Offenbach, 24 November 2000. The purpose of this meeting was to discuss and assess some discrepancies in the provisional work packages and to prepare the final form of the COSMO work plan. A number of additional proposals for the Steering Committee have also been formulated. The main results of this meeting are summarized below.

- ***Z-coordinate model version***
  Since the development of the z-coordinate version of LM is time-critical, a detailed work plan for this work package (WP 2.5), including the rewriting of the dynamical core, the definition of external parameters, the interpolation program for initial and boundary conditions and the formulation of the physics has been elaborated.

- ***LM-update procedure for larger changes to the system***
  A number of aspects concerning a common update procedure have been formulated. A central and crucial point is the set-up of a parallel suite with a parallel verification system. Three strategies for test environments and their implications have been discussed and a time schedule including the implementation of technical components has been set up. These are:

  – Test suite for single cases at ECMWF
  – Test suite for fixed time periods with data assimilation at ECMWF
  – Parallel test suites at DWD and MeteoSwiss

  A central requirement for this test environments is a common verification system or an agreement on methods and common products such that partners can rely on the verification scores of one centre. The items related to verification will be discussed in detail at the upcoming verification workshop in Bologna.

- ***SRNWP test cases***
  We agree that the COSMO group should actively take part in the SRNWP community. Therefore, a new Work Package in WG2 has been added (WP 2.11: Evaluation of the LM dynamical core using the SRNWP test cases)

- ***COSMO Web-site (www.cosmo-model.org)***
  The basic structure of the public part of the COSMO web-site has been defined. Also a proposal for the internal part, the member area, was formulated. Both proposals will be assessed by the Steering Committee.

- ***Reporting Cycles***
  The COSMO-agreement plans regular reporting cycles to inform the WP coordinators and the SPM on the progress of work, where the SPM has to define the intervals. The SPM and the WP coordinators agreed on a quarterly reporting cycle.

- ***COSMO Technical Reports***
  We plan to have a COSMO series named 'Technical Reports' to document scientific research, technical changes and bigger changes to the model system at non-regular intervals. The series is mainly for internal use, but also to document progress to other groups.

- ***COSMO Newsletters***
  At the SRNWP meeting in Toulouse (October 2000) the SPM was encouraged to initiate an annual report of the COSMO group - as already exists for the other European NWP groups. This is lot of additional work, but we agreed on an annual report named 'COSMO Newsletter' containing information on recent changes to the model system, a review of the operational system, a summary of our meetings, a summary of verification results and interesting scientific work. A table of contents for the first issue was formulated.

- ***Missing Work Packages***
  We decided to add two work packages in WG 2. These are:
  WP 2.12 Check of the LM water mass budget, and
  WP 2.13 Tuning of basic dynamics.

A more detailed protocol of the WPC-meeting has been formulated by the SPM which was submitted to the StC and the WPCs. These minutes are also available from the member area of our web-site.

(9) Meeting of the COSMO Steering Committee

The fifth meeting of the COSMO Steering Committee was held in Zürich at MeteoSwiss on 28 November 2000. The SPM (G. Doms) presented the work plan for upcoming COSMO period and summarized the main results and proposals from the WPC meeting (see above). All work packages have been accepted with a few modification. The final form will be available at the member area of our web-site. Also, the other proposals from the WPC meeting have been accepted.

The draft agreement for COSMO is still under discussion. Some modifications have to be added for legal reasons. The final version of the agreement is expected early 2001.

The IMGW (Institute of Meteorology and Water Resource Management) of Poland will be a new member of COSMO. Prof. Dr. Jan Zielinski from IMGW received on the 13.10.2000 a letter from the StC chairman confirming the acceptance of the four COSMO core partners.

The Steering Committee of COSMO will enter in contact with the Polish Meteorological Institute after the signature of the agreement by the four core partners.

The Steering Committee decides to start the new COSMO Working Group 4: Interpretation and Applications. The responsible work package coordinator for this group will be Dr. Pierre Eckert (Pierre.Eckert@meteosuisse.ch or pek@sma.ch) from MeteoSwiss.

The Steering Committee decides, on the recommendation of the respective Directory Boards of the Partners, to elect Dr. Massimo Capaldo from UGM as its chairman for the period 2001-2002.

7.2 Guest Scientists

Luca Bonaventura from the University of Trento (Italy) stayed at DWD as a guest scientist for three weeks in February/March and for one week in September 2000. During his first visit, the concrete work on the new z-coordinate was started. At the second visit, specific numerical questions related to the shaved element discretization have been addressed.

In November 2000, Zavisa Janjic from NCEP (Washington, USA) stayed for four weeks as a guest scientist at DWD. Several points where improvements for the LM could be made have been addressed and worked on by Z. Janjic. These points were:

- the conversion between kinetic and potential energy,
- the non-cancellation instability of the potential enstrophy conserving scheme used for horizontal advection of momentum,
- the advection of passive scalars
- the two time-level scheme
- PBL and surface layer schemes

Also, a number of experimental integrations with the SAM nonhydrostatic model (developed within the Serbian Academy of Sciences) were made and compared to the corresponding runs with LM. Moreover, considerable additions and modifications have been suggested concerning the draft of a review paper on numerical methods (planned by J. Steppeler et al.) used in nonhydrostatic models. A detailed report on the work done during this visit will be prepared for the member area of the COSMO web-site.

For next year it is planned to have Jack Kain (NSSL, Norman, USA) as a guest scientist at MeteoSwiss for final implementation and tuning of his convection scheme. DWD plans to invite Louis Wicker (NSSL, Norman, USA) for implementation and testing of his new two-time level integration scheme.

7.3 Internal Visits

During spring 2000, J. Papageorgiou from HNMS visited DWD two times for a couple of days. He will take over the work package on 2-way interactive nesting from J. Rissmann who left DWD.

J. Steppeler and U. Schättler visited L. Bonaventura at the University of Trento (Italy) from 5-9 June. The visit aimed at the definition of a strategy for the implementation of the new z-coordinate system in LM using shaved element finite-volume discretization and the set-up of analytical test cases. Also, a more close cooperation on C-grid triangular elements was agreed on. On the 9th of June, D. Cesari from ARPA-SMR and E. Minguzzi from SMR-Piedmont joined this meeting. The two Italian regional meteorological centres plan to contribute to the z-coordinate development and to testing by evaluating real cases (i.e., the Piedmont case and the Boulder case).

In spring and autumn 2000, M. Arpagaus from MeteoSwiss visited DWD. The current status, progress and problems in work packages in WG 3, which mostly reside at DWD, have been discussed.

J. Steppeler visited G. Papageorgiou and G. Sakellarides at HNMS in Athens from 20-21 November. Problems with the implementation of the 2-way nesting version as well as some numerical issues related to the z-coordinate version have been discussed.

7.4 Upcoming Events

The following COSMO workshops and meetings are planned for 2001. Some other meetings related to COSMO are also included.

March 22-23: COSMO-Workshop on Verification and Interpretation
at ARPA-SMR, Bologna (I)
Discussion on the status and problems of the activities in WG4 and WG5. A special point will be the definition of a common COSMO verification system to be installed at ECMWF. Pierre Eckert will prepare a draft agenda and circulate it in February.

April/May: Meeting of the Work-Package Coordinators
at DWD, Offenbach (D).
Discussion of the progress of WPs and preparation of the basic goals and a draft work plan for the next COSMO period. The SPM will invite for this meeting during spring.

May 21-23: Seminar on Scientific Applications of the LM
at DWD, Langen (D)
This seminar is dedicated to research activities with the LM at various universities and research institutes in Germany. Due to the interest of the COSMO group and other European countries, this year's seminar will be held in English language. For information on the seminar and the preliminary program, please contact J. Steppeler (juergen.steppeler@dwd.de).

September 24-26: 4th International SRNWP-Workshop on Nonhydrostatic Modelling
at DWD, Bad Orb (D)
The aim of the workshop is to provide a forum for information concerning all questions related to fine scale modelling. The special topic this year is "Numerical Techniques for Nonhydrostatic Modelling", but papers on all other topics are also welcome. Deadline for abstracts is 1 July 2001. For more information please contact Jürgen Steppeler (juergen.steppeler@dwd.de).

October 2: COSMO-Workshop on Numerical Methods
HNMS, Athens (GR)
Discussion on new numerics and dynamical cores. J. Steppeler will invite for this workshop during the year.

October 3-5: Annual Scientific Meeting of the COSMO Consortium
HNMS, Athens (GR)
Progress Reports from the Working Groups and presentation of results from the work packages; discussion and set-up of a scientific work plan for 2002.

October 8-12: 23rd EWGLAM and 8th SRNWP meeting
IMWG, Warsaw (Poland)
The status report of the COSMO Consortium will be given by G. Doms. The scientific topic of this meeting is *High Resolution Mountain NWP* and is strongly related to the MAP experiment. The COSMO group should be represented by one or two talks from WG2 and/or WG5.

November: Meeting of the Steering Committee
UGM, Rome (I)
Regular business meeting, revision of work packages and definition of the final COSMO work plan for 2002.

7.5 Announcements of other events

At the recent COSMO annual meeting we agreed to have more active participation at international conferences, workshops and seminars. This section lists a number of meetings which are of specific interest (besides the EWGLAM and SRNWP meetings already mentioned above). Of course, this list is by no means complete. But everyone of the COSMO scientists is strongly encouraged to submit contributions to these meetings (or other ones). For some events, participants from COSMO have already been found.

1st SRNWP Workshop on Verification
22-24 April 2001, De Bilt, Netherlands.

MAP Meeting 2001
14-14 May 2001, Schliersee, Germany (www.map.ethz.ch).
A. Gassmann and J. Steppeler will attend this conference.

SRNWP Workshop on Numerical Techniques
June of July 2001 in Bratislava, Czech Republic.
J. Steppeler intends to take part in this workshop.

8th Scientific Assembly of IAMAS
10-18 July 2001, Innsbruck, Austria (http://meteo.uibk.ac.at/IAMAS2001)

9th Conference on Mesoscale Processes
30 July - 2 August 2001, Fort Lauterdale, Florida (USA)

ECMWF Seminar on Key Issues in the Parameterization of Subgrid Physical Processes
3-7 September 2001, Reading, UK (www.ecmwf.int/services/training/index.html).
ECMWF has invited G. Doms to give a lecture on the role of parameterization in high resolution nonhydrostatic NWP models.

DACH Meteorologentagung 2001
18-21 September in Vienna, Austria (www.zamg.ac.at/~DACH2001)
G. de Morsier and A. Gassmann have submitted contributions.

HIRLAM/SRNWP Workshop on Soil Analysis and Soil Processes
Autumn 2001 in Madrid, Spain.

8 Verification and Diagnostics

This section summarizes some of the operational verification results for the LM forecasts at various COSMO meteorological centres. Also, recent research and development work on regional verification, new verification methods and diagnostical tools is considered.

8.1 Verification of Surface Weather Parameters

8.1.2 Operational Verification at DWD

(U. Damrath, DWD)

For objective verification of surface weather elements predicted by the LM running at DWD, the standard verification package of the research and development department is used. Verification scores are derived on a daily, weekly and monthly basis for various sets of SYNOP observation stations.

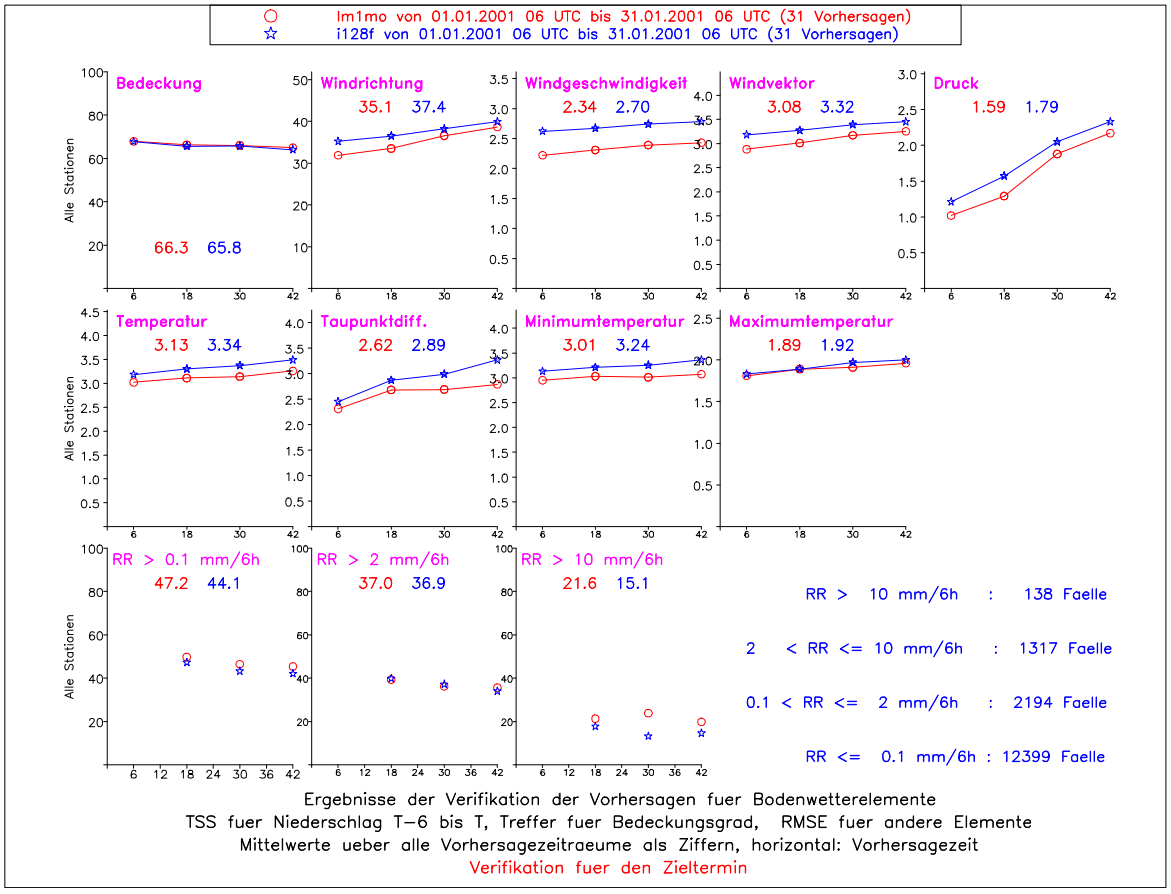

Figure 23: *Mean verification scores for January 2001 at 6 UTC as a function of forecast time (00,12,24,36 and 48 hrs). Red: LM, blue: GME. RMSE for all elements except for cloud cover (hit rate) and precipitation (TSS); numbers are mean values over all forecast times. Top: cloud cover, wind direction, wind speed, wind vector and surface pressure (from left to right). Middle: temperature, dew point difference, minimum and maximum temperature (from left to right). Bottom: 6 hr precipitation amounts for 3 thresholds: 0.1mm, 2mm and 10mm. The observed numbers of observations in each class is also indicated.*

As an example, Figure 23 shows the verification results for LM and the driving global model GME obtained for January 2001 for all stations in Germany and Switzerland and at all EWGLAM stations in the model domain. The root mean square errors of predicted 2m-temperature and dew point, of wind direction, wind speed and wind vector as well as of surface pressure are significantly smaller in LM than in the coarse grid global model GME. This is expected because the impact of the topography is much better represented in a high resolution model. No clear advantage can be seen for cloud cover where the hit rate has about the same values in LM and in GME. For predicted precipitation, the LM has a slight advantage compared to GME, especially for the yes/no-decision (>0.1mm class) and for heavy precipitation events (>10mm class). This is different to the preceding months, where the GME had often a slight advantage over LM concerning the precipitation scores. The better scores for LM in January 2001 might indicate a positive impact of the filtered topography which was introduced in mid December 2001.

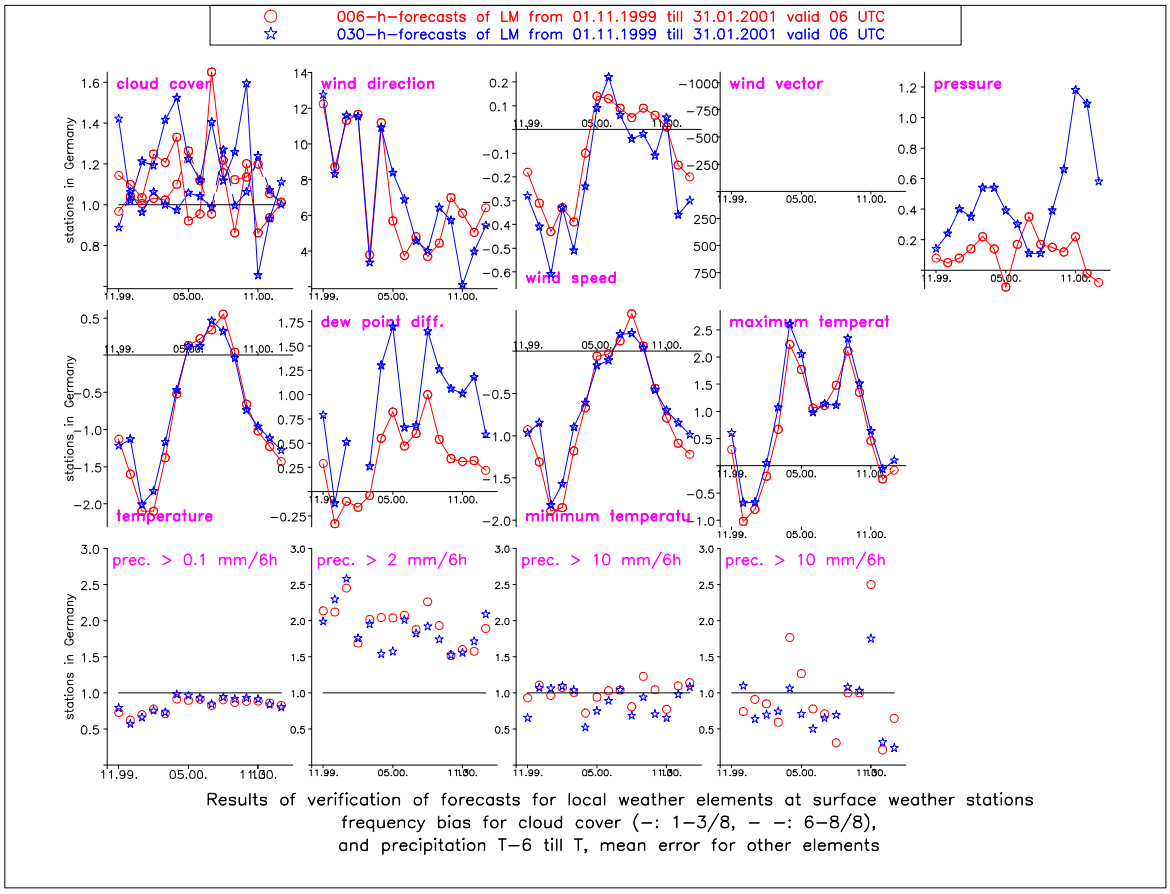

Figure 24: *Mean verification scores at 6 UTC as a function of time for two forecast times (red: + 6h, blue: + 30h). Mean error for all elements except for cloud cover (frequency bias) and precipitation (frequency bias). Top: cloud cover, wind direction, wind speed, wind vector and surface pressure (from left to right). Middle: temperature, dew point difference, minimum and maximum temperature (from left to right). Bottom: 6 hr precipitation amounts for 3 thresholds: 0.1mm, 2mm and 10mm.*

The time series of the scores in Central Europe (all stations in Germany and Switzerland and all EWGLAM stations) from November 1999 until January 2001 is shown in Figures 24 and 25 for two forecast times at 6 UTC verification time: + 6 h and + 30 h. The mean errors of wind speed and (Fig. 24) show an annual variation with a large negative bias during winter,

whereas a slight positive bias occurs during the summer months. Also, the rmse error of wind speed is smallest during summer (Fig.25).

A similar effect can be seen for temperature: the mean errors have a large negative bias during winter, but an only small positive bias during summer (Fig. 24). The temperature rmse error is smallest for the summer months (Fig.25). The reduction of 2m-temperature errors for late spring until autumn can be attributed to the impact of the soil moisture analysis scheme.

The precipitation scores (frequency bias in Fig. 24, thread skill score in Fig. 25) do not show a large annual variation. Heavy precipitation events (> 10mm/6h) appear to be underpredicted.

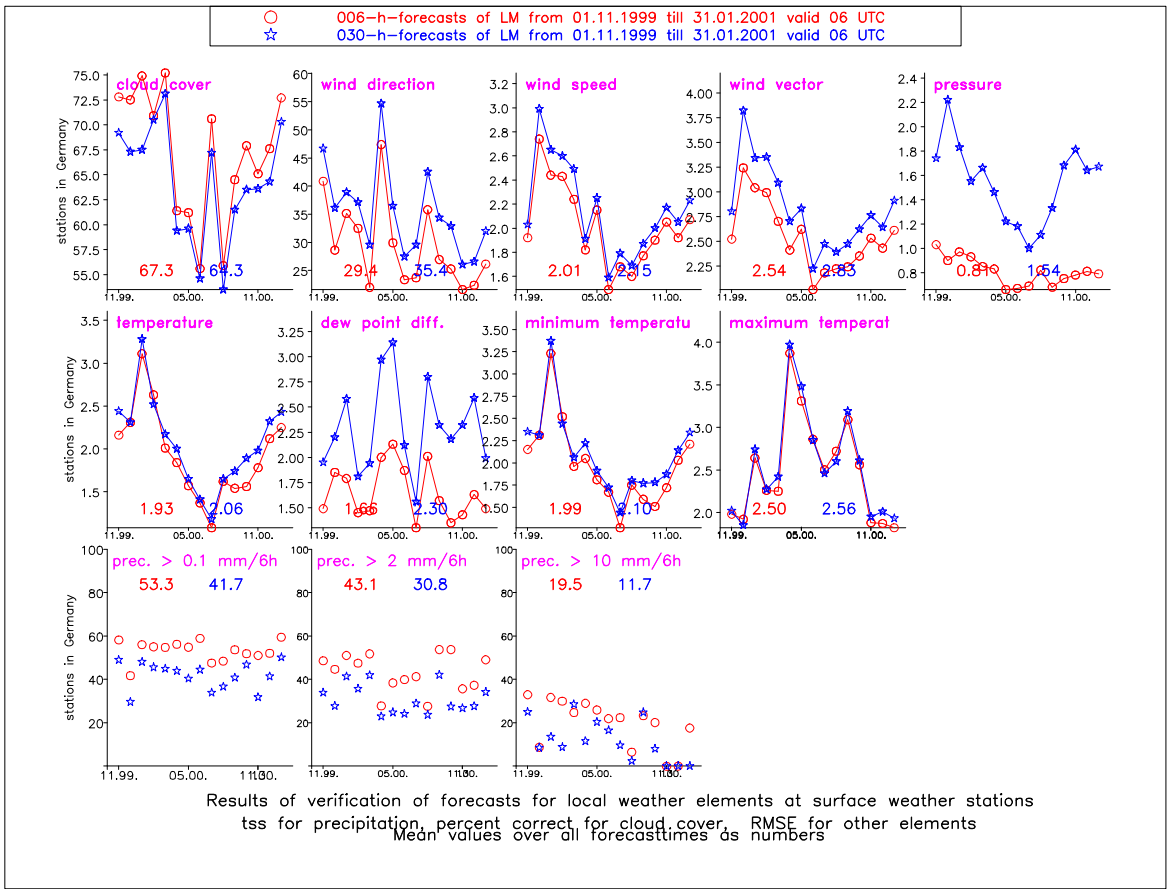

Figure 25: *Mean verification scores at 6 UTC as a function of time for two forecast times (red: + 6h, blue: + 30h). RMSE for all elements except for cloud cover (hit rate) and precipitation (TSS); numbers are mean values over all forecast times. Top: cloud cover, wind direction, wind speed, wind vector and surface pressure (from left to right). Middle: temperature, dew point difference, minimum and maximum temperature (from left to right). Bottom: 6 hr precipitation amounts for 3 thresholds: 0.1mm, 2mm and 10mm.*

An example for the spatial variation of errors of the predicted surface weather elements is shown in Figures 26 and 27. The monthly mean error of the predicted maximum 2m-temperature (Fig. 26) for July 2000 is mostly in the range of ± 0.5 K except for regions in southern Germany. The rmse errors are below 2.5 K in large parts of the domain.

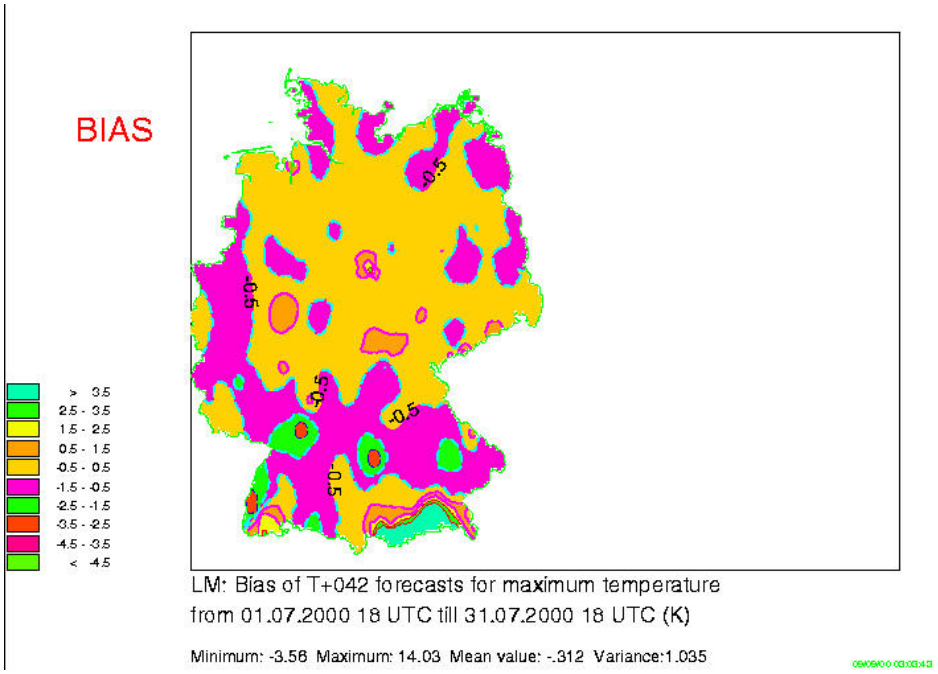

Figure 26: *Monthly mean bias of maximum 2m-temperature for + 42hr LM-forecasts at 18 UTC verification time in July 2000.*

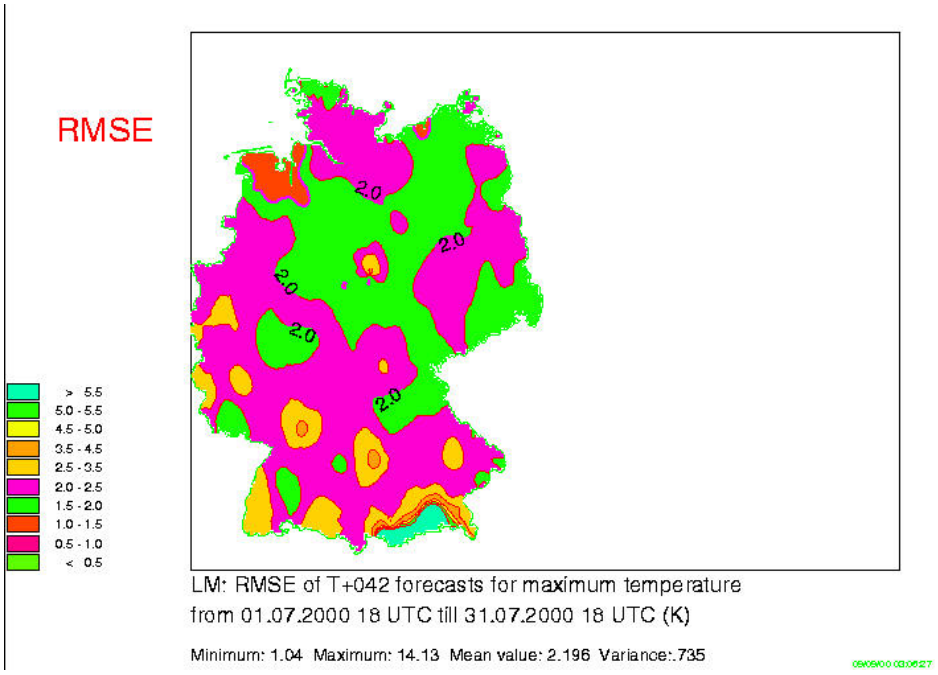

Figure 27: *Monthly mean rmse error of maximum 2m-temperature for + 42hr LM-forecasts at 18 UTC verification time in July 2000.*

8.1.2 Operational Verification at MeteoSwiss

(F. Schubiger, MeteoSwiss)

The following nomenclature for LM is used in the text below: LMS means the LM version of MeteoSwiss that was in preoperational mode since July 2000, LMD means the operational LM version of DWD.

(a) High resolution verification of daily cycle over Switzerland

Results of LMD, LMS (since July 2000) and SM have been computed monthly and seasonally for 2m-temperature, 2m-dewpoint and 2m-dewpoint depression, 10m-wind, precipitation (hourly sums for daily cycle and 6h sums for scores) and for cloud cover (3-hourly intervals).

The following points are of main interest:

- the 2m-temperature negative bias was quite pronounced in wintertime. In January 2000 it was of the order of 3K for gridpoints < 800m and even $\sim 8K$ (!) for gridpoints > 1500 m. Cooling in the night is too pronounced in LMD and LMS. The diurnal amplitude is about 1 K larger in LMD than in LMS and SM (but already SM has too large amplitude, see Figure 28a. New results of test runs for November 2000 when LMS run with filtered orography show better results, i.e. a reduced diurnal amplitude.

- The 2m dewpoint depression shows that the models are too dry, especially during night (see Figure 28b). But the results of LMS compared to LMD are surprising and need to be further studied: over Switzerland the bias is reduced with LMS (i.e. LMS is not so much too dry as LMD), despite the fact that LMS has not yet a nudging assimilation cycle and soil-moisture analysis as in the LMD (LMS run in the pre-operational phase with interpolated fields of the global model GME of DWD).

- The results of precipitation still had be interpreted as a mean for an area of at least $\sim$ 14x14 km: the variability of total monthly precipitation for neighboring grid points remained very large. During summer and autumn LMS and LMD gave too little precipitation (see Figure 29): LMS $\sim$ 10% and LMD $\sim$ 30% (LMD has about 25% less precipitation than LMS). Results of LMS with filtered orography (in operations since 01.11.00) gave a greatly reduced variance from one gridpoint to the other. Test runs for November 2000 with filtered orography and a modified horizontal diffusion (developed at DWD) showed no more an exaggerated horizontal variance and overall better results of LMS compared to SM.

- Verification of 10m-wind (for stations below 800m) gave for direction the same good results for LMD and LMS as for SM, but for wind speed the existing positive bias in the SM has become even larger with LMS and LMD.

- LMD and LMS have a reduced negative bias in total cloudiness compared to SM.

(b) Daily verification of LMS/SM cloudiness with the Meteosat VIS-Channel

This verification is operational with the SM since 01.02.00 and since 01.10.00 with LMS over its enlarged domain.

(c) Verification of the vertical profiles at TEMPs stations

The vertical verification package (i.e., verification of the vertical structure by comparison of the model atmosphere with radiosonde observations) for the LMS is operational. Apart from monthly, seasonal and yearly verifications, it also allows to study the behaviour of the model depending on weather type by providing daily skill scores.

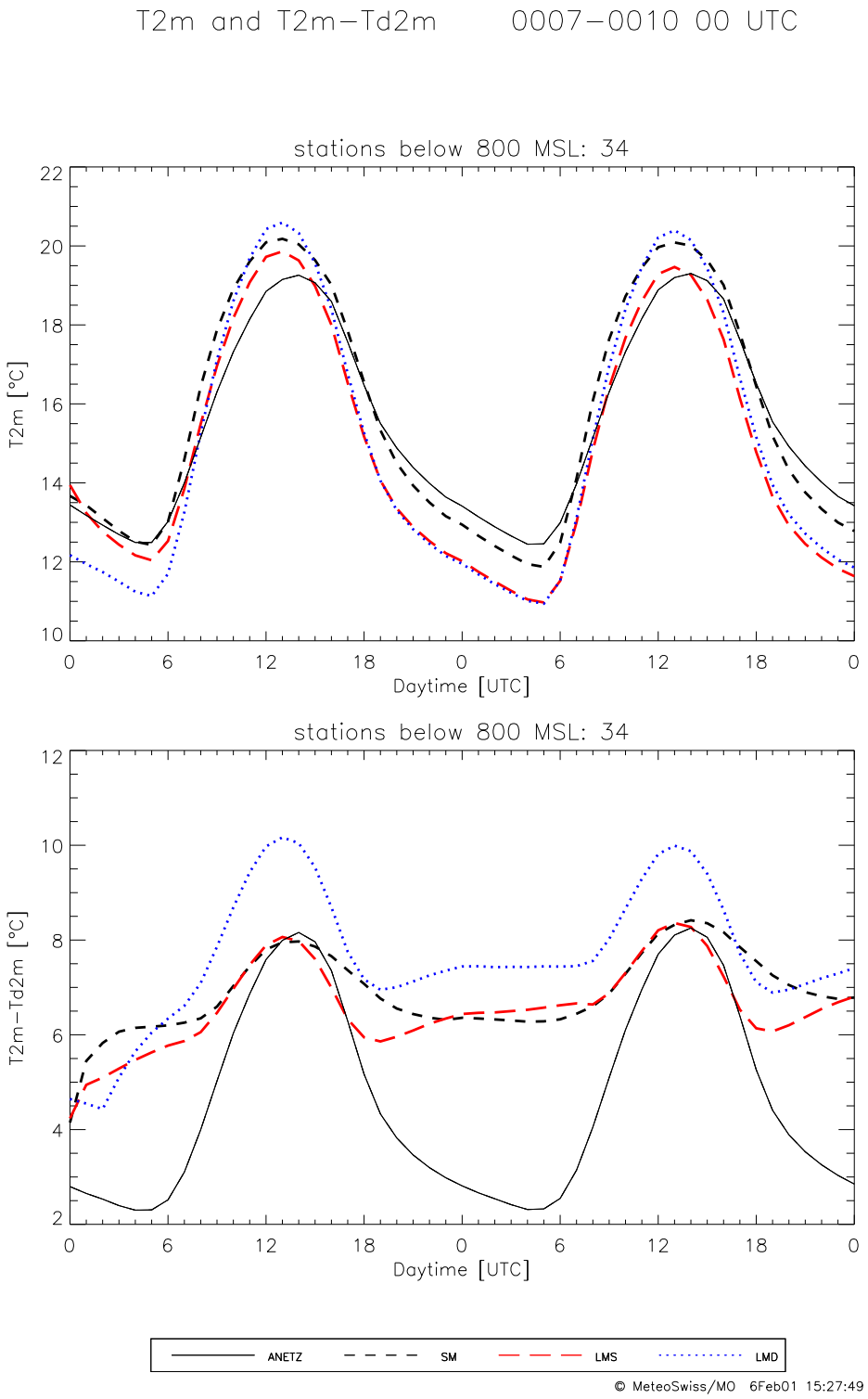

Figure 28: *Mean daily variation of 2m-temperature (a: upper part) and 2m-dewpoint depression (b: lower part) for stations (resp. gridpoints) < 800m for all 00 UTC forecasts from July to October 2000. The full (black) line are the hourly observations of the automatic network ANETZ of MeteoSwiss (34 stations < 800m). Dashed line (black) is SM, long dashes (red) is LMS and dotted (blue) line is LMD. The horizontal axis is daytime for observations and forecast length from +0h to +48h for the models.*

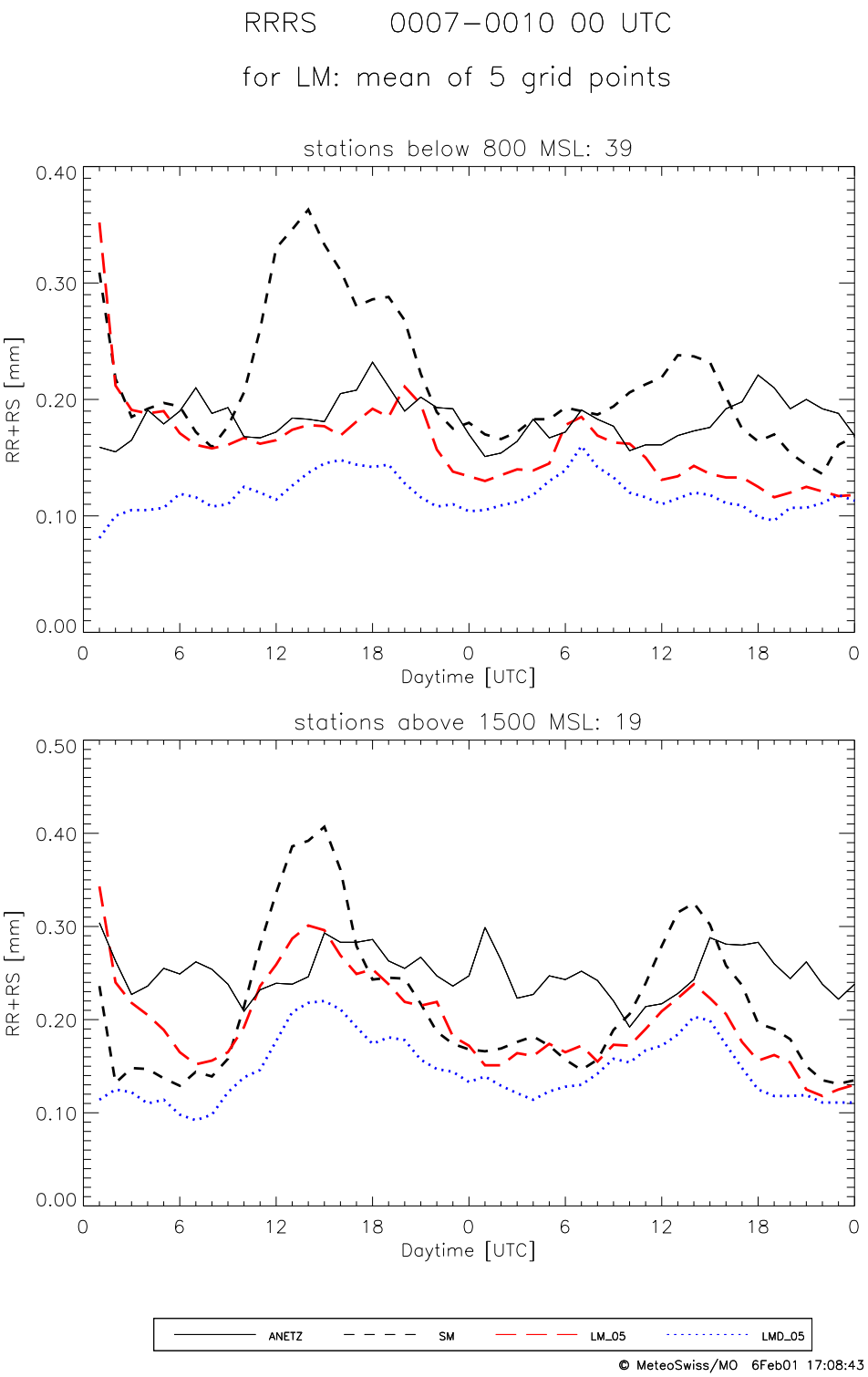

Figure 29: *Mean daily variation of hourly precipitation sums for stations < 800m (a: upper part) and > 1500m (b: lower part). For the rest of the legend: see Figure 28.*

(d) Subjective verification of LMS by bench forecasters

Since end of July 2000 the bench forecasters of MeteoSwiss make a subjective verification of LMS. The nine elements under consideration are frontal structures, timing of fronts, precipitation (maxima, distribution and timing), 10m wind, vertical profiles and low-level clouds. Emphasis is given to the general performance of the LMS and to the relative performance as compared to the SM. The questions have to be answered by a five step ranking. The results obtained till end of the year show that the forecasters judged the LMS quite similar as the SM: MS provides a little bit superior forecasts compared to SM for fronts (structure and timing) and the vertical profiles (at Payerne). 10m-wind of LMS were judged as frequently better as also more badly than SM. Precipitation were judged a bit worse in LMS than SM (results with filtered orography and the modified horizontal diffusion will be available in early 2001).

8.2 Verification of Vertical Profiles

Both at MeteoSwiss and DWD a software package for the verification of the vertical structure by comparison of the model atmosphere with radiosonde data has been developed and is operational. The packages allow for monthly, seasonal and yearly verification at individual TEMPs stations and for sets of stations.

As an example, Figures 30 and 31 show the mean and rmse errors of vertical profiles at all TEMPs stations within the model domain for 00 UTC and 12 UTC LM runs at DWD, respectively.

When looking at the geopotential, a drastic increase of the mean and root mean square error in the stratosphere is obvious. The reason for this increase could not be traced back yet, but is probably related to the interpolation scheme for temperature and pressure. The strong fluctuations in the temperature errors at and above the tropopause level might result from the same effect. This has to be checked for.

The forecasted mean errors of temperature have on the average a large negative bias from the middle atmosphere up to the tropopause level for both 00 UTC and 12 UTC run. This indicates a model deficiency which is not yet understood, but could be related to an erroneous cloud-radiation interaction for upper level cloudiness or to problems with vertical transports at the tropopause.

When comparing the mean errors form 00 and 12 UTC runs, some interesting points can be noticed, which need clarification in future.

- The mean error of geopotential has a slight negative bias at analysis time, but is constant within the troposphere. For 12 UTC runs, however, the bias is positive initially and increases with hight.
- The mean error of relative humidity is close to zero throughout the atmosphere for both 00 and 12 UTC runs at analysis time. However, for 00 UTC runs a slightly negative bias evolves with forecast time, whereas a slight positive bias evolves for the 12 UTC runs.
- For temperature, the mean error of 00 UTC runs has a constant negative bias of about 0.15 K within the atmosphere at analysis time. For 12 UTC runs, however, the initial mean error is close to zero (but slightly tilted).
- The mean errors of wind direction are close to zero in both 00 and 12 UTC runs. At analysis time, a slight positive bias can be observed in the boundary layer for the 00 UTC runs, unlike for 12 UTC runs.

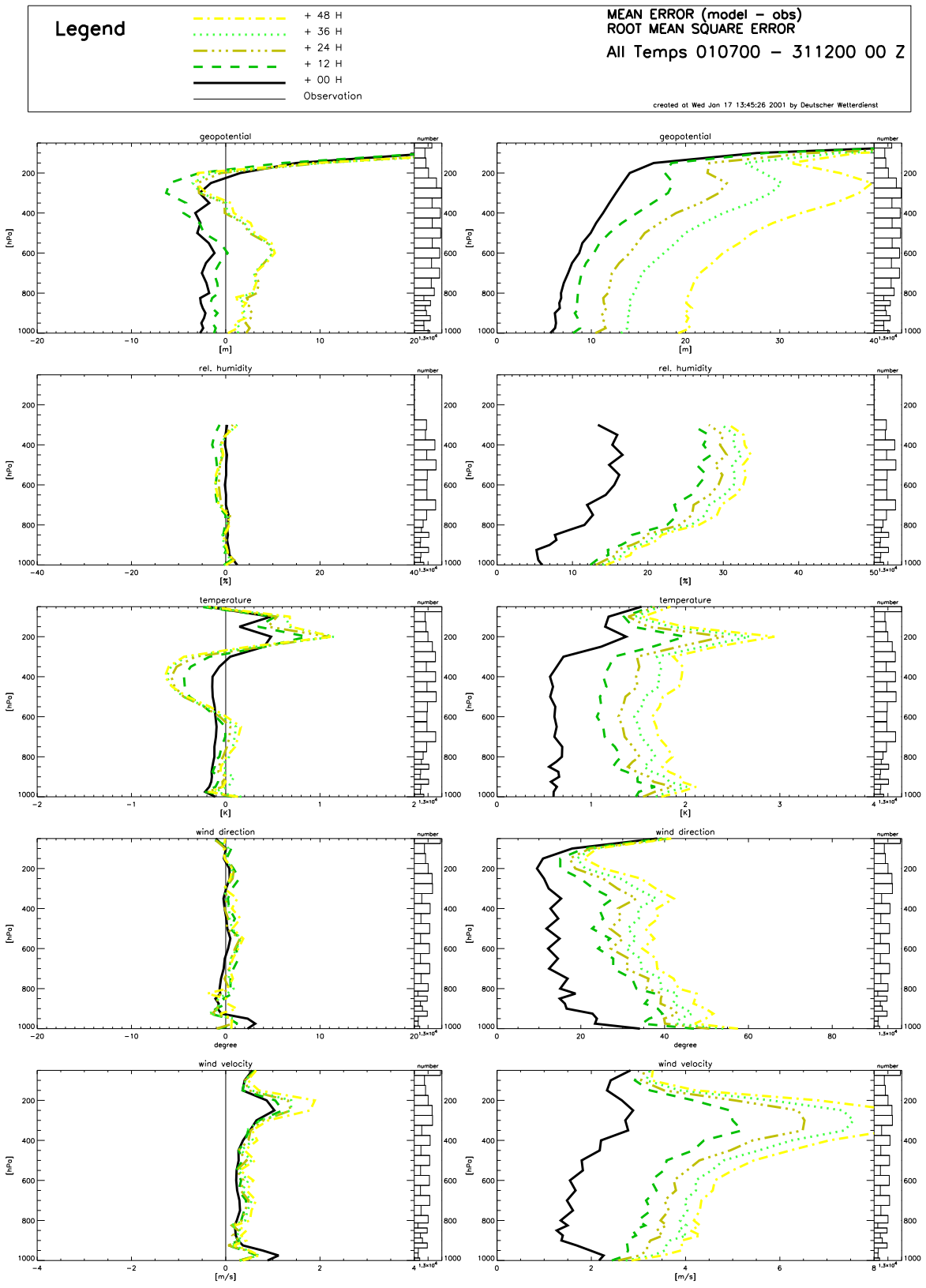

Figure 30: *Vertical profiles at all TEMPs stations for 00 UTC LM runs at DWD from July - December 2000 for different forecast times. From top to bottom: geopotential, relative humidity, temperature, wind direction and wind velocity. Left: bias. Right: rmse*

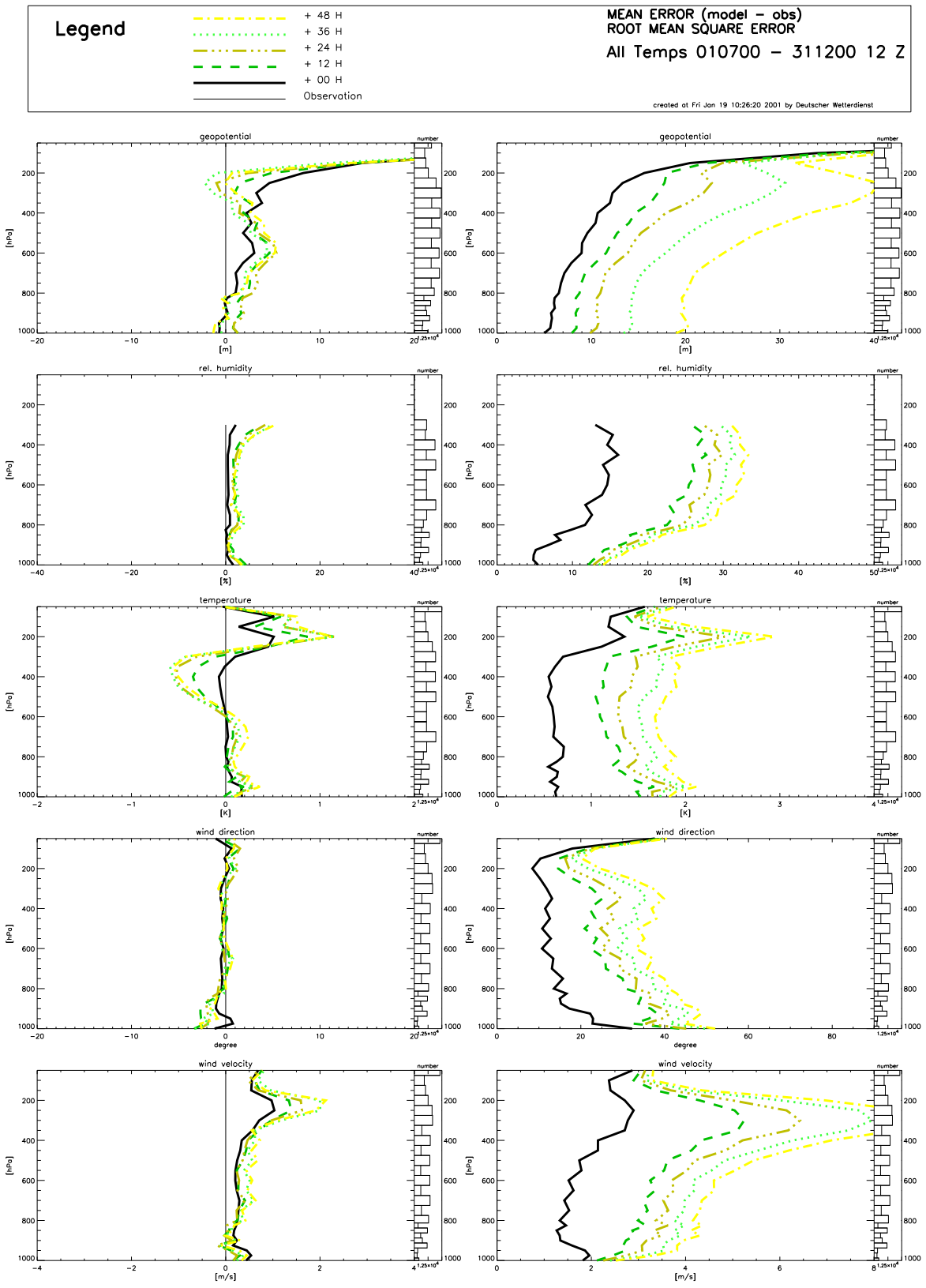

Figure 31: *Vertical profiles at all TEMPs stations for 12 UTC LM runs at DWD from July - December 2000 for different forecast times. From top to bottom: geopotential, relative humidity, temperature, wind direction and wind velocity. Left: bias. Right: rmse*

- The mean errors of wind velocity have a slight positive bias for both 00 and 12 UTC runs. Similar to wind direction, the mean errors are somewhat larger within the boundary layer for 00 UTC runs. This might indicate a parameterization problem related to the nocturnal stable boundary layer or a problem in the assimilation of 10m winds.

As expected, the rmse errors increase with forecast time for all verified variables. The geopotential rmse error shows a quite gradual increase for the 12 hour increments of forecast time. All other variables, however, behave quite different: starting from relatively rmse errors, the values jump to much higher level within the first 12 hour forecast time. Thereafter, the increase in rmse error is quite gradual. This indicates a relatively tight coupling of the observed variables to the model variables by the nudging analysis scheme, and it also reflects the fact that TEMP and PILOT are the only upper-air data sources used currently.

8.3 Verification of Precipitation

Precipitation is a very important weather parameter and a demanding task for numerical weather prediction. To find a valid analysis of precipitation measurements to compare with gridded model results of precipitation forecasts is equally demanding and not yet conclusively resolved. A specific problem, especially at high model resolution, is that the spatial and temporal variability of precipitation is much larger than those of the standard observations.

The operational daily verification of precipitation at meteorological centres is mostly based on the coarse SYNOP observations. This section summarizes work of the COSMO verification group which is related to regional verification of precipitation using special observational networks of high resolution in space and/or time.

8.3.1 Spatial Distribution of Precipitation over Germany and Switzerland

(U. Damrath, DWD)

This verification product is based on the climate observation networks of DWD and MeteoSwiss. The data have a high spatial resolution (more than 5000 stations in Germany and Switzerland), but a coarse temporal resolution (24 h precipitation sums).

Figure 32 shows the distribution of monthly precipitation amounts for March 2000 as obtained from the climate networks and form the corresponding 00 UTC LM runs at DWD. Most details resulting from orographical forced enhancement of precipitation are well represented by the LM forecasts, e.g. the high rain amounts along the northern ridge of the Alps, over the Black Forest and over various low mountain ranges in Germany and along its southeastern border. In most of these mountainous areas the peak values are somewhat overestimated, but in southern Switzerland the precipitation amount is underestimated.

The situation changed during summer and autumn 2000, where the LM tended to underestimate precipitation, especially over mountainous areas. Fig. 33 shows the verification result for October 2000. The rain amounts in the northern parts of Germany were captured quite well by the model. However, in the southwestern regions of Germany and the northern and western parts of Switzerland, the precipitation amounts were significantly underpredicted. In October and November 2000, a southerly Föhn-flow over the Alps prevailed in the synoptic-scale weather situation. Obviously, the LM simulated a too strong Föhn effect resulting in a blocking of fronts coming from southwest. Meanwhile, a filtered topography has been introduced as a short-term remedy to cure this problem.

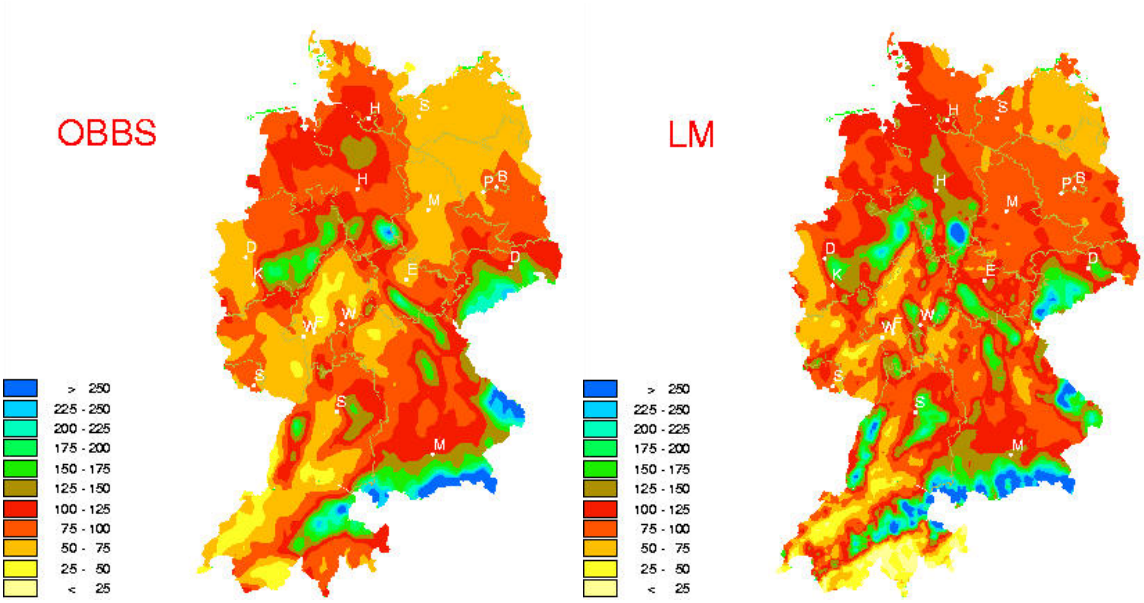

Figure 32: *Monthly precipitation sum (mm) for March 2000 as observed (OBBS) by climate networks (max: 481 mm, mean: 103mm) and derived from 00 UTC LM forecasts at DWD (max: 995 mm, mean: 103mm).*

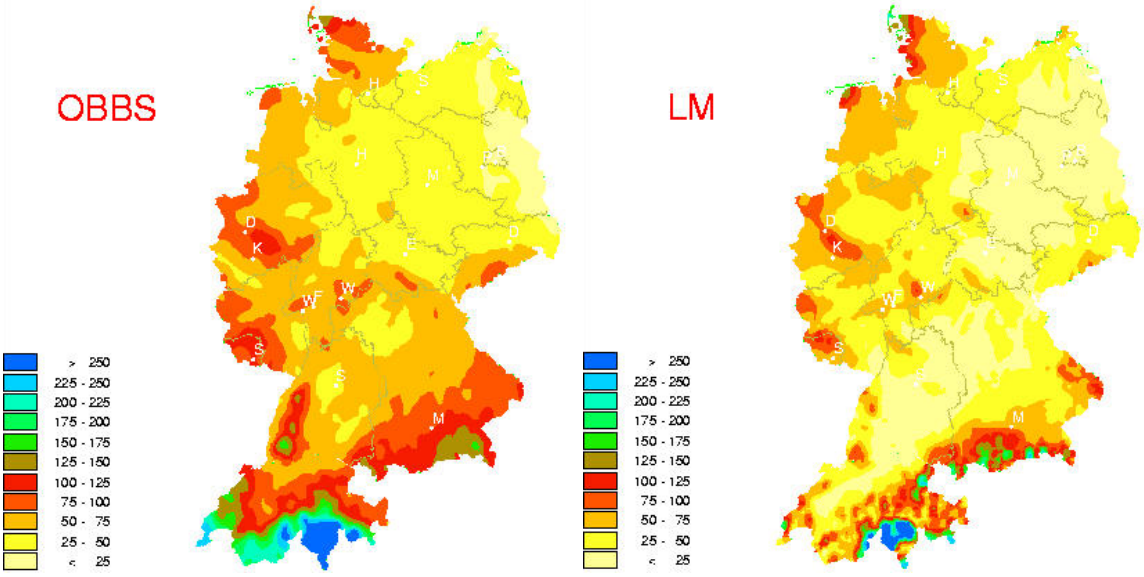

Figure 33: *Monthly precipitation sum (mm) for October 2000 as observed (OBBS) by climate networks (max: 525 mm, mean: 63mm) and derived from 00 UTC LM forecasts at DWD (max: 999 mm, mean: 69mm).*

8.3.2 Recent Results of Lokal-Modell Verification in Emilia-Romagna and Marche Regions, Italy.

(Carlo Cacciamani (ARPA-SMR), Laura Mannozzi (OSGM Marche) and Laura Sandri (ARPA-SMR))

The goal of this study, performed in collaboration between ARPA SMR and OSGM, is to assess the quality of Lokal-Modell (LM) quantitative precipitation forecast (QPF) over the Emilia Romagna and Marche regions in Italy, from February 1999 to January 2000. In this short report, we will discuss the results obtained during the last 5 months of verification (from September 1999 to January 2000). The verification has been carried out by means of the synoptic and local stations, in both regions. In order to measure the quality of the QPF, we selected two different verification methods, meant to explore different aspects of the model forecast.

The first and less strict method, called areal method, is applied to obtain important insights regarding the integral quantities of the simulation. It is sensitive to errors in the magnitude of the precipitating structures and not in their location, provided that both the observed and forecast structures fall into the verification area. The areal verification is carried out by computing the spatial average over all the model grid points that fall into the verification area, and comparing it (daily and monthly) with the observed one.

Regarding the daily comparison, we found out that during the last 5 months of verification the model generally underestimated the total precipitation over both regions, especially during November 1999 (see Figure 34). The behaviour of LM was generally better in Emilia Romagna than in Marche, where also in September 1999 LM underestimated the rainfall amount. In the Marche region, on Dec. 15 th , 1999, a heavy precipitation event was recorded (over 70mm/day observed on average over the whole area) which was seriously underpredicted (less than 20mm/day forecast on average over the whole area).

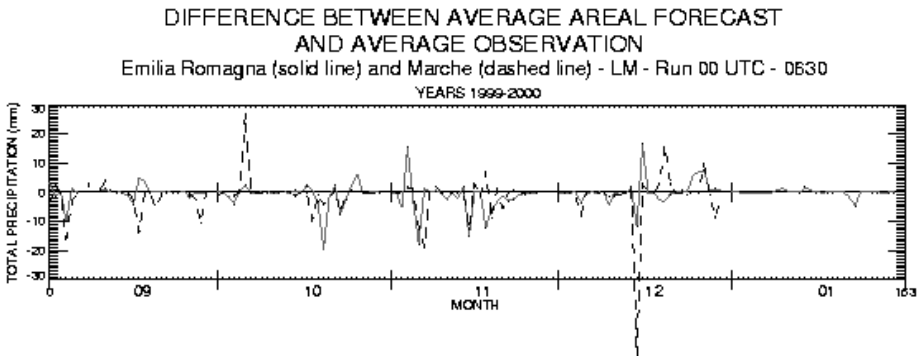

Figure 34: *Difference between average areal forecast and average observation of precipitation in the Emilia Romagna (solid line) and the Marche (dashed) regions.*

It is interesting to analyse the behaviour of LM during the so-called Christmas storms occurred in Europe on the 26 th and 28 th of December 1999. During these events, in Emilia Romagna there was almost no observed precipitation but strong winds, and LM correctly forecast low rain amounts (less than 10mm/day on the 26 th and 2mm/day on the 28 th on average over the whole area). In Marche almost no precipitation was recorded on the 1 st event, but 10mm/day on average fell during the 2 nd one. The LM forecast was quite wrong, because the simulation yielded 12mm/day on the 26 th and less than 2mm/day on the 28 th, always on average over the whole area of Marche.

As concerns the monthly comparison of spatial averages, we computed Mean and Root mean

Square Errors (ME and RMSE). For 24-hour cumulated precipitation forecasts, in both regions the bias is very different from the high and positive one we observed during spring and summer 1999. In fact, in Emilia Romagna the ME is close to zero (although slightly negative in November 1999) and in Marche is negative. This confirms the above discussed considerations regarding the daily comparison. We also checked the first 6 and 12 hours into forecast ME, and found out that the spin-up problem is much less significant in autumn and winter than in summer.

We also compared the daily maximum observed value with the forecast one, regardless of the correspondence between the station and the grid point where they were respectively recorded. This was done to measure the realism of the LM forecast, that is how realistic are the precipitation maxima produced by LM. The results show a more realistic behaviour over the Marche region, where the forecast maxima do not exceed significantly (like they do over Emilia Romagna) the observed ones.

The second method we use is called punctual. It is a stricter method if compared to the areal one, because it is sensitive to errors both in the magnitude and in the location of precipitating structures. The punctual verification is performed by comparing the daily value recorded at each station with the one forecast at its closest model grid point. The comparison for each station at different precipitation thresholds (we used 1mm/day, 5mm/day, 10mm/day, 20mm/day, 50mm/day) produces a 6x6 contingency table, which is then reduced, for a given threshold, to a 2x2 yes(event above threshold)/no(event below threshold) contingency table. Thus, we obtained monthly tables at different thresholds, from which bias and some accuracy measures, such as the Hit Rate (HR), the Hit Rate Rain (HRR), the False Alarm Rate (FAR), the Threat Score (TS) and the Heidke Skill Score (HSS) were computed. Due to the scarce number of high rainfall rates events in these Italian regions, we cannot give results for thresholds higher than 10mm/day.

However, the bias for both regions is about one for the 1 to 10mm/day thresholds during the autumn and winter months, being less than 1 in November 1999. During these months, there is also a much lower FAR, and a much higher TS (up to 0.55-0.6 at 1mm, up to 0.5 at 10mm) and HSS (up to 0.6 for 1 and 10mm) in both regions, compared to the spring and especially the summer scores. The most remarkable feature of our punctual verification, apparent for both regions at all the significant thresholds (1 to 10mm/day) is a systematic improvement of bias, FAR,TS and HSS during the whole year of LM QPF verification, apart from the summer overprediction problems outlined in the September 1999 COSMO meeting in Bologna.

8.3.3 Lokal-Modell Verification in Piemonte Region, Italy

(Enrico Minguzzi (CSI, Torino))

Introduction

In the framework of the COSMO project, the precipitation forecast of the Lokal-Modell from February to half December 1999 was verified using the raingauge network of Regione Piemonte; this short report summarize some of the main results of this work.

The verification was focused on precipitation cumulated in 24 hours, from +12 to +36 in the 00Z run: this interval was chosen in order to remove spin-up period, and also because it is the most important for our operational forecasts. The observational network is relatively dense, which allow to restrict the analysis to heated raingauges (removing observational errors due to unregistered snow falling and lagged snow melting), and to examine the precipitation pattern on 3 different spatial ranges: the station point, the hydrological catchments (Piemonte was divided in 10 sub-domains, each about 2000 km2 wide) and the whole region. Several

statistical scores were evaluated, such as Bias (B), Threat Score (TS), Hit Rate Rain (HRR) and False Alarms (FAR), considering 5 precipitation thresholds (1,5,10,20,50 mm).

Punctual Verification

The amount of precipitation observed at each station was compared with the one forecasted at the nearest model grid-point, and then contingency tables and scores were computed.

Considering the whole year and thresholds lower than 50 mm, scores achieved are not unusual: there is not a remarkable bias (B about 0.9) and the other scores decrease uniformly with increasing precipitation (TS = 0.33 at 1mm and 0.23 at 20mm). For intense precipitation (>50mm/24h), the model overestimates the total amount (BIAS = 1.5), but nevertheless it does not predict the correct time and place (FAR = 0.82, HRR = 0.27).

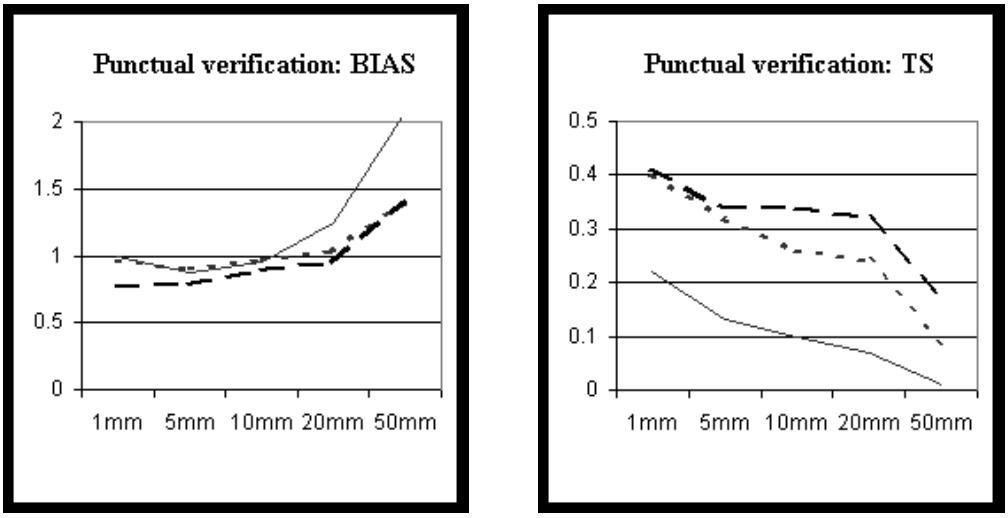

Figure 35: *Seasonal scores for punctual verification (see text)*

As regard to the monthly trend, summer is by far the worse time, with an overprediction at higher thresholds (BIAS = 2.1 at 50 mm), and an unbiased but unreliable forecast for weak precipitation (FAR = 0.64 at 1mm). On the other hand, in autumn months the model predicts less precipitation (with a small negative bias at lower thresholds) but with a more realistic distribution (TS = 0.33 at 10 and 20 mm); this behaviour can suggest that model performance has improved in the last part of the year, although scores are also good in March and poor in the first part of December.

Catchments Verification

The observed and predicted precipitation were averaged over each of the 10 sub-domains and then contingency tables were built, considering each averaged value as a single observation; these "averaged" values are of crucial importance for hydrological forecasts, and moreover this approach provides scores which are independent from model resolution. As it could be expected, scores are generally better than in the punctual verification.

In this analysis the model performance turns out to be rather good: TS is always greater than 0.32, but the most remarkable feature is that scores decrease very little at the high thresholds. Considering the entire 1999, there is a small underprediction of precipitation (B = 0.77 at 20mm), but the forecast is very reliable: HRR is about 0.5 and FAR about 0.4-0.5, and the model hardly ever makes big errors (all of the 13 cases of forecasted precipitation ¿50mm correspond to observations of at least 20mm).

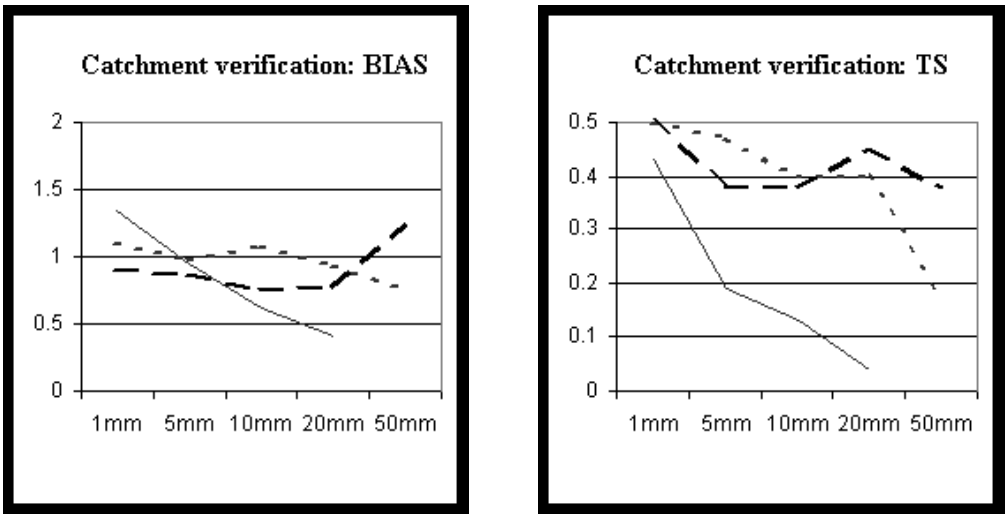

Figure 36: *Seasonal scores for catchment verification (see text)*

The seasonal behaviour is similar to that seen for the punctual verification. During summer the model strongly underestimate precipitation, but the forecast is nevertheless unreliable (at 10 mm, B=0.62 and FAR=0.71); it should be noticed, however, that in these months large amounts of averaged precipitation are rather infrequent. There appears indeed to be an evolution in model performance through the year: in autumn there is less precipitation predicted with respect to spring (B reduces from about 1.0 to about 0.8), but this does not affect significantly HRR and TS, and strongly reduces FAR (at 20 mm FAR=0.41 in spring and 0.29 in autumn)

Regional Verification

Due to the lower number of data, the analysis of precipitation averaged over all Piemonte was restricted to seasonal means and to thresholds not greater than 10 mm.

The model shows the same small negative bias already discussed in catchment analysis, but this appears evident at lower thresholds (B=0.76 at 5mm); nevertheless the forecast is very reliable, with FAR always less than 0.3, and this explains the high values of TS reported (TS $>$ 0.45). To reinforce this conclusion, it can be noticed that all of the 4 events of precipitation $>$ 20mm were correctly forecasted, with only 2 false alarms (where the observed precipitation was anyway $>$ 10mm)

8.3.4 Verification of Lokal-Modell precipitation at CMIRL, Genova: Seasonal Report (winter 1999/2000)

(G. Contri and E. Trovatore (CMIRL, Genova))

The Lokal Modell verification was carried out for the 00UTC and 12UTC Lokal Modell runs using the available stations located in the Liguria region. The period we have considered is from December, 21st to February, 29th, and it was characterized by very dry meteorological conditions all over the North-Western Italy due to prevailing northerly winds.

This fact, together with the very poor data received from our rain-gauges, also during the very few rainy periods, made this season particularly unlucky for the verification over Liguria. The problem of the few available data should be resolved in the next months, the Liguria region being now in a period of transition in the management of the local meteorological stations.

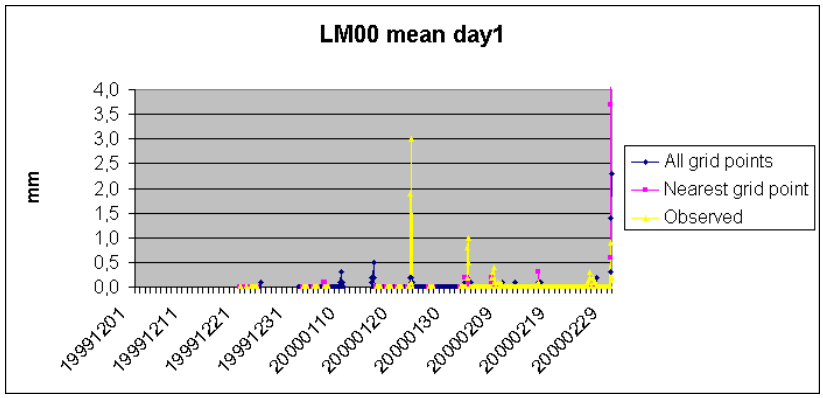

Figure 37: *Spatial average of 3 hr precipitation amounts for LM 00 UTC runs (day1)*

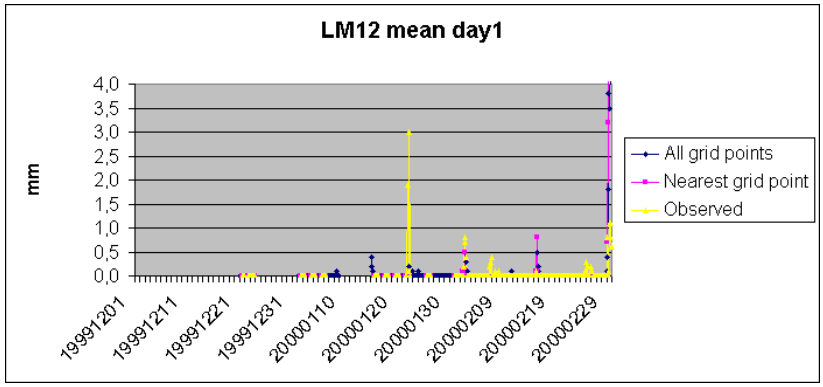

Figure 38: *Spatial average of 3 hr precipitation amounts for LM 12 UTC runs (day1)*

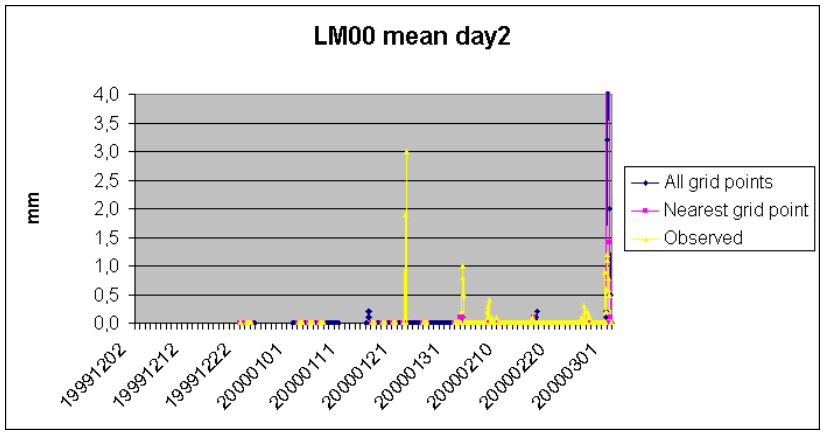

Figure 39: *Spatial average of 3 hr precipitation amounts for LM 00 UTC runs (day2)*

We concentrated on 3 hours cumulated precipitation. The results for the all season are shown in Figures 37 - 40 (spatial average) and Figures 41 - 44 (maximum value). The number of observations is often very low, and we have no observations at all for the Christmas period, the only interesting rainy period in this winter. At the end of the period (the very beginning of March), we put the forecast values out of range in our graphs: if not, all the previous values, not exceeding a few mm, would be badly visible.

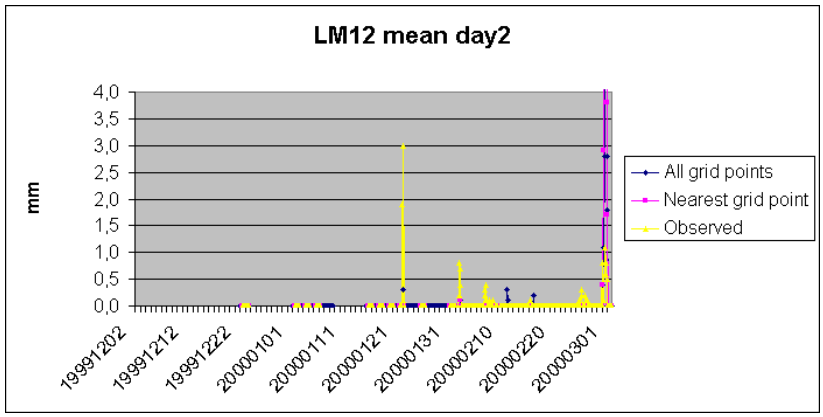

Figure 40: *Spatial average of 3 hr precipitation amounts for LM 12 UTC runs (day2)*

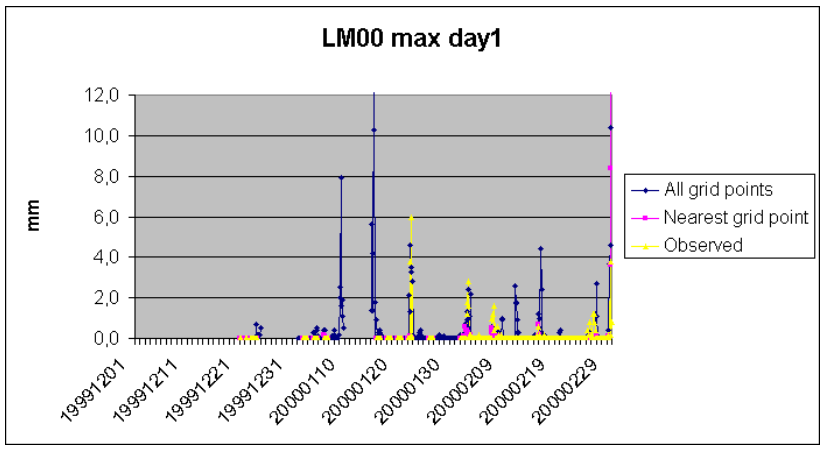

Figure 41: *Maximum value of 3 hr precipitation amounts for LM 00 UTC runs (day1)*

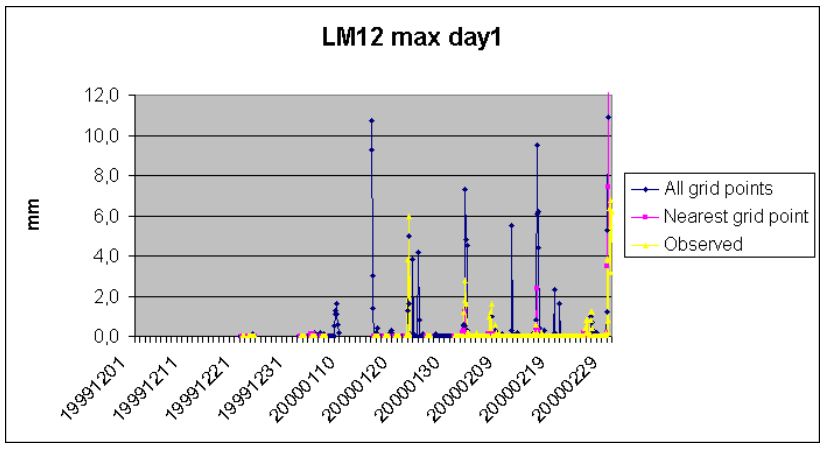

Figure 42: *Maximum value of 3 hr precipitation amounts for LM 12 UTC runs (day1)*

We can say that both LM00 and LM12 underestimated the areal average of total precipitation in three cases, comprised since the middle of January till the middle of February, without a great difference of behaviour between day1 and day2, while very overestimated was the precipitation of the last day of the period, with the exception of LM00 day1 which gave a more realistic amount of rain.

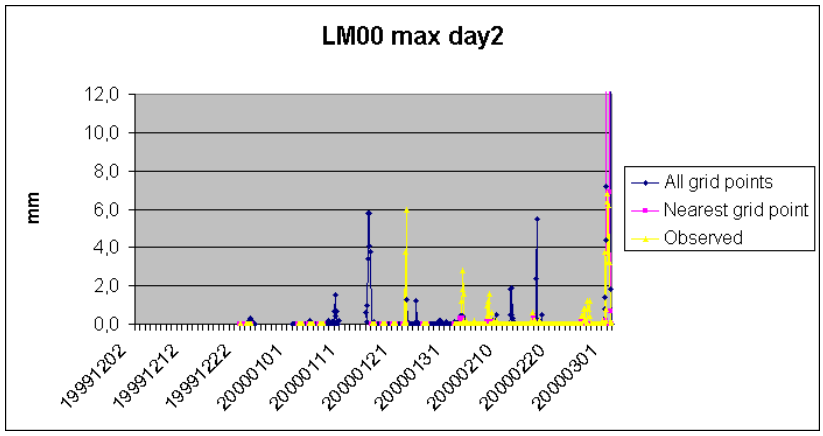

Figure 43: *Maximum value of 3 hr precipitation amounts for LM 00 UTC runs (day2)*

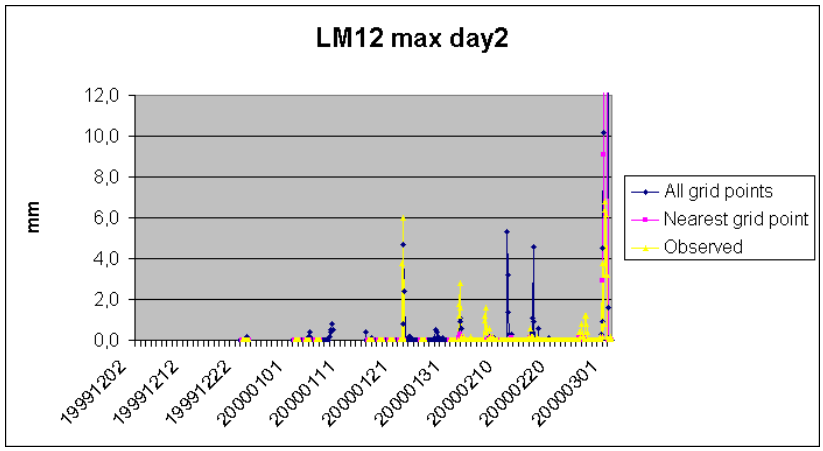

Figure 44: *Maximum value of 3 hr precipitation amounts for LM 12 UTC runs (day2)*

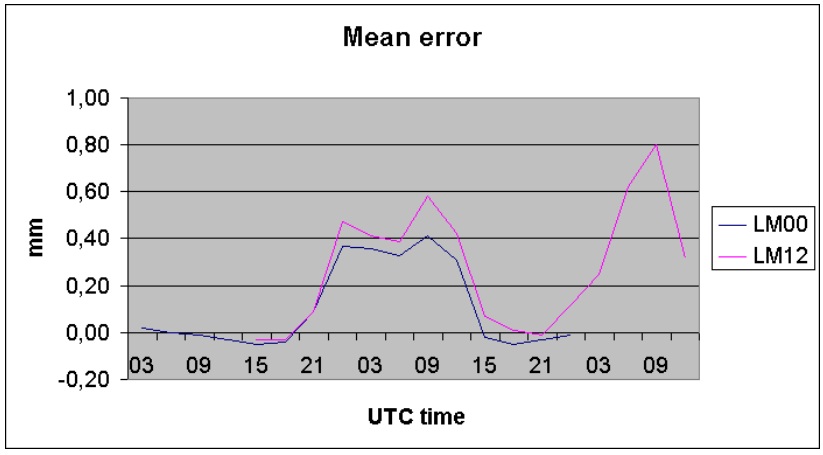

Figure 45: *3 hours accumulated rain mean error for 00 UTC (LM00) and 12 UTC (LM12) runs.*

The forecast maxima are generally overestimated: this is more evident in day1 and especially for the 12UTC run. Perfectly forecasted were the maximum amount of rain for the 22 January and the 2 February by the 00UTC run for day1. Like for the areal average, in the last day we have a great overestimation of precipitation.

In Figure 45 we computed the 3 hours cumulated rain mean error every three hours time steps for LM00 and LM12 considered for the same observation period (UTC time). In general we have a sort of periodic behaviour for both runs, and a slightly better performance for LM00. In any case, it is important to remark again that the absolute values are very low (less than 0.5 mm).

The most striking exception is the very good value for the first 12 hours of LM00: this feature, and the waving behaviour with 24 hours period, can be explained by the great amount of precipitation forecasted for the first half of the 1st of March: this day was not included in the LM00-day1 computations. This consideration demonstrates how much a single day can influence the verification of a season when there are very few data and, above all, very low observed precipitation.

Note: in this report we didn't include any index derived from the contingency table: this is due to the fact that the quasi-totality of data is comprised in the first square, giving us not useful indexes.

8.4 Verification Methods Using Remote Sensing Observation Systems

8.4.1 Verification of Vertical Profiles of Water and Ice Content Using a Radiative Transfer Model on Selected Case Studies

(L. Mannozzi and M. Lazzeri (OGSM, Regione Marche); R. Rizzi and R. Amorati (ADGB-Bologna); C. Cacciamani and T. Paccagnella (ARPA-SMR))

The aim of this work is to verify the vertical profiles of some variables forecast by the Lokal-Modell (LM) using an indirect technique based on the comparison between the simulated radiances and the METEOSAT measured ones. The LM fields we need to carry out the verification are the following:

- Temperature at the model levels;
- Mixing ratio at the model levels;
- Cloud fraction at the model levels;
- Cloud ice content at the model levels (not yet available at DWD);
- Cloud water content at the model levels;
- The value of pressure on the model levels;
- The surface parameters: pressure, skin temperature, 2mt temperature, 2mt dew point temperature and Land sea mask.

These parameters are given for each LM grid point in the chosen domain and at three different forecast times: 6, 12, 18 hours after the run time of the model.

The computation of simulated radiances at each Field of View (FOV) of the METEOSAT satellite requires both time and space interpolation of the LM fields. Two kinds of tools are necessary: an algorithm to compute the FOV geometry and timing, given the satellite orbital parameters and an interpolation algorithm to generate the horizontal grid and the vertical profiles of the meteorological variables to be used in the computation of the radiances. In this way, starting from the LM fields, the horizontal interpolation of each three dimensional meteorological parameter to the latitude and longitude of each FOV follows. Finally a vertical interpolation / extrapolation to the pressure levels is required.

These interpolated profiles are used as input for a radiative transfer model. In general, a radiative transfer model solves the basic radiative transfer equations of the whole atmosphere taking into account the absorption of the gases and the scattering by the aerosols and clouds. Some different numerical methods to resolve the radiative equations exists. The ADGB

group performed a comparison between a fast radiative transfer model (RTTOV5) and a full scattering radiative transfer scheme, where the gaseous and cloud optical properties are computed at high spectral resolution by a line by line code. The results are satisfactory and they encourage us to use the fast model RTTOV5 in order to have an operative system with a short computation time.

The Radiative Transfer for TIROS Operational Vertical sounder (RTTOV5) is operationally used at the European Centre for Medium-Range Weather Forecasts (ECMWF) for radiance assimilation and it is implemented to calculate radiance in NOAA and METEOSAT instruments spectral channels. An absorption-type radiation scheme is incorporated in the model to take into account the cloud presence. It is a sub-grid cloud overlap scheme leading to the computation of some columns with different vertical structures. In this scheme the radiative properties of the clouds are defined by the absorption coefficient. A parameterization of the absorption coefficients has been developed at the ADGB group. However this parameterization was developed for spherical particles, so at the moment the ADGB group and L. Mannozzi are testing a new parameterization for non-spherical particles. The RTTOV5 run produces the simulated radiances at each METEOSAT FOV and these ones can be immediately compared with the satellite data.

8.4.2 Verification of Lokal-Modell Cloudiness at CMIRL (Genova): Seasonal Report Winter 1999/2000

(S. Gallino (CMIRL-DIFI,Genova); V. Levizzani and M. Cervino (ISAO-CNR (Bologna))

Present Status of the Work

The verification task of LM cloudiness is carried in co-operation with CNR-ISAO (Bologna, Italy). OGS (Macerata, Italy) is no more active on it. By the time, a bi-spectral classification software (Porcu and Levizzani, 1992) of High Resolution Images in IR and VIS METEOSAT channels is available and operates at DIFI. Data are acquired daily at CMIRL in Genoa.

The procedure uses calibrated VIS and IR radiance data, applying a normalization of VIS radiance taking into account the actual SZA (Solar Zenith Angle). The bi-spectral classification is performed in the LM verification area (42N-47N, 6W-16W), using 165x77 pixels.

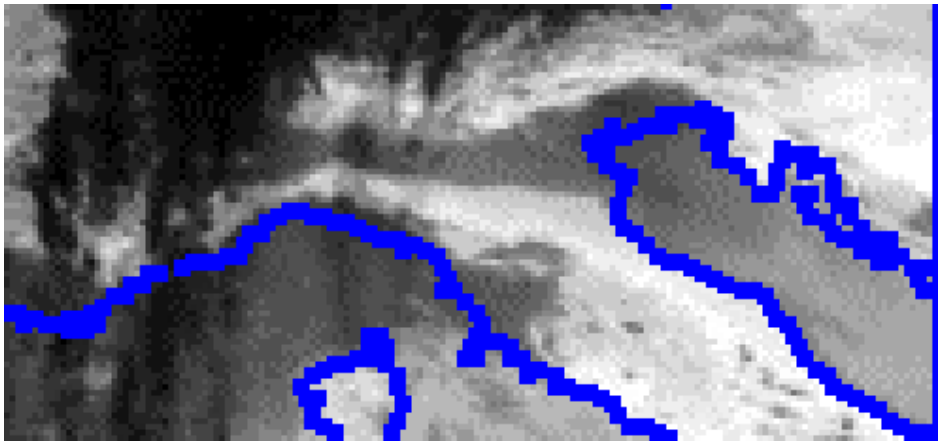

Figure 46: *IR image for 6 February 2000, 12 UTC.*

The performances of the bi-spectral classificator were qualitatively tested for 12UTC of 06th February. At that time, IR image shows (see Figure 46) the presence of high clouds over western Alps, VIS image indicates the presence of low clouds over Ligurian sea and fog over

Po Valley (see Figure 47). The applied procedure gives a spectral classification of IR-VIS histogram (see Figure 48) and a correspondent spectrally classified image (see Figure 49). At this stage, the main cloud fields, such as fog over Po Valley and high clouds over Alps, are well identified by the classifier.

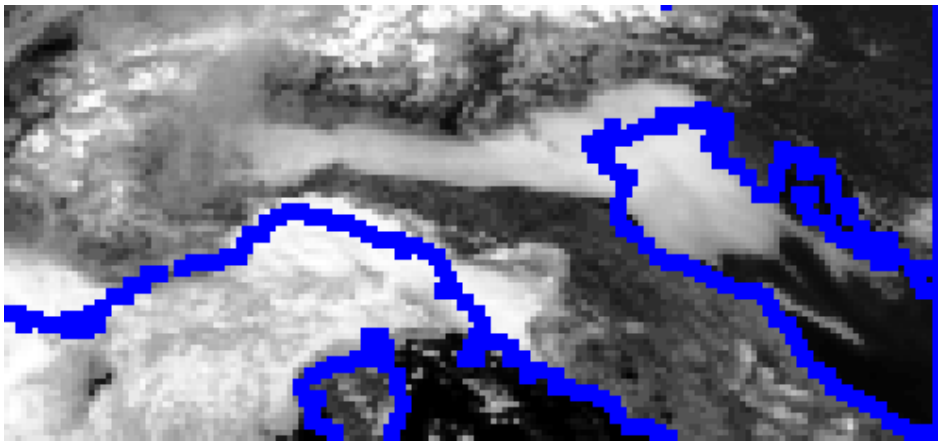

Figure 47: *VIS image for 6 February 2000, 12 UTC.*

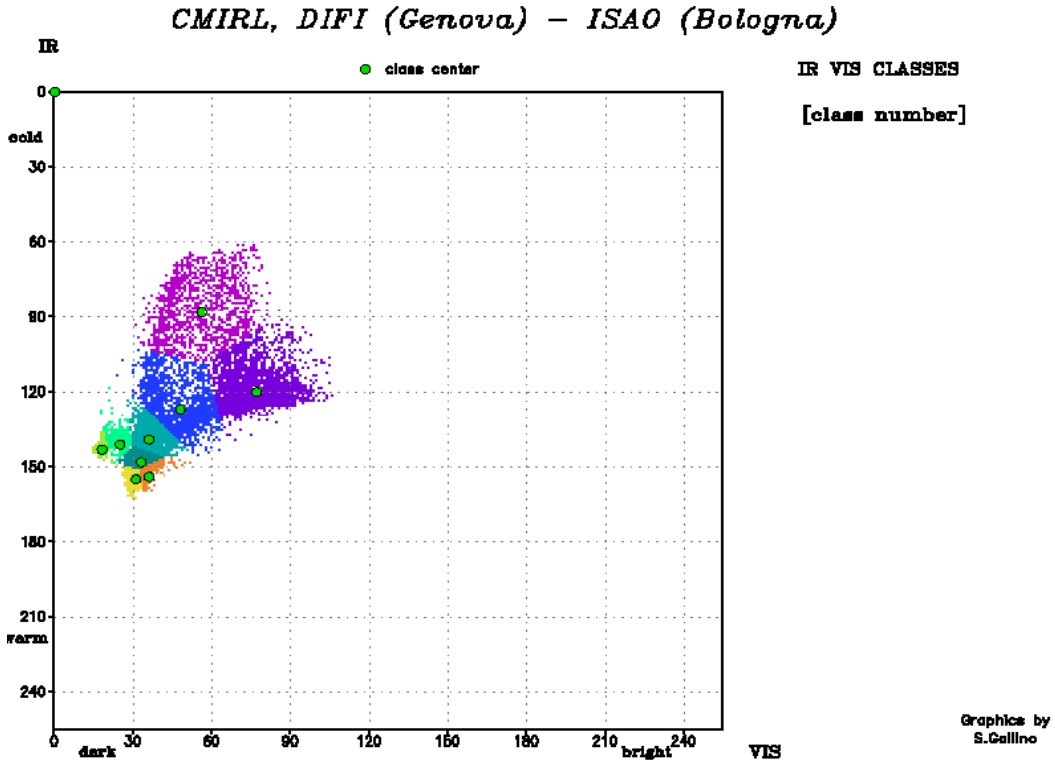

Figure 48: *Spectral classification of IR-VIS histogram for 6 February 2000, 12 UTC.*

LM low, medium, high and total cloudiness for the same time and over the same area are reported in Figures 50 - 53. The analysis of only this preliminary case shows that low clouds over Ligurian sea and high clouds over Alps are well simulated by LM; on the other hand, fog in Po Valley is missed.

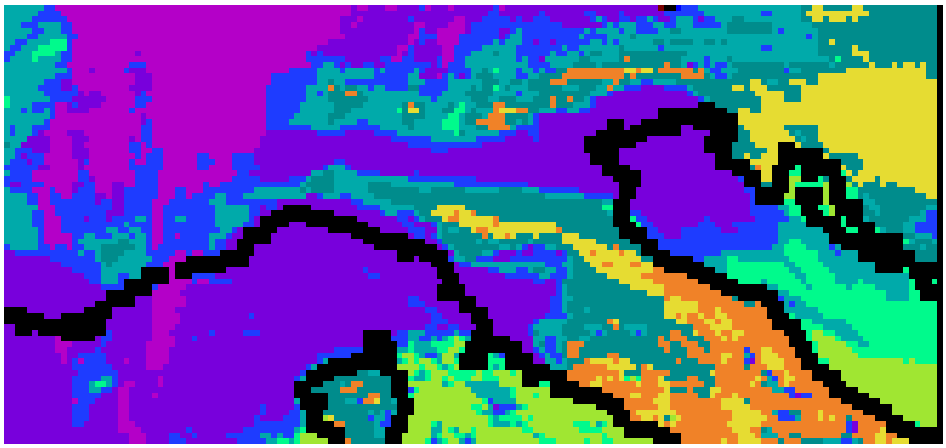

Figure 49: *Spectrally classified image for 6 February 2000, 12 UTC.*

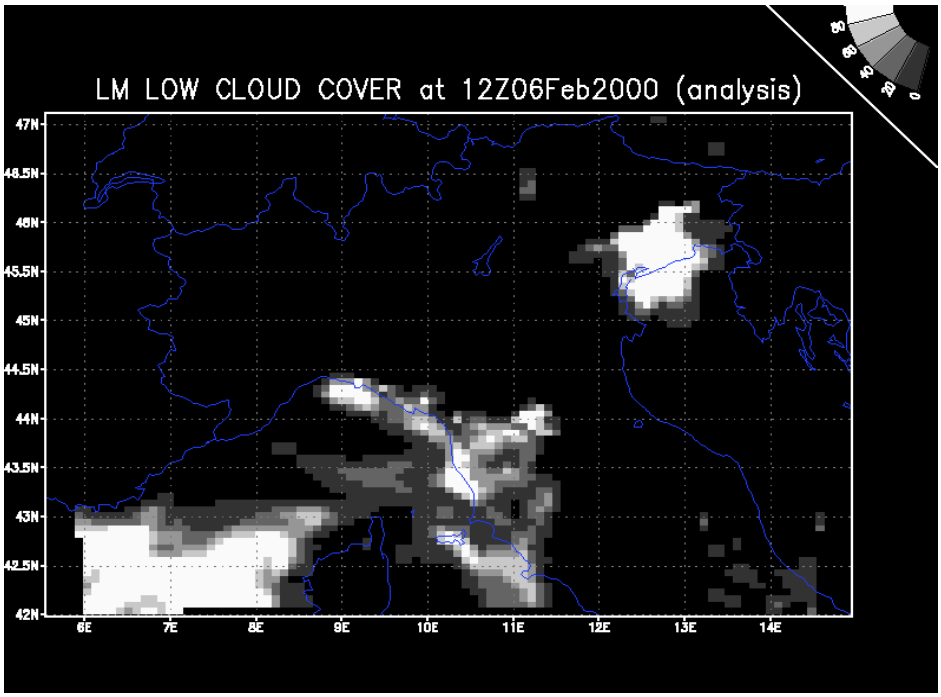

Figure 50: *LM low cloud cover at 6 February 2000, 12 UTC.*

Future Work

The spectral signature of clouds during one year (1999) over selected surfaces (for example Tyrrhenian sea) is scheduled. The aim is to deduce threshold values for IR and VIS counts in order to classify clouds not only according to their height (low, medium and high) but also by same WMO categories (Ci, Cb, St, etc.). This work will be done for different values of SZA and for different kind of surface (mountain, plain, etc). After that, verification of LM cloudiness will be performed.

References

Porcu, F., and Levizzani V., 1992: Cloud classification using METEOSAT VIS-IR imagery. *Int.J.Remote Sensing*, 13, 893-909.

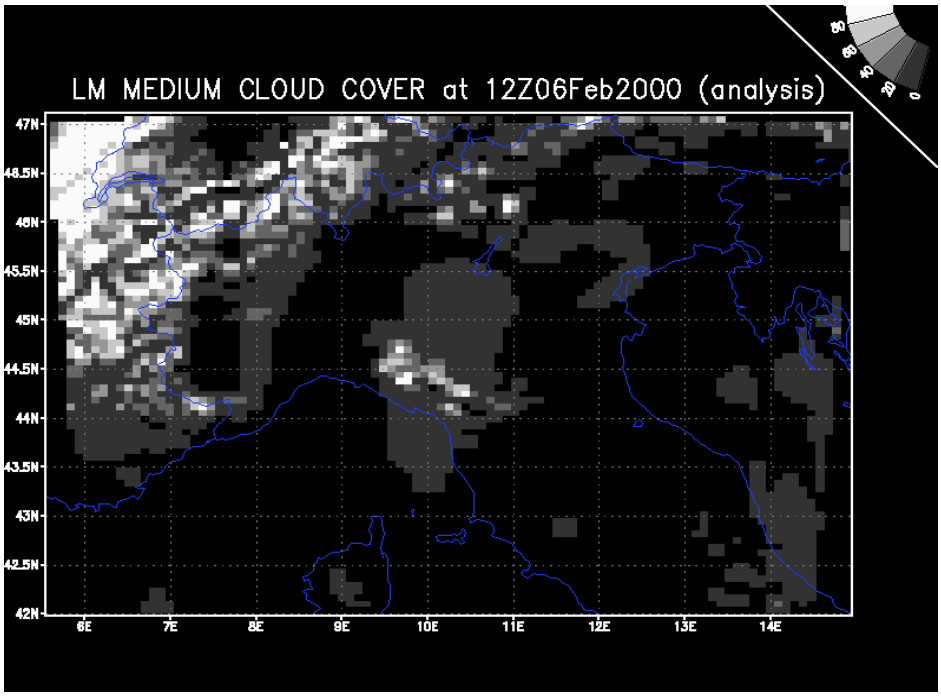

Figure 51: *LM medium cloud cover at 6 February 2000, 12 UTC.*

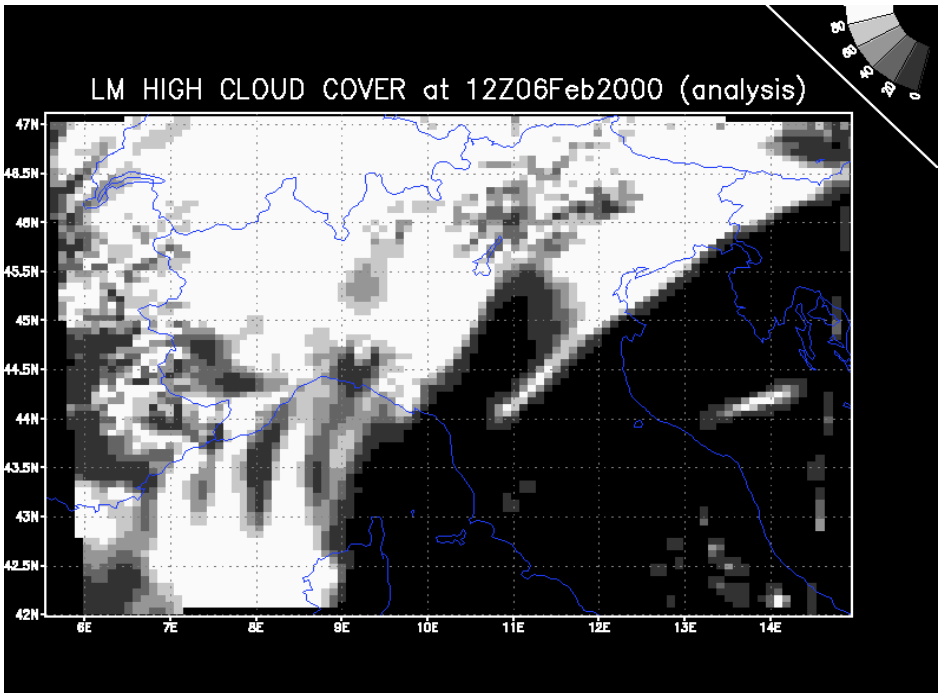

Figure 52: *LM high cloud cover at 6 February 2000, 12 UTC.*

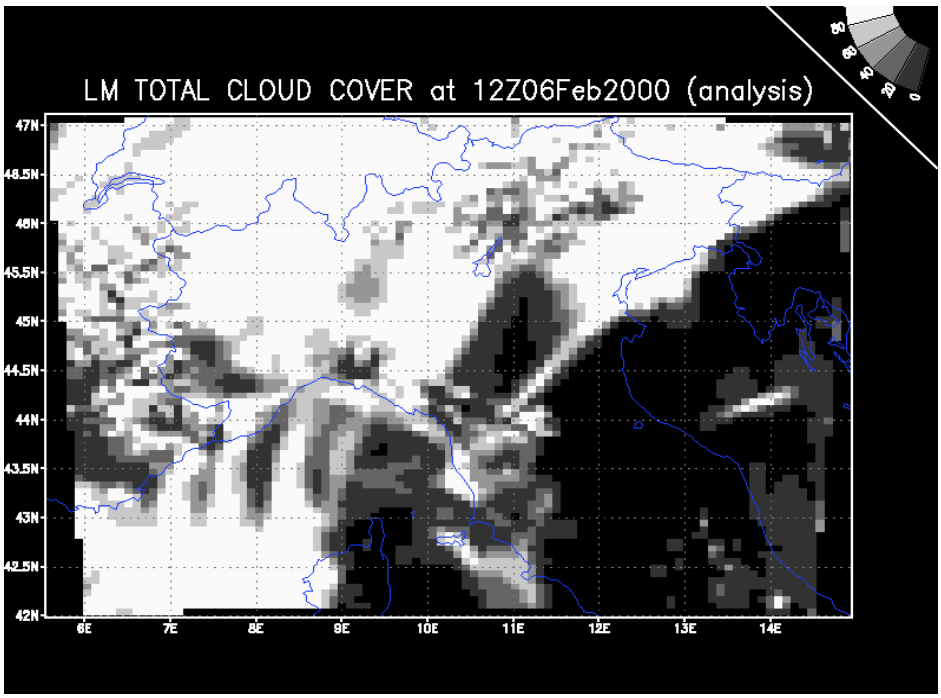

Figure 53: *LM total cloud cover at 6 February 2000, 12 UTC.*

8.5 Assessment of Model Performance

This section summarizes certain aspects of the general model behaviour in the operational application. Also, some conclusions on model deficiencies from the recent verification results as well as from diagnostic evaluations and from case studies are summarized.

(a) General

During the course of the operational and pre-operational applications of the LM at COSMO meteorological centres, the model has proven to run stable, robust and efficient. Only one blow-up (due to a CFL instability) for the Lothar Christmas Storm (24 December 1999) has been recorded up to now.

Also, no significant problems related to the lateral relaxation boundary conditions or to the use of nonhydrostatic dynamics have been encountered. In general the relaxation boundary conditions with an updating frequency of 1 hour work well despite of the quite large GME/LM grid spacing aspect ratio of about 1:9. Unlike for inflow boundaries, where the flow systems in general are adaptated consistently from the driving model (even for fast moving storm systems) problems may sometimes arise along the outflow boundaries whenever the inner solution evolves much different from the imposed solution of the driving model (e.g a faster movement of fronts or a different evolution of convective systems). As the two solution do not fit, the relaxation results in artificial divergence or convergence generating vertical accelerations. In such cases, this can produce narrow bands of clouds and precipitation along the lateral boundaries. However, any significant detrimental impacts on the inner solutions have not been observed so far.

Grid-point storm like effects have not been noticed up to now. This is a clear advantage compared to hydrostatic models, which at high resolution often tend to generate grid-point storms (which even may result in blow-ups) in case of convectively unstable stratification. Also, subgrid-scale convection seems to be reasonable represented by LM (but with known deficiencies); that is, no worrying problems have been encountered from using a large-scale convection scheme at 7 km grid-spacing in a nonhydrostatic dynamic framework.

The prediction of cyclones and of frontal clouds and precipitation is in general well simulated by the LM. Exceptions occur for large errors in position and timing of storm systems from the driving model along the lateral boundaries. A prominent example of miss-positioning of cyclones by GME is the Lothar Christmas Storm. Meanwhile, a revised data assimilation for GME has been introduced to cure this type of problem.

The simulation of convective systems such as squall-lines or air-mass thunderstorms seems to be of about the same quality as with the old hydrostatic model DM (or SM). Position and timing errors occur quite often, but a better localization of air-mass convection is achieved when topographical forcings are relevant. As with the old models, the diurnal cycle of convection is not well represented.

(b) Model Deficiencies

From the verification results for the last year, we can summarize some basic problems:

- Below frontal clouds, the 2m-temperature appears to be larger than observed (by up to about 4 K), and the temperature error moves with the cloud system. Thus, the simulated clouds seem to be too transparent for radiation.
- During nighttime the 2m-temperature has a quite large cold bias, especially during winter (this could also result from a too small amount of low clouds)
- The diurnal cycle of the 2m-dewpoint-temperature is not well captured.
- 10m-winds appear to be too high over Switzerland.
- The evaluation of monthly mean forecasts show a trend to decrease cloudiness with the forecast time. This can come from problems in the surface scheme, in the turbulence parameterization (PBL entrainment), or from numerical problems.
- Over regions with complex and steep topography (especially over the Alps), the simulated precipitation patterns are not very satisfactory. Within deep alpine valleys, the precipitation amount is strongly underestimated. On the other hand, there is an overestimation on the windward side and on the top of mountains.
- For typical Föhn situations with a southerly flow over the Alps, the corresponding subsidence in the regions north of the Alps seems to be overestimated. In autumn 2000, there were a large number of wrong precipitation forecasts for norther Switzerland and southern Germany due to a too strong Föhn effect which blocked fronts coming from southwest.

At the recent COSMO meeting, several new work packages have been defined to investigate these problems and to find short-term remedies (e.g., work on the cloud-radiation interaction, on the tuning of the new surface layer scheme, on a check of the water-mass budget and on positive definite advection schemes for humidity). The latter two problems in the list above seem to be related to more general deficiencies in the model formulation. The use of terrain-following coordinates implies that

(1) the errors in the pressure gradient term discretization increases with increasing steepness of topography at higher resolution,

(2) the errors in 3-d advection increase at higher resolution and

(3) the errors from horizontal diffusion will also increase.

Additionally, topographical structures on the grid-scale cannot be resolved by the dynamics, that is the flow around singular structures (which are alway present when using a mean topography) is never correctly represented and can be completely wrong. All these numerical errors drive and interact nonlinear with the physics, which for instance can result in a complete thermodynamical decoupling of deep valleys.

As short-term remedies for this problems, current work considers the introduction of a filtered topography (see Section 9.1), a reformulation of horizontal diffusion using monotonic and orographic flux limiting and the introduction of a horizontal averaging for convective forcings. On the long-term, we aim at the introduction of the z-coordinate using shaved element discretization to get rid of the numerical topography problem.

9 Research Reports

This section includes selected reports on special research topics as well as progress reports of the COSMO Working Groups.

9.1 Filtering of LM-Orography

Almut Gassmann
Deutscher Wetterdienst (DWD)
P.O. Box 100465, D-63004 Offenbach, Germany
almut.gassmann@dwd.de

1 Introduction

High resolution models often suffer from unrealistic forecasts in precipitation fields in mountainous areas. The LM exhibits large maxima in precipitation amount on the top of the mountains and conversely valleys are dry desert areas. In turn, the hydrological cycle will be modified in a strange way. This model behaviour is not confirmed by observations and obviously a fault.

Dynamics govern the precipitation forecast. We should test the dynamics on reliable flow fields in mountainous areas. In a study we examine four test cases. First, a mountain (height: 1500 m) is represented by only one gridpoint on a 7 km grid. Successively, the horizontal mesh size is reduced and the mountain is represented by more and more gridpoints. This refinement is done until the flow pattern doesn't change any longer. This state will be recognized as truth. From this study we deduce the height structure of a mountain that gives a reliable forecast.

With this result, we know whether the orography of the mountain should be smooth in some way. We can apply a filtering operation to the orography for the flow field will develop in a numerical clean way. As a result, the precipitation forecast should improve significantly. But this filtering operation should not damage meteorological important and correct information.

We examine the problem of horizontal resolution in relation with the precipitation field. Other problems with orography should also be mentioned. The circulation in valleys represented by only one gridpoint does not develop in a right way. Sometimes in winter, these gridpoints are completely decoupled from the dynamics and forcing is only done by radiation and horizontal diffusion. This may lead to unrealistic cooling in the valley.

2 Idealized Experiments

2.1 Configuration of Experiments

The configuration of idealized experiments is shown in the table below.

Number	Resolution	dlam dphi	zda	ie_tot	dt	i(hmax)
1	1*	0.0625	0.5	32	60	17
2	2*	0.03125	1	32	40	17
3	4*	0.015625	2	64	20	33
4	8*	0.0078125	4	128	10	65

Following values are used for all calculations.

- zhmax = 1500 m
- u = 10 m/s
- TSL = 5 ^{o}C
- 95% relative humidity in middle troposphere
- 6.5 K decrease of temperature / 1000 m
- 12 h forecast time

The mountain is represented by a bell shaped profile.

$$H(x,y) = \frac{zhmax}{(1+(\frac{x}{zda*dlam})^2+(\frac{y}{zda*dphi})^2)^{\frac{3}{2}}} \tag{1}$$

In the coarsest grid resolution, the mountain is represented by more than one gridpoint, but the height of the surrounding points beside the peak is negligible.

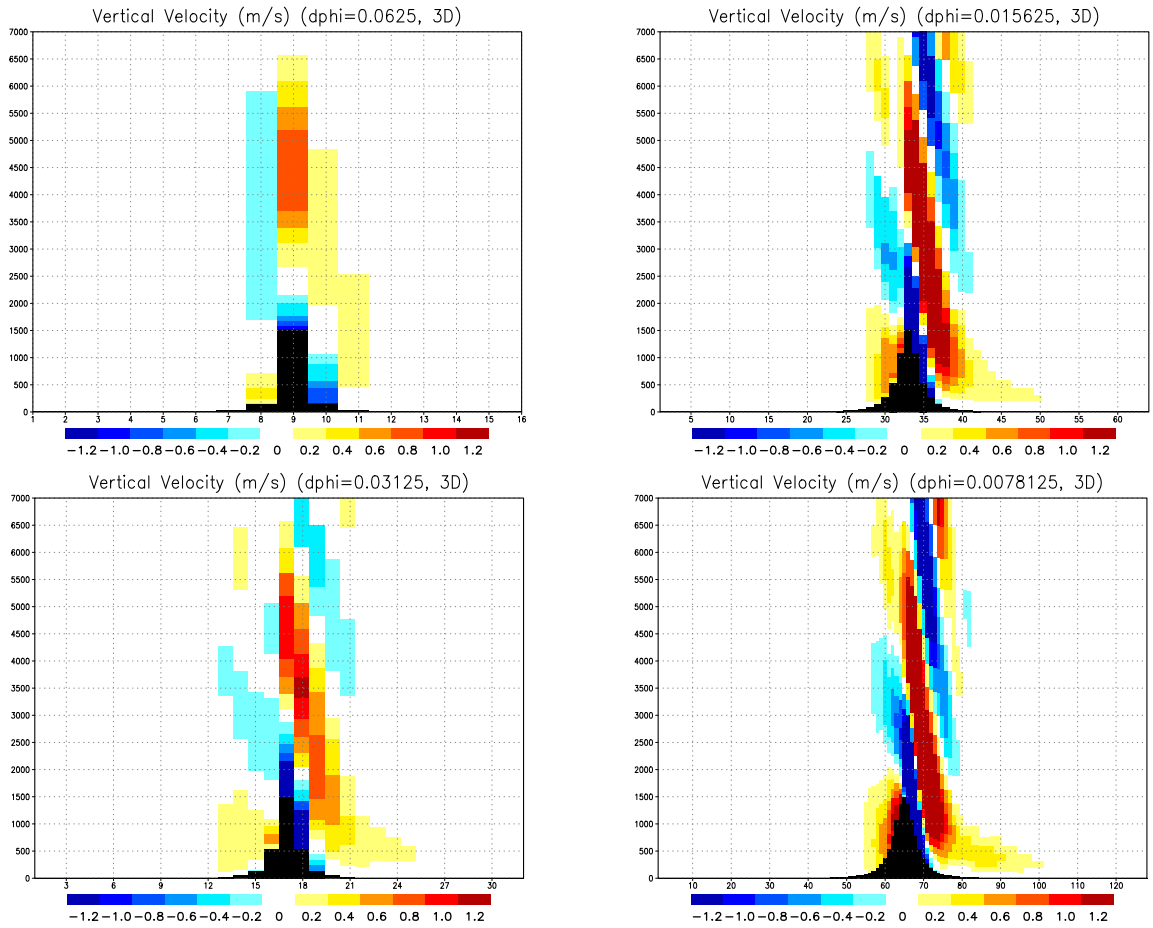

Figure 1: *Vertical velocities for different resolutions*

2.2 Results

A lee wave should develop in all experiments. Figure 1 shows the vertical velocity w in a vertical cross section. Mean flow is coming from the left. In all cases lee waves are forming, but their structures differ remarkably. Locations of maximum upwind areas in the two coarser resolution experiments do not coincide with the pattern formed with the finest resolution. But for the resolution with dphi=0.015625 the coincidence with the finest resolution flow is quite well. This is elucidated in figure 2 (top picture) showing the horizontal velocity u in the lowest model layer. Even negative u-values occur for coarser resolutions. The disturbed flow area is larger for coarser resolutions. Other model layers show similar results. The vectors of horizontal velocity in the lowest model layer (figure 3) give an impressive picture of different scales of the flow in different resolutions. In a coarse resolution, flow patterns are translated to a larger scale. This is not in common with the true solution.

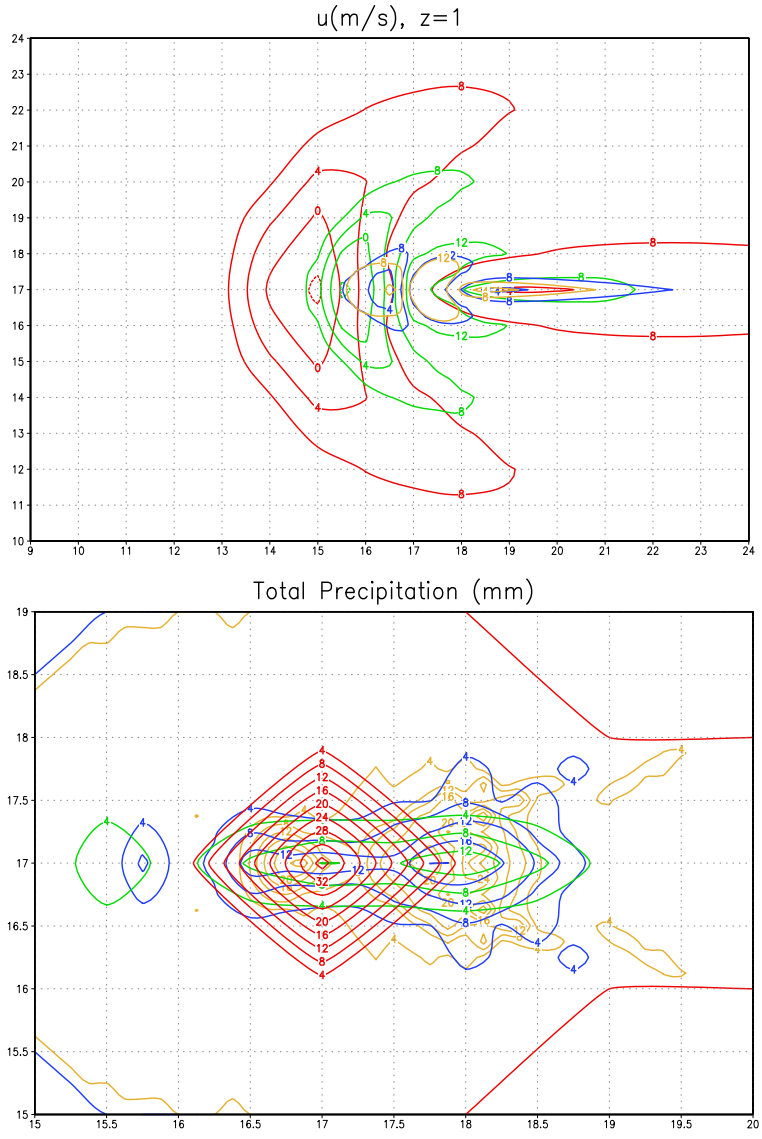

Figure 2: *Horizontal velocity u in the lowest model layer (top) and precipitation after 12 hours (bottom) for different resolutions;*
red: dphi=0.625, green: dphi=0.03125, blue: dphi=0.015625, yellow: dphi=0.0078125

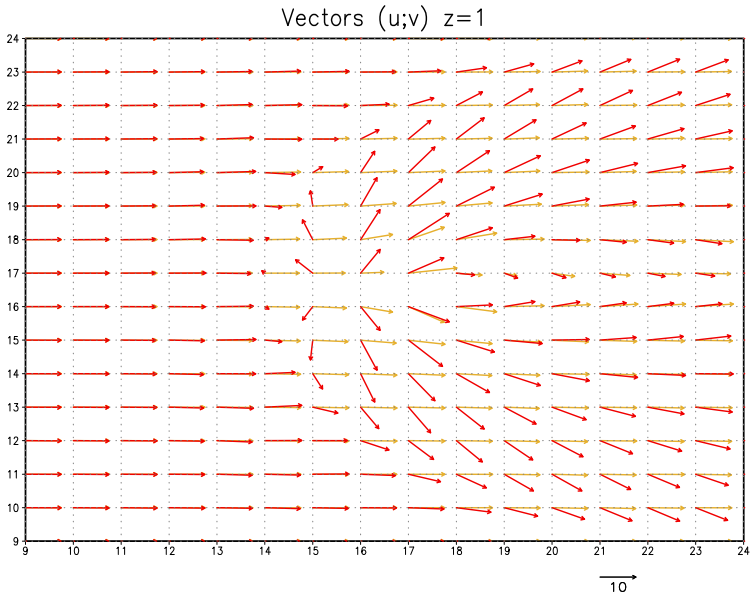

Figure 3: *Vectors of horizontal velocity in the lowest model layer. Colors as in figure 2.*

Precipitation amount should converge to the true solution if mesh size is refined. But if the flow is not in the correct scale, precipitation field (figure 2 bottom picture) is neither. But as with the flow field, convergence is achieved from the resolution of dphi=0.015625. Due to the false representation of vertical velocity maximum on the top of the mountain, the coarsest resolution has a peak in precipitation just there. The overall precipitation amount is very different in the two coarser resolution cases from that of the two finer resolution cases which have an almost equal precipitation amount. A table shows the overall precipitation amount after 12 hours related to that of the finest resolution case (100%).

Number	Resolution	Precipitation amount [%] related to the finest resolution
1	1*	118
2	2*	60
3	4*	98
4	8*	100

We can conclude: A steep mountain represented by only one gridpoint is not able to produce a realistic flow pattern and, in turn, is not able to produce the right precipitation field. This error appears the more dramatic, the steeper the mountain is. Only a four times finer resolution can give a reliable solution, because it provides a sufficient number of degrees of freedom.

3 Filtering of Orography

The desired filter for orography should smooth all small scale structures until a grid size of $4\Delta x$. A suitable filter is the filter of Raymond (1988). It is very selective for short waves and does not damp the longer waves. This characteristic is controlled by the order of the filter and the filter parameter ϵ. The filter is defined by

$$[S^{2p}]u_n^F + (-1)^p \epsilon [L^{2p}]u_n^F = [S^{2p}]u_n. \tag{2}$$

In that, u_n are the original values of the field, u_n^F are the filtered values. The operators S and L are the sum operator and the finite difference operator of an order given by $2p$, ϵ is the filter parameter. From the amplitude response function

$$F(l) = \left(1 + \epsilon \tan^{2p}\left(\frac{\pi}{l}\right)\right)^{-1} \tag{3}$$

we know the properties of the filter. Here, the function is written in dependency of l, the wave length in gridpoints. Figure 4 shows the amplitude response function for different orders and different filter parameters. A suitable configuration for our aim is a 10th order filter with $\epsilon = 10$.

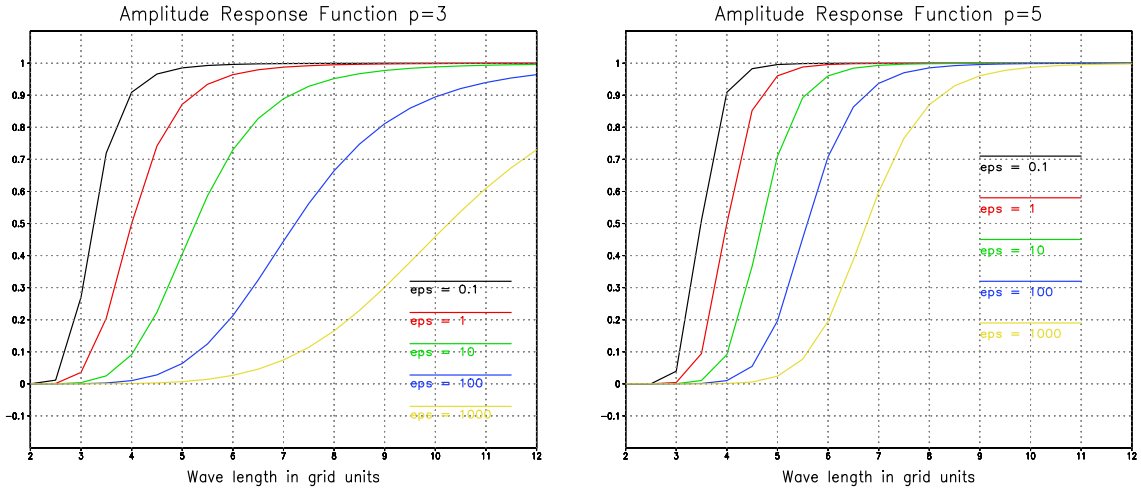

Figure 4: *Amplitude response functions for different filtering parameters*

The idealized mountain on the grid with dphi=0.0625 from the previous section will then be filtered in the following way. It will be represented by 5 gridpoints with a maximum height of 640 m. The structure is similar to that of the mountain in experiment 3 from the previous section, but on a larger scale. This height structure is sufficient to produce a realistic flow.

Figure 5 shows the original and the filtered orography of the Alps for the LM with the mesh size of 7 km. The original curve in Figure 6 is an example with a valley and a mountain represented by only one gridpoint each. After filtering, all valleys and all mountains provide enough degrees of freedom (gridpoints) for the proper flow field.

This filter produces, like many other filters, so called Gibbs phenomena. These oscillations near steep gradients have only a small amplitude, but can cause systematic errors. Consequently, the height of gridpoints over sea (land-see-mask smaller than 0.5) surrounded by at least 4 other sea gridpoints is set to the original value after filtering. Additionally, the sign of filtered orography should be the same as the original sign, otherwise height is set to the original value too.

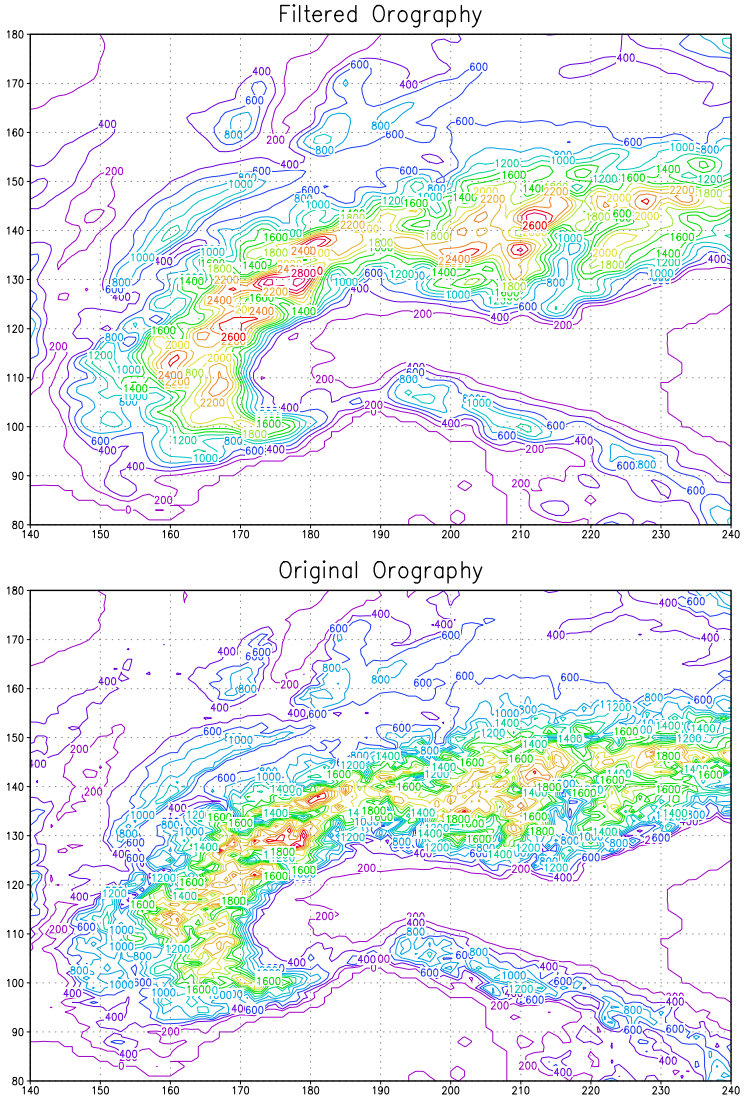

Figure 5: *Orography of the Alps (mesh size 7 km)*

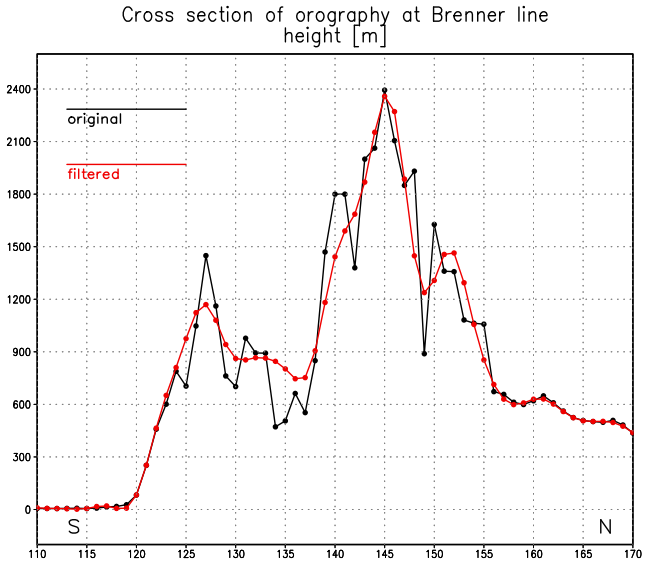

Figure 6: *Cross section of orography in the Alps along the Brenner line*

4 Realistic experiments

We carried out an experiment for 8th of February 2000 and compared it with the routine run (figure 7). The routine run exhibits the well known features with unrealistic minima and maxima in the precipitation field in the Alps. In contrary, a smooth field can be found in the experimental run. Larger scale precipitation patterns are the same in the experimental and the routine run. The mean value of precipitation in both runs is the same, whereas the maximum and the variance of precipitation drops to one half in the experimental run with filtered orography. The new field seems to be much more realistic than the routine one. There is no loss of reliable information. In regions outside the high mountains, differences are negligible. This filtering has a positive influence on the hydrological cycle and the prediction of precipitation as well as on other dynamically driven processes.

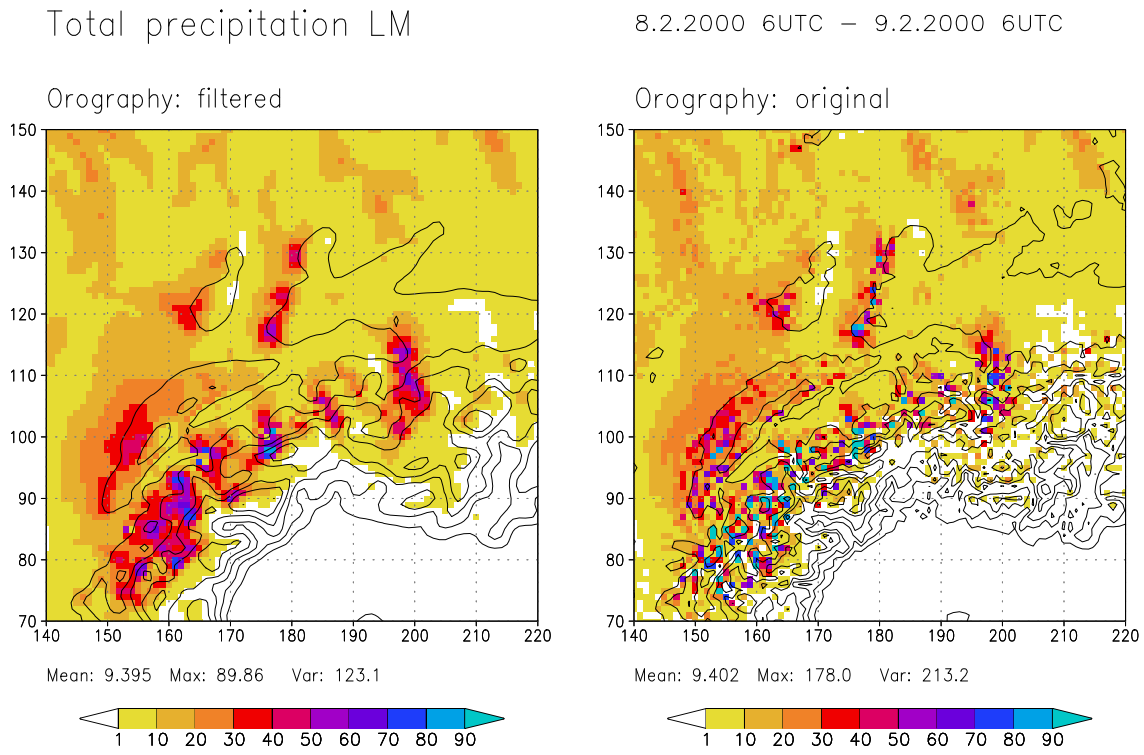

Figure 7: *Precipitation fields of experiments with and without filtered orography.*

Another test case was the Christmas storm "Lothar" on 26th of December 1999 (figure 8). Here, we wanted to test the LM with the filtered orography with an extreme weather situation. Provided the right boundary values, wind maxima and sea level pressure are as well recognized as in a comparable run. The local patterns of wind maxima seem reasonable and are similar to those in a comparable run. Filtered orography does not remove any meteorological relevant information.

5 Conclusion

This study gave us a positive result. The real numerical resolution of phenomena is on a larger scale than the grid scale. Forcing below the scale of numerical resolution is not only without any sense, it even causes errors by translating the response to larger scales. By filtering orography, the forcing scale is comparable to the numerical resolvable scale. Important information is retained and structures that could produce false information are not forced. There is a necessity to filter the orography.

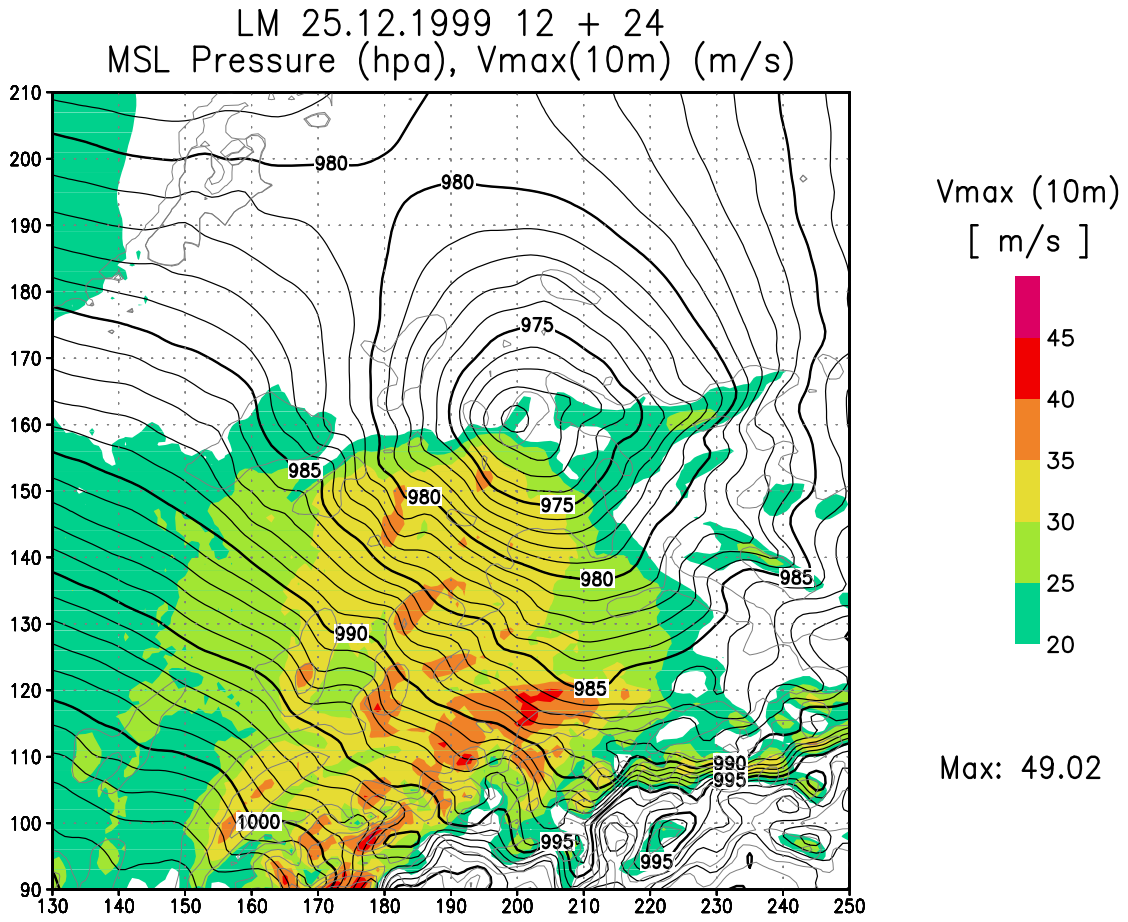

Figure 8: *Christmas storm "Lothar"*

6 References

Raymond, W.H. 1988: High-order low-pass implicit tangent filters for use in finite area calculations. *Mon. Wea. Rev.*, **116**, 2132-2141.

9.2 Variational Soil Moisture Analysis with First Operational Results

Reinhold Hess
Deutscher Wetterdienst (DWD)
P.O. Box 100465, D-63004 Offenbach, Germany
reinhold.hess@dwd.de

1 Introduction

Model forecasts for screen–level values of temperature and relative humidity depend during clear–sky days (i. e. low cloudiness and high radiative impact) strongly on the specified soil water contents, that determine the relationship between sensible and latent heat fluxes. Inaccurate values can result in temperature forecast errors up to several degrees centigrade. An often experienced cold bias of the previously operational forecast model DM of DWD during early sunny spring days results from unrealistic high evaporative fluxes caused by overestimated soil moistures contents (compare Rhodin et al., to appear). Moreover, on longer time scales the entire hydrological budget of the simulation is influenced. E. g. Schär et al. (1999) report that model–precipitation climatology heavily depends on soil moisture contents in summertime.

Since representative measurements of soil moisture contents are rarely available, its initialization is a severe problem in numerical weather forecasts. Up to now the soil moisture fields of the DM and also of the new operational Local Model LM were never analyzed by observations: Rather, they are free–running and only influenced by the hydrological balance between precipitation, evapotranspiration, and water runoff using a bucket soil model.

Currently two soil layers are implemented in the LM: The moisture content of the top layer (thickness 0.1 m) prescribes the evaporation of bare soil. The the wetness of the root layer (thickness 0.9 m) provides the transpiration by plants, that becomes the dominant part of evapotranspiration in summertime. The two soil layers exchange water due to gravity and capillary forces. Because only variations are used to compute the soil moisture contents, a drift to inaccurate values is unavoidable in longer time scales.

The need for soil moisture initialization without representative measurements has led to the development of indirect solutions. In case of high solar radiative impact, screen–level temperature and relative humidity strongly depend on the specified soil moisture contents. This soil–atmosphere coupling can be used to exploit information on the soil moisture contents from synoptic measurements. Mahfouf (1991) compared two methods of soil moisture analysis that use near surface observations of temperature and relative humidity: The first, optimal interpolation, adds increments with statistically derived soil–atmosphere dependencies to the moisture fields and the second, variational analysis, retrieves soil moisture contents as minimum of a cost functional that expresses the differences between model derived and observed screen–level values. The variational method is potentially superior, since it is possible to take nonlinear soil–atmosphere dependencies into account, however it is computationally more expensive and the application to general weather conditions including precipitation and cloudiness is difficult (Bouyssel et al., 1998).

For these reasons the optimal interpolation method has been applied in some NWP–centers (e. g. at Météo–France, Giard and Bazile, 1997). Approaches to derive soil moisture contents by use of satellite data exist as well (Bart et al., 1997), however further research is necessary for operational application.

At DWD a variational soil moisture analysis (SMA) has become operational in March 2000 for the two soil layer of the Local Model LM. It is applied once per day in order to provide improved soil moisture fields to be used for the next forecast. Because the soil–atmosphere coupling is not always strong enough to compute the soil moisture contents accurately in operational conditions, a background state along with background error estimates is incorporated. The background and its error variances and covariances are updated in a Kalman–filter–like cycled analysis that takes an assumed model error into account. In case of low radiative impact, the retrieved moisture fields remain close to the background and the background errors increase. High radiative forcing, on the other hand, results in improved moisture fields and reduced background error estimates. The variational Kalman–filter analysis requires only one additional short–term forecast for each analyzed soil moisture layer and does not depend on a specific soil model nor on physical parameterizations. Tangent linear or adjoint models are not required.

By their indirect determination the soil moisture fields are basically adapted so that the model forecasts of near surface temperature and relative humidity approximate the observed values. General forecasts errors that are not related to soil moisture (e. g. misspecification of cloudiness, errors in radiation and boundary layer parameterizations) are likely to be reflected in errors of the retrieved values therefore. Consequently, the method SMA developed at DWD does not attempt to provide accurate and realistic moisture fields, but uses the soil moisture values to some extend to compensate for biases in the physical parameterizations. In this way the forecasts are improved and the computed heat and moisture fluxes at the bottom of the atmosphere model are likely improved as well.

The outline of the paper is as follows: Section 2 gives an overview of the variational soil moisture analysis SMA. Section 3 provides results for a six week experiment with soil moisture analysis and comparisons to routine forecasts. Section 4 gives conclusion and outlook.

2 Variational Soil Moisture Analysis

The optimal soil moisture contents minimize a cost functional that expresses the differences between model derived and observed screen–level values. This method is potentially superior to optimal interpolation, since the actual soil–atmosphere dependencies for the present synoptic and seasonal meteorological conditions are computed instead of statistically derived average values. Nonlinear dependencies are taken into account in this way (Mahfouf, 1991, Bouyssel et al., 1998). On the other hand the computational costs of variational methods are higher and the concrete set up (e. g. the definition of the background weights) in order to achieve stable and robust results in an operational environment is more complex.

To reduce the computational costs of the variational analysis, horizontal soil–atmosphere couplings are neglected, see Section 2.1, and the minimization of the cost functional is computed directly without need for an iterative solver, see Section 2.2 . Background fields are used to stabilize the soil moisture retrieval and the background weights are computed in a Kalman–filter scheme using the previous analysis error covariance matrix and an assumed soil model error, see Section 2.3 .

2.1 Horizontal Decoupling

The minimization problem is of high dimension in general; the moisture contents of each vertical grid column of every soil layer has to be retrieved. However, since the screen–level values for temperature and relative humidity are mainly vertically coupled to the soil moisture contents, horizontal decoupling is assumed. In this way, the high–dimensional minimization problem reduces to a large series (i. e. one minimization for each vertical grid column) of

low–dimensional minimizations and the computational requirements are essentially reduced.

In order to confirm the assumption of horizontal decoupling, every second point of an original moisture field of the top layer is decreased by 20 kg/m^2 in a chessboard–like way (see Figure 1, left). An experimental 3–hour forecast starting at 12 UTC with this field shows chessboard–like variations of 2 m–temperature compared to the original forecast (right). At grid points with reduced soil moisture content the 2 m–temperature is increased, whereas it remains almost stable at undisturbed points, which shows weak coupling to the surrounding grid points. The horizontal resolution of this experiment is 14 km and the near surface wind speed ranges between 5 and 10 km/h.

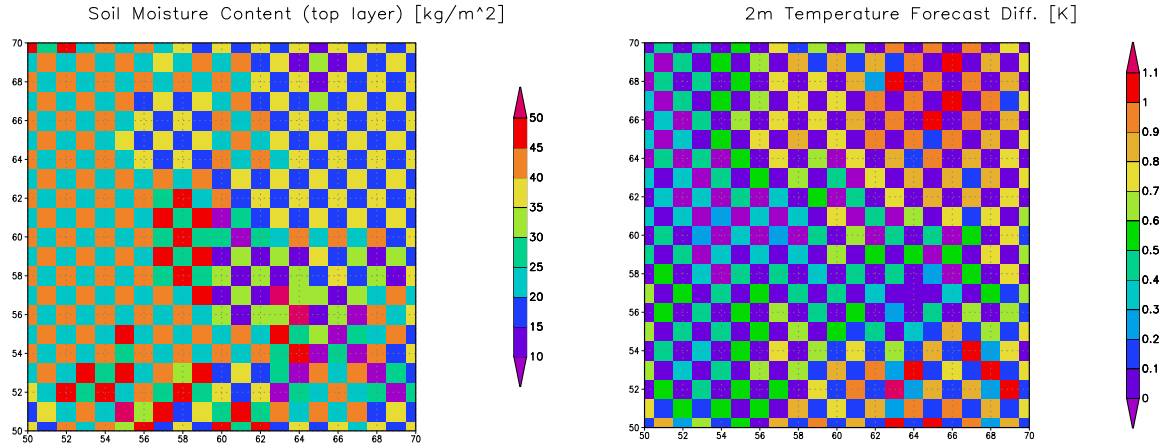

Figure 1: *Chessboard–like reduced soil moisture content of top soil layer (left) and resulting variation of 3–hour 2 m–temperature forecast (right).*

2.2 The Cost Functional

Assuming horizontal decoupling, the formulation of the variational soil moisture analysis scheme is given for an arbitrary horizontal grid point in the following. Let η and η^b denote vectors containing the moisture contents of the n^{soil} analyzed soil layers[1] and their background states, respectively. The vector T^o of length n^{obs} contains synoptic 2 m–temperature observations that are interpolated to model grid points[2] at specified observation times[3]. Vector $T(\eta)$ consists of corresponding values from a short–term forecast that started at 0 UTC with soil moisture fields η. Observations of relative humidity are not considered here, but can be included in the cost functional and assimilated likewise.

The cost functional $\mathcal{J}$ to be minimized at each analysis step (i. e. daily) reads

$$\mathcal{J}(\eta) = \mathcal{J}^o(\eta) + \mathcal{J}^b(\eta) \tag{1}$$

with observation term

$$\mathcal{J}^o(\eta) = \frac{1}{2}\Big(T^o - T(\eta)\Big)^T \mathbf{R}^{-1} \Big(T^o - T(\eta)\Big) \tag{2}$$

and background term

[1] Currently two soil layers are analyzed within the LM.
[2] Interpolation to grid point space is performed using successive correction with height adjustment.
[3] Since the soil-atmosphere coupling is strongest with high radiative impact, observations at 12 and 15 UTC are assimilated.

$$\mathcal{J}^b(\eta) = \frac{1}{2}(\eta - \eta^b)^T \mathbf{B}^{-1} (\eta - \eta^b) \quad , \tag{3}$$

with $ADP \leq \eta_j \leq PV\,, \quad j = 1, \ldots, n^{soil}$. The components of η (indicated with lower indices) are limited by air dryness point (ADP) and pore volume (PV) of the soil type of the grid point in concern. Matrix $\mathbf{R}$ denotes the observation error covariance matrix, which is diagonal and includes constant observation error variances.

The background term $\mathcal{J}^b(\eta)$ provides information from the past and is necessary to stabilize the soil moisture retrieval and to reduce undesirable daily variation in the soil moisture analysis (Rhodin et al., to appear). The soil–atmosphere coupling by itself is not every day strong enough to derive the soil moisture contents accurately. If the coupling is weak (for low radiative impact) the analyzed fields stay close to the given background.

Matrix $\mathbf{B}$ is the background error covariance matrix, which is symmetric and positive definite for physical reasons. Its relation to $\mathbf{R}$ prescribes the sizes of the resulting analysis increments (for defined 2 m–temperature–soil moisture dependencies). Background values η^b and background error covariance matrix $\mathbf{B}$ are computed within the Kalman–filter cycling, see Section 2.3 .

Minimization of $\mathcal{J}$ results in the analyzed soil moistures η^a. Although the soil moisture–2 m–temperature dependency is nonlinear in general, linearization around the background state provides good approximations as long as the retrieved values are not too far from the background state. Linearization of the model 2 m–temperatures $T(\eta)$ around η^b gives

$$T(\eta) \doteq T(\eta^b) + \mathbf{\Gamma}\,(\eta - \eta^b) \quad , \quad \text{with} \quad \mathbf{\Gamma} = \nabla T\Big|_{\eta=\eta^b} \quad , \tag{4}$$

where the Jacobian $\mathbf{\Gamma}$ is approximated by one–sided finite differences. This approximation requires n^{soil} additional forecast runs with varied soil moisture contents. Because of horizontal decoupling, $\mathbf{\Gamma}$ is computed for all horizontal grid points simultaneously.

Using the linearization (4) the gradient of the cost function can be analytically expressed as

$$\nabla\mathcal{J}(\eta) = -\mathbf{\Gamma}^T \mathbf{R}^{-1} \left(T^o - T(\eta^b) - \mathbf{\Gamma}\,(\eta - \eta^b)\right) + \mathbf{B}^{-1}\,(\eta - \eta^b) \quad . \tag{5}$$

For the low–dimensional minimization problem it is highly efficient to solve $\nabla\mathcal{J}(\eta^a) = 0$ directly rather than performing several steps of an iterative method. Little calculus gives the minimum directly as

$$\eta^a = \eta^b + \left(\mathbf{\Gamma}^T \mathbf{R}^{-1}\mathbf{\Gamma} + \mathbf{B}^{-1}\right)^{-1} \mathbf{\Gamma}^T \mathbf{R}^{-1} \left(T^o - T(\eta^b)\right) \quad . \tag{6}$$

Worth to mention that the applied minimization by linearization and direct solution is no degradation in accuracy of the retrieved soil moisture fields.

2.3 Kalman–filter Cycling

The cycled soil moisture analysis is performed daily. Background state $(\eta^b)^{t+1}$ and background error covariance matrix $(\mathbf{B})^{t+1}$ for the following day are computed in a Kalman–filter–like scheme[4] (the valid times of the variables η^a, η^b, $\mathbf{A}$, and $\mathbf{B}$ are from now on indicated by upper indices outside brackets).

[4] At the initial start of the cycled scheme η^b and $\mathbf{B}$ have to be initialized with first guess moisture fields that are used as initial background and estimates for their error variances and covariances, respectively.

The background $(\eta^b)^{t+1}$ is computed as

$$(\eta^b)^{t+1} = (\eta^a)^t + \left(M_t^{t+1}((\eta^b)^t) - (\eta^b)^t \right) \quad , \tag{7}$$

where $M_t^{t+1}((\eta^b)^t)$ are the 24 h model values that result from the routine forecast that is started at 0 UTC with background fields $(\eta^b)^t$. Changes in soil moisture contents by precipitation, evapotranspiration, and water runoff during the 24 hours are taken into account in this way.

The confidence in the retrieved values $(\eta^a)^t$ is given by the analysis error covariance matrix $\mathbf{A}$,

$$(\mathbf{A})^t = \left(\nabla^2 \mathcal{J} \right)^{-1} = \left(\mathbf{\Gamma}^T \mathbf{R}^{-1} \mathbf{\Gamma} + ((\mathbf{B})^t)^{-1} \right)^{-1} \quad , \tag{8}$$

which is the inverse of the Hessian of $\mathcal{J}$ (e. g. Tarantola, 1987). In case of weak soil–atmosphere coupling ($\mathbf{\Gamma} \approx 0$) matrix $(\mathbf{A})^t$ almost equals the background error covariance matrix $(\mathbf{B})^t$. The higher the soil–moisture–2 m–temperature dependence is, the smaller the estimated analysis errors become.

The new background error covariance matrix $(\mathbf{B})^{t+1}$ finally is computed as

$$(\mathbf{B})^{t+1} = \mathbf{M} \, (\mathbf{A})^t \, \mathbf{M}^T + \mathbf{Q} \quad , \tag{9}$$

where matrix $\mathbf{M}$ is an estimation of the tangent linear of the forecast operator M_t^{t+1}. Matrix $\mathbf{Q}$ expresses the assumed error of M_t^{t+1}. This additive term reduces the sensitivity of the background to past observations and is important to keep the retrieved moisture contents variable in long–term cycled analyses. In this way, the soil moisture contents are adapted every day so that they would have provided optimal forecasts during the previous days. The weighting of older dates is reduced through $\mathbf{Q}$.

3 Results

An experiment with soil moisture analysis for a six–week period in May/June 1999 was carried out for the LM and the results are compared to routine forecasts without soil moisture adaptation. The selected period comprises severe weather conditions in order to prove the stability of the method as well as clear–sky days with high radiative impact to show the benefits. Comparisons of the retrieved moisture values to measurements are available.

An experiment with soil moisture analysis for the period May 1 until June 15 1999 was carried out that included a complete assimilation cycle based on the adapted soil moisture contents. Figure 2 (left) displays rmse and bias of experiment and routine forecast for all landpoints (beside 10 boundary lines) of the LM–domain. Short wave net radiation and total precipitation are given in Figure 2 (right) in order to asses the weather situation.

Especially for the days with high radiative impact (May 16 until May 21 and May 24 until June 3) the rmse has truly declined for the experiment compared to the routine forecast. The biases of experiment and routine forecast are small and become negative for sunny days. The soil moisture analysis reacts soon and reduces the cold bias that results from overestimated evapotranspiration further on essentially.

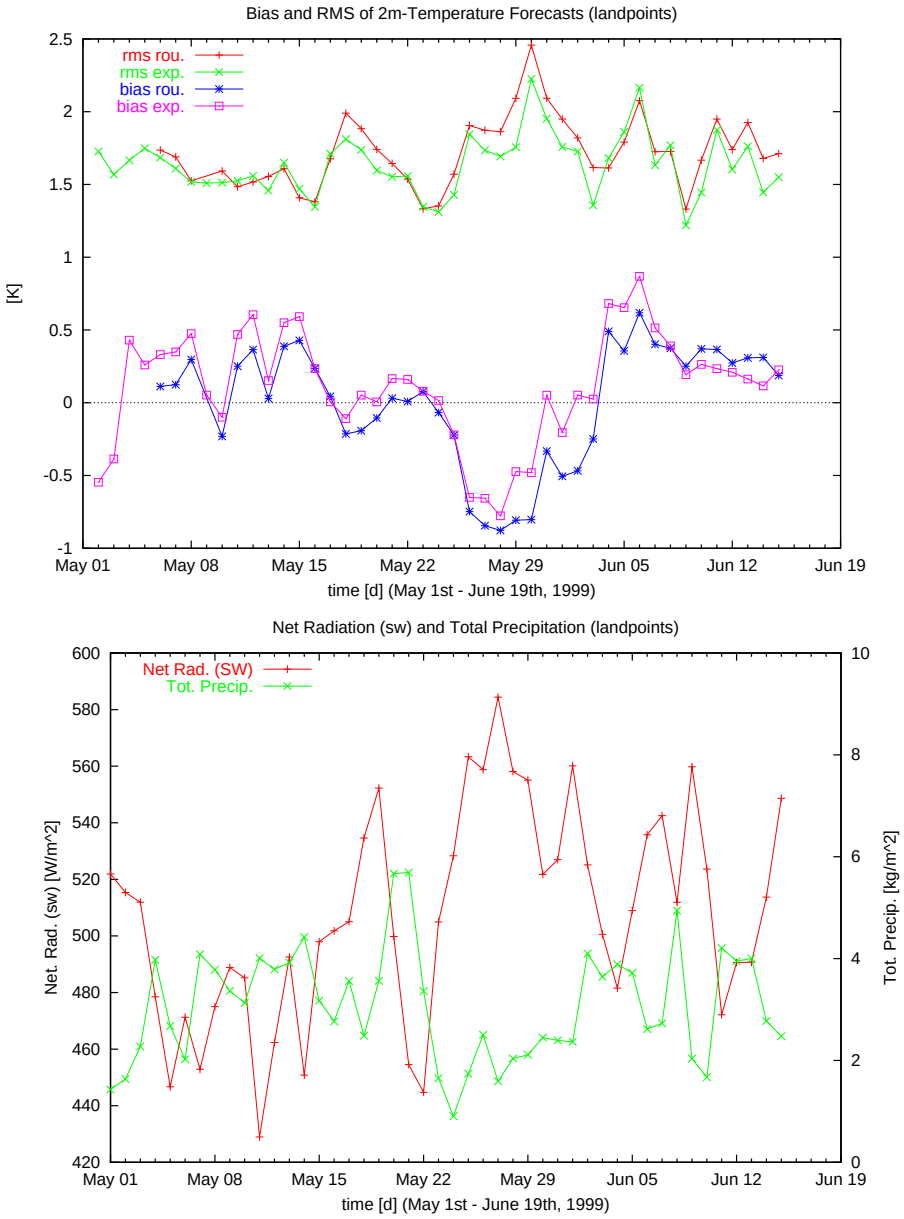

Figure 2: *RMSE and Bias of experiment with SMA and routine, statistic of all landpoints (beside 10 boundary lines) within LM–domain (top). Short wave net radiation (averaged between 9 and 15 UTC) and total 24 h precipitation (bottom).*

Figure 3 shows measured soil moisture values of meteorological observatory Lindenberg and averages of 4 surrounding LM–gridpoints of experiment and routine forecast for top layer (left) and bottom layer (right).[5] The vertical lines of the experiment data are variations of soil moisture contents introduced by the analysis (analysis increments), the lines from left to right represent changes of the soil model within the forecast due to precipitation, evaporation, and runoff (model increments).

[5]The displayed soil moisture values are very local and especially the absolute value of the measurements has to be considered with care.

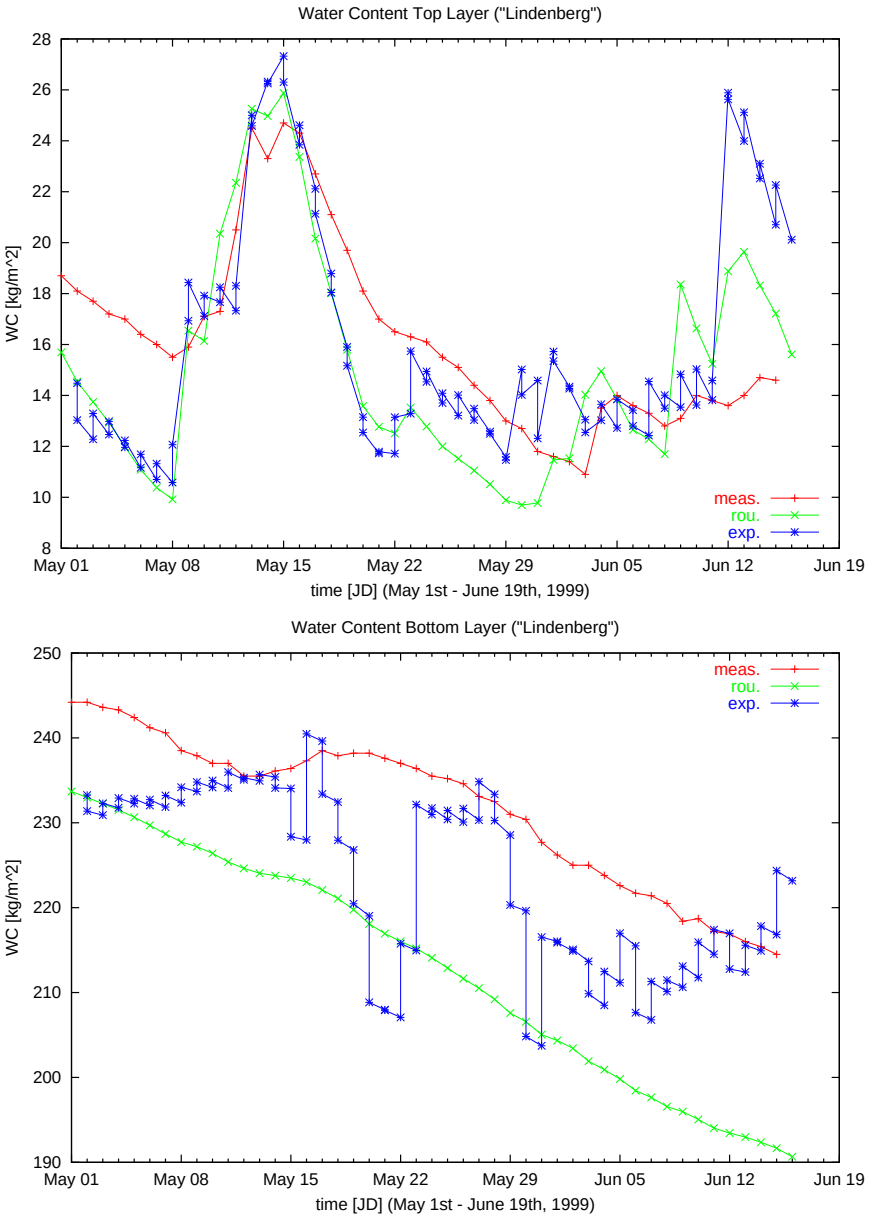

Figure 3: *Soil moisture contents measured at meteorological observatory Lindenberg and model values of the 4 surrounding LM–gridpoints of experiment and routine. Top layer (left) and bottom layer (right).*

The soil moisture analysis reacts reasonably to the weather conditions and forecasts errors given in Figure 2 . The negative analysis increments during the clear–sky periods from May 17 until May 20 and May 28 until May 30 reduce overestimated evapotranspiration and negative bias in subsequent experimental forecasts.

The large variations especially for the bottom layer and the strong moisture increase (e. g. for May 22 and 23) result from general model errors (e. g. misspecification of cloudiness) the soil moisture analysis SMA tries to compensate. The comparison to measurements should be taken carefully, since measurements are known to be very little representative. Nevertheless, Figure 3 shows that the analyzed values still reside in realistic ranges.

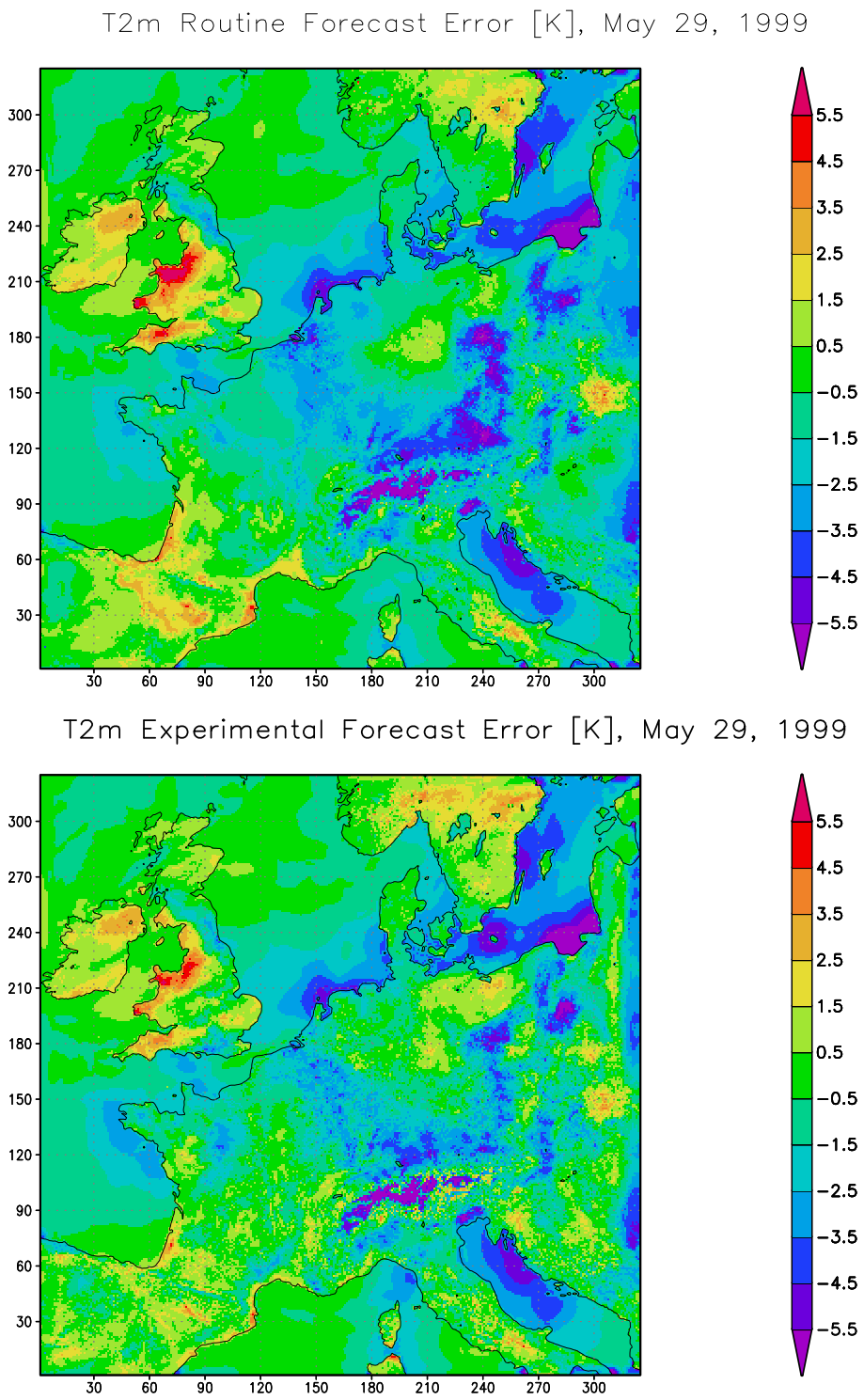

Figure 4: *Forecasts error distribution of 2 m–temperature averaged over 12 and 15 UTC. Routine forecast (top) and experiment (bottom) starting from 0 UTC, May 29 1999.*

Forecast error distributions (forecast values $T(\eta)$ versus interpolated observations T^o) of 2 m–temperature (averaged over 12 and 15 UTC) of experiment and routine forecast starting at 0 UTC, May 29 1999 are displayed in Figure 4 (top and bottom, respectively).

In large parts of central Europe the negative bias of the routine forecast has considerably improved in the experiment. However, there are not only warmer temperature forecasts due to reduced soil moisture contents, also reduced temperatures from increased moisture values (e. g. in Spain) exist.

4 Conclusion and Outlook

The variational soil moisture analysis SMA has proven stability and positive impact on 2 m–temperature forecasts during a six–week experiment from May 1st until June 19th 1999 and in several other experiments not mentioned here. It has become operational within the LM at DWD in March 2000.

Misspecification of model cloud cover and radiation is regarded as most harmful problem for SMA. An overestimation of radiative impact leads to incorrectly high 2 m–temperature–soil moisture dependencies and to large erroneous analysis increments that try to compensate forecast errors that does result from inaccurate radiative impact. Since in most cases the cloud cover is sufficiently accurate, the soil moisture values are improved. The use of background values in the cost function relates the analyzed moisture contents to history and model errors average out to some extent. Although experiments have shown improvement in general, cloud cover analyses based on satellite data are prepared daily in order to perform monitoring and long time studies.

SMA has been set up in order to improve near surface temperature forecasts rather than computing real and accurate soil moisture contents. The comparison to measurements shows, that the retrieved moisture values are nevertheless in realistic ranges. Further adaptation especially in combination with the currently developed improved soil and boundary layer models of the LM will take place. It is assumed that the large artificial variations of the moisture contents will reduce with improved model physics.

Further improvements of SMA concerning the usage of analyzed precipitation and cloud cover in order to provide accurate model increments and radiative impacts are under concern.

Acknowledgments
The work was carried out within the EU–Project NEWBALTIC–II. Thanks to colleagues who contributed to this work: Mr. Buchholt implemented the 2 m–temperature analysis, Mr. Hanisch supported the environment for executing SMA operationally and Mrs Kirchner provided a set of soil moisture measurements from meteorologic observatory Lindenberg. Thanks also to Dr. Wergen for discussions and for reading the manuscript.

5 References

B. J. J. M. van den Hurk, W. G. M. Bastiaanssen, H. Pelgrum, and E. van Meijgaard: *A New Methodology for Assimilation of Initial Soil Moisture Fields in Weather Prediction Models Using Meteosat and NOAA Data*, J. App. Met., vol. 20, no. 11, pp. 1271–1283, November 1991.

F. Bouyssel, V. Cassé, and J. Pailleux, *Variational Surface Analysis from Screen Level Atmospheric Parameters*, Tellus, 51 A, 4, 1999.

U. Callies, A. Rhodin, and D. P. Eppel, *A Case Study on Variational Soil Moisture Analysis from Atmospheric Observations*, J. Hydr., no. 212–213, 95–108, 1998.

D. Giard and E. Bazile, *Soil Moisture Assimilation in a Global Variable Resolution NWP Model*, 13th Conference on Hydrology. Am. Meteorol. Soc., 163–166, Longbeach, California, 2–7 February 1997.

A. Rhodin, F. Kucharski, U. Callies, D. P. Eppel, and W. Wergen, *Variational Soil Moisture Analysis from Screen–Level Atmospheric Parameters: Application to a Short–Range Weather Forecast Model*, Quart. J. Met. Soc., to appear.

A. C. Lorenc, *Analysis Methods for Numerical Weather Prediction*, Quart. J. Met. Soc., 112, 1177–1194, 1986.

J.-F. Mahfouf, *Analysis of Soil Moisture from Near–Surface Parameters. A Feasibility Study*, J. Appl. Meteor., 7, 506–526, 1991.

C. Schär, D. Lüthi, U. Beyerle, and E. Heise, *The Soil–Precipitation Feedback: A Process Study with a Regional Climate Model*, Jour. Clim., 12, 722-741, 1999.

A. Tarantola, *Inverse Problem Theory*, Elsevier, 1987.

9.3 The New Turbulence Parameterization of LM

Matthias Raschendorfer
Deutscher Wetterdienst (DWD)
P.O. Box 100465, D-63004 Offenbach, Germany
matthias.raschendorfer@dwd.de

1 Introduction

DWD has developed two versions of a non-hydrostatic model. One version (LM) is designed as a meso-γ-scale model and will be used as a high resolution numerical weather prediction model. The other micro-α-scale version (LLM), which is a quasi LES-model, will be a tool for testing parameterization schemes (mainly for the surface layer) and may also be used in a later version for local climate modelling purposes. For the sake of having an almost unified 'root model' with as far as possible a unique source code for both versions (LM and LLM), we attempt to build up a fairly general parameterization scheme for all subgrid-scale flow patterns in both non-hydrostatic model versions. To this end, the turbulence scheme contains some considerable generalizations which make it possible to use it in both, LM and LLM.

As an extension of our operational level 2.0 turbulence closure scheme with a diagnostic equation for turbulent kinetic energy (TKE) it seems now to be important to consider (resolved as well as unresolved) transport of TKE (that is advection and diffusion), too. Thus we decided to use a prognostic TKE-equation, that is a level 2.5 closure scheme according to Mellor and Yamada (1982). As we are interested in a realistic simulation of the lower boundary layer we have the intention to resolve the surface layer, which may be interspersed with a variety of irregular roughness elements, such as plants of a canopy, buildings of a city and hills of subgrid-scale orography, in the vertical direction. The fact that volume averaging and spatial differentiation do not (in general) commute, if the averaging volume is intersected by obstacles, provides the effect of those elements in the form of surface integrals over the inner boundaries of the obstacles. A parameterization of these surface integrals gives additional terms in the budget equations for the mean quantities and therefore in those for the second order moments, too. This leads to a more general turbulence closure scheme, which fortunately can be reduced to a simple flux-gradient form similar to that in case of no obstacles. However, the stability functions are now influenced by (say) canopy terms, and the TKE-equation has an additional drag production term.

The new scheme includes the transition of turbulence which contributes mainly to the fluxes (diffusive turbulence) to very small scale (dissipative) turbulence by the action of very small scale roughness elements, and the handling of non-local vertical diffusion due to boundary layer scale turbulent motions. Most important seems to be the introduction of a parameterization of the pressure transport term in the TKE-equation, that accounts for the TKE-production by subgrid-scale thermal circulations. The whole scheme is formulated in conservative thermodynamic variables (with respect to moist adiabatic processes) together with a statistical cloud scheme according to Sommeria and Deardorff (1976), in order to consider subgrid-scale condensation effects.

Since the turbulence scheme is designed to be applicable both in LM and LLM, some of its components will not yet be used in the forthcoming operational version of LM. This mainly applies to the detailed treatment of the roughness layer (canopy model). This part will first be tested in LLM in the context of the LITFASS project. Depending on the results of these tests the missing components will be implemented in later versions of the operational LM step by step.

2 Theory and Major Modifications

The most important term which appears after volume averaging, when roughness elements are present in the grid box, is the so called wake production term in the TKE-budget. This is due to the averaging of subgrid-scale pressure gradients along the surface of a fixed body within an air flow. This concept has been introduced by Raupach and Shaw (1981). But a revised application of this method showed that there must appear an additional term, describing the reduction of the air volume fraction, r_{air}, due to the presence of rigid obstacles in the grid box.

A specific problem within plant canopies is the short cut of the turbulence spectrum by the action of very small bodies, such as leaves and branches, which transform the kinetic energy of large eddies with a big mixing potential to that of very small ones being on the dissipative scale. Band pass filtered 2-nd order equations may be applied in a way that they do not contain the dissipative part of the spectrum. The whole procedure can be done in the framework of the level 2.5 closure in a way that the only difference to the previous scheme are different canopy dependent values of the model constants, representing enhanced dissipation.

Some new development was done by the parameterization of TKE-production connected with subgrid-scale thermal circulations, which are forced by subgrid-scale patterns of the surface temperature. This effect is hidden in the pressure covariance term and has a big input especially in very stable nocturnal boundary layers over heterogeneous terrain. This term forces the scheme to simulate more mixing in stable boundary layers and thus removes to some extent a well known shortcoming of traditional turbulence schemes. But single column simulations showed that this positive effect is suppressed to a large extent, if Monin-Obukhov similarity theory is used to describe the turbulent surface fluxes of heat and moisture. That is due to the simulation of a strong decoupling between soil and atmosphere, if the surface temperature is much lower than that of the air above. This problem could be solved by simply applying the TKE-scheme down to the lower boundary of the turbulent Prandtl-layer. This was achieved by the evaluation of vertical gradients with the help of the logarithmic Prandtl-layer profiles. The main effect of this unified approach is a consistent formulation of the surface layer scheme and the TKE-scheme used above the surface layer.

The additional TKE-production terms all together come from the following expansion of the term $\overline{\mathbf{v}'' \cdot \nabla p}$, which originally appears in the TKE-equation:

$$-\overline{\mathbf{v}'' \cdot \nabla p} \;=\; P_t + P_c + P_d$$

Here, the overbar describes the appropriate averaging operator, and for any generic variable ψ, we use the mass-weighted Hesselberg-mean $\hat{\psi} = \overline{\rho\psi}/\overline{\rho}$ together with the corresponding fluctuation $\psi'' = \psi - \hat{\psi}$. On the right side, we have the following terms:

(a) the buoyancy-term, defined by (this is state of the art)

$$P_t \;=\; -\,\overline{\mathbf{v}''} \cdot \nabla p \;\simeq\; \frac{g}{\overline{\theta}_v}\overline{\rho w'' \theta_v''}\,,$$

(b) the thermal circulation term defined by

$$P_c \;=\; -\,\overline{\mathbf{v}'' \cdot \nabla p'} \;\simeq\; -\nabla \cdot (\overline{\mathbf{v}'' p'}) \;\simeq\; \frac{\partial}{\partial z}(H \cdot P_t)\,,$$

(c) and the wake production term given by

$$P_d \;=\; \hat{\mathbf{v}} \cdot \overline{\nabla p'} \;\simeq\; \overline{\rho} \frac{|\hat{\mathbf{v}}|^3}{l_{ele}} .$$

In (b), H denotes the vertical length scale of coherence which is approximated by

$$H \;\simeq\; l_{pat} \frac{R_d}{g} \frac{\partial \overline{\theta_v}}{\partial z} ,$$

where l_{pat} is the length scale of subgrid-scale thermal surface patterns. The term l_{ele} in (c) is defined by

$$l_{ele} \;=\; \frac{r_{air}}{1 - r_{air}} L_{ele}$$

where L_{ele} is the length scale of big canopy elements.

Further, ρ, p, θ_v and $\mathbf{v}$ represent air density, pressure, virtual potential temperature and the vector of wind velocity, respectively. g is the acceleration due to gravity and R_d is the specific gas constant of dry air.

Errors due to non-local effects, which may occur in the convective boundary layer or within a plant canopy (where sometimes counter gradient fluxes are present), are related to simplifications in the second order equations. This is, in particular, the neglect of the third order moments, which describe turbulent transport of second order moments. Those errors are significant, when the length scale of vertical turbulent diffusion at a point is larger than the depth of the vertical interval belonging to this point, where the vertical profiles of the first order moments can be treated as linear. As we intended to stay within the framework of a level 2.5 scheme, we tried to solve this problem by a modified determination of vertical gradients, using vertical profiles, which are smoothed with the help of a stratification dependent length scale of vertical diffusion.

A further modification is related to the consideration of subgrid-scale clouds and their interaction with turbulence. In order to include condensation effects during subgrid-scale vertical movements to the turbulence scheme, the second order budgets are formulated in terms of the thermodynamic variables θ_l (liquid water potential temperature) and q_w (total water content). The turbulent fluxes of those quantities then have to be transformed in those of the model variables T (temperature), q_v (water vapour content) and q_c (cloud water content), which is done by the use of a statistical subgrid-scale cloud model proposed by Sommeria and Deardorff (1976). Their model calculates the volume fraction and the water content of subgrid-scale clouds with the aid of the variance of the saturation deficit distribution in a grid box which can be expressed in terms of turbulent quantities.

Finally, we introduced a laminar surface layer. This makes it possible to discriminate between the values of the model variables at the rigid surfaces (e.g. radiative surface temperature) and values at the level z_0 (lower boundary of the turbulent atmosphere). This innovation results in the increase of the diurnal variation of the soil surface temperature, which is now in better agreement with measurements.

3 The Potential of the New Turbulence Scheme

The former parameterization of atmospheric turbulence and turbulent soil-atmosphere transfer showed some significant shortcomings. The new turbulence scheme introduces some more physical mechanisms to the model, which have the potential to reduce the errors in relation with the following deficiencies of the former scheme:

- Too little vertical mixing during stable stratification:
  - ▷ nocturnal inversion layers are too shallow and too cold near the surface
  - ▷ diurnal minima of 2 m-temperatures are often too low
  - ▷ semi-diurnal wave of 2 m-humidity during high pressure situations is almost not to be seen

  This can be improved mainly by the additional thermal circulation term in the TKE-budget.

- No distinction between the values of model variables at the rigid surface of the soil and those of the lower boundary of the turbulent atmosphere:
  - ▷ too small diurnal amplitude of the radiative surface temperature
  - ▷ too much evaporation of bare soils, which leads to strong underestimations of the maximum temperature in the 2m level (especially in early spring , just before the plants become active)

  This can be improved mainly by the introduction of the laminar surface layer which represents an additional resistance between the surface and the atmosphere.

- Convective development is strongly coupled with the amount of evaporation:
  - ▷ maximum convective activity occurs at noon, which is too early

  This may be improved with the explicit simulation of deep convection (which is not possible until we run LM with the 2.5 km resolution) together with the non-local TKE-scheme in conservative variables, combined with the statistical cloud scheme, in order to capture shallow convection with the turbulence parameterization.

- Insufficient mixing at the top of the inversion layer:
  - ▷ stratiform boundary layer clouds do dissolve too slowly

  This can be improved by the diffusion term in the TKE-budget, the non-local formulation and the increased mixing by the presence of subgrid-scale condensation.

- Inadequate representation of the surface layer within large surface elevations, such as buildings, trees or subgrid-scale orography:
  - ▷ considerable errors in the 2m values over such regions
  - ▷ difficulties with the definition of the roughness length in regions with high subgrid-scale orography

  This may be improved by resolving the roughness layer with the concept of the flow through a porous medium, which provides a model of such surface layers and makes it possible to get prognostic values of the 2m quantities. In this case subgrid-scale orography should be handled as a series of obstacles within the roughness layer, which act as an additional form drag resistance in the momentum equation and as a corresponding source of wake turbulence in the TKE-equation. Thus the roughness length of the surface must no longer be effected by subgrid-scale orography or high trees and buildings, but should represent the small scale surface elements only, such as short plants.

- The turbulence scheme gives no solution in situations, where the Richardson number exceeds its critical value. Here, an arbitrary minimum value for the diffusion coefficients is prescribed:

  ▷ Almost no mixing in the higher troposphere, that is above the boundary layer, and nearly no entrainment at the upper border of the boundary layer

  This can be improved due to the prognostic treatment of the TKE equation together with a formulation of the stability function being well defined at any positive Richardson number.

4 The Actual Implementation in LM and Further Steps of the Development

The scheme to be implemented in the forthcoming operational version of LM uses the following components:

- Prognostic TKE equation, including
  - diffusion of TKE
  - production due to subgrid-scale thermal circulations
  - well defined formulation of the stability function for stable stratification
- Consideration of subgrid-scale condensation using
  - conservative thermodynamic variables
  - a statistical subgrid-scale cloud scheme
- Non-local estimate of vertical gradients (optionally)
- Consistent formulation of transport through the surface layer
  - extending the TKE-equation to the lower boundary of the turbulent Prandtl layer
  - introducing an additional laminar layer just above the rigid surface
  - using an adopted diagnosis of 2m temperatures and 10m winds, being consistent with the new surface layer parameterization

Of minor importance are the following points:

- Consideration of thermal TKE sources in the heat budget
- Reformulation of the Charnock formula (to estimate the roughness length over see) using the TKE

Implemented but not used yet are the following components:

- Calculation of an additional form drag resistance for momentum within the roughness layer
- Calculation of an additional wake production of TKE within the roughness layer
- Conversion of diffusive turbulence in dissipative turbulence due to small canopy elements

At present, we have no methodology to deduce the additional external parameters, required to simulate the roughness layer as a part of the atmospheric model. These parameters are the height of the roughness layer, the volume fraction and the length scale of each type of obstacles. Furthermore, we have a parameterization of the source terms due to the roughness elements only in the budgets for momentum and TKE. A parameterization of these sources for heat and water vapour (the complete canopy model including radiative transfer through the canopy) is missing yet. On the other hand, the canopy model will be more important with finer horizontal resolution and will be mainly a matter of LLM. Thus, as a first step, LM will run without a resolved roughness layer.

The completion of the canopy model will be done as a part of the LLM development, which is related to the LITFASS project. LITFASS also has a big measurement part, which provides very detailed external parameters about the Lindenberg (special observatory of the DWD) area and a great variety of atmospheric, hydrologic and soil measurements. Those measurements will be used to support the development and are necessary for validation purposes as well.

As the next step, we intend to incorporate the canopy model to LM. Then we should be able to introduce additional model layers at the synoptic levels (2 m and 10 m above the model ground) in order to calculate the model variables at those levels no longer by a diagnostic approach but simply by the prognostic model equations. Furthermore the roughness length (used for soil-atmosphere transfer calculations) will be independent of obstacles resolved in the vertical direction and thus will represent only short vegetation.

In future, it should be possible to apply the canopy model to large scale models (e.g. GME) as well. On that scale, the canopy elements would consist of the elevations of subgrid-scale orography, and the roughness length would be independent of this kind of obstacles, only representing the plant cover.

The present LM version has a horizontal resolution of about 7 km. This seems to be too coarse in order to resolve deep convection. Thus, convection is still to be parameterized on this scale, and the problem remains, how to separate this correctly form turbulence parameterization, which now may be able to describe shallow convection. Perhaps, with the introduction of the 2.5 km version by 2002, it will be possible to get rid of a convection parameterization at all.

5 First Results

The influence of the thermal circulation term on boundary layer development is exemplified in Figs. 1 and 2. In order to test this effect without the influence of a presumably not very accurate surface scheme and soil model, respectively, single column simulations, forced by observed temperatures and dew points at 2 m height, were performed. The simulations started with vertical profiles obtained by radio soundings at midnight (hour = 0). All measurements are taken from the Lindenberg observatory of DWD and the external parameters of course belong to this area. The simulations belong to a high pressure situation in July 1997, when the wind was low, so that the single column simulations are easier to compare with data from measurements.

In Fig. 1 measured (mes) and simulated profiles of potential temperature (Tet) are shown after 18 hours (well mixed layer) and 24 hours (stably stratified layer) of simulation time. The left picture shows the simulation without using the circulation term ($l_{pat} = 0m$) and the picture to the right shows the case with $l_{pat} = 2000m$.

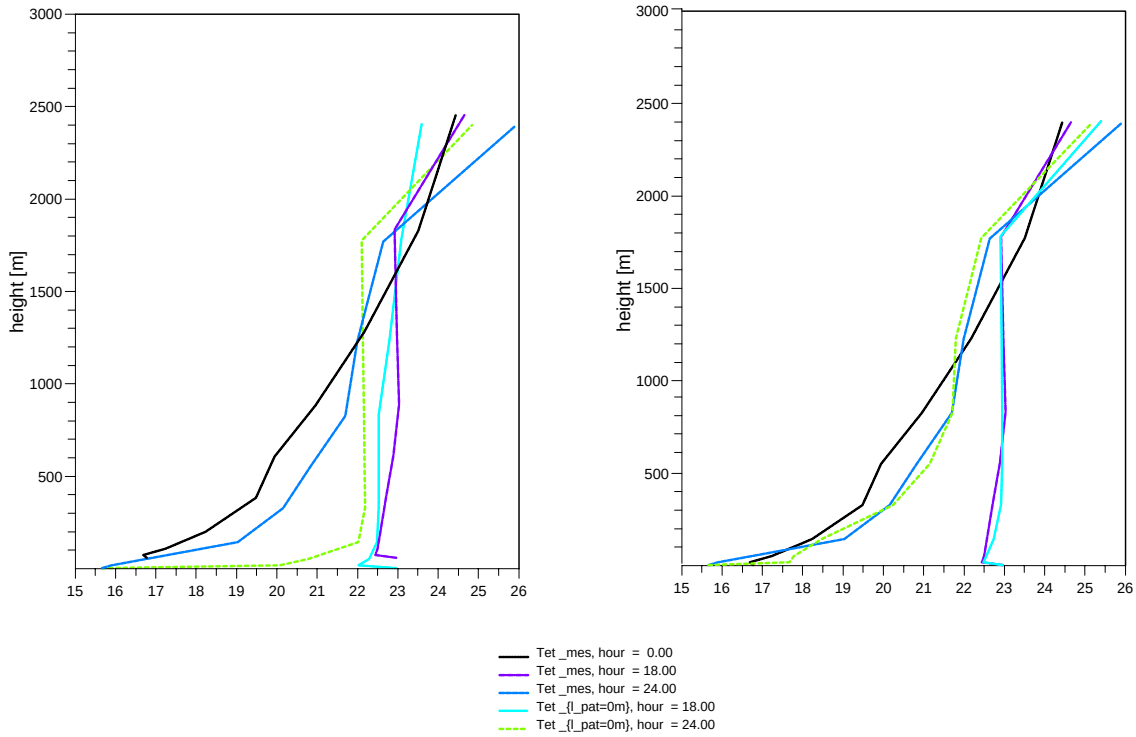

Figure 1: *1-D boundary layer simulation for 10 July 1997 at Lindenberg. Left: simulation without the circulation term. Right: simulation including the circulation term.*

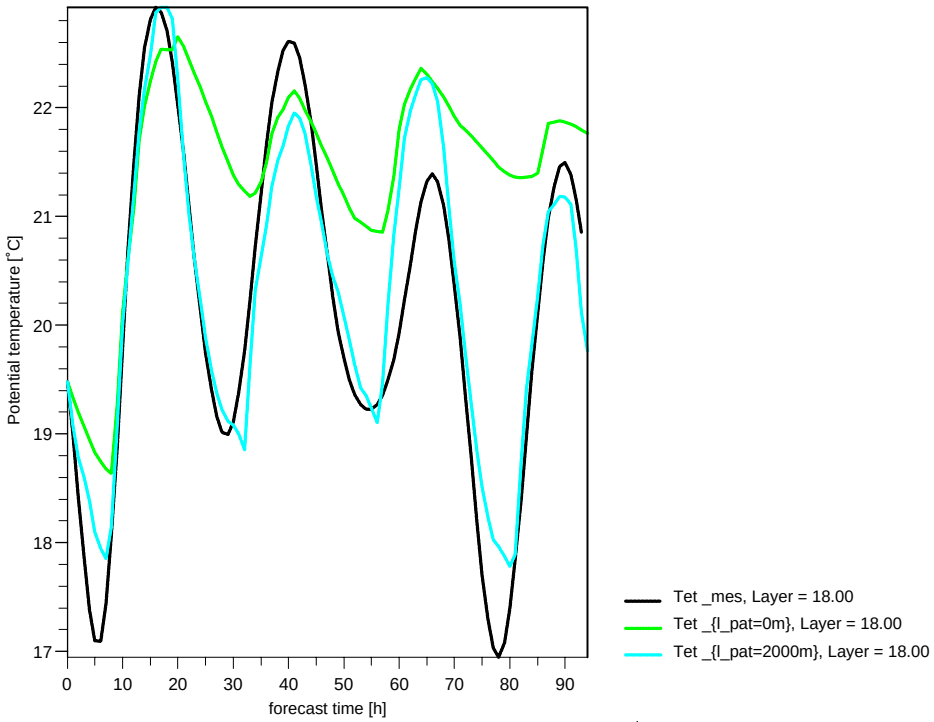

Figure 2: *Time series at the 18-th layer in 300 m height (for 10 July 1997 at Lindenberg)*

Figures 3 and 4 show some results of 12 hour forecasts with LM during the low pressure situation over Germany of 22.07.1999, starting at 00 UTC. Obviously, both, the old model version (ref) and the new version (new) reproduce a jet stream, as is seen in Fig. 3. Although the new version produces more mixing at stable stratification (Fig. 4), it completely retains the jet stream structure.

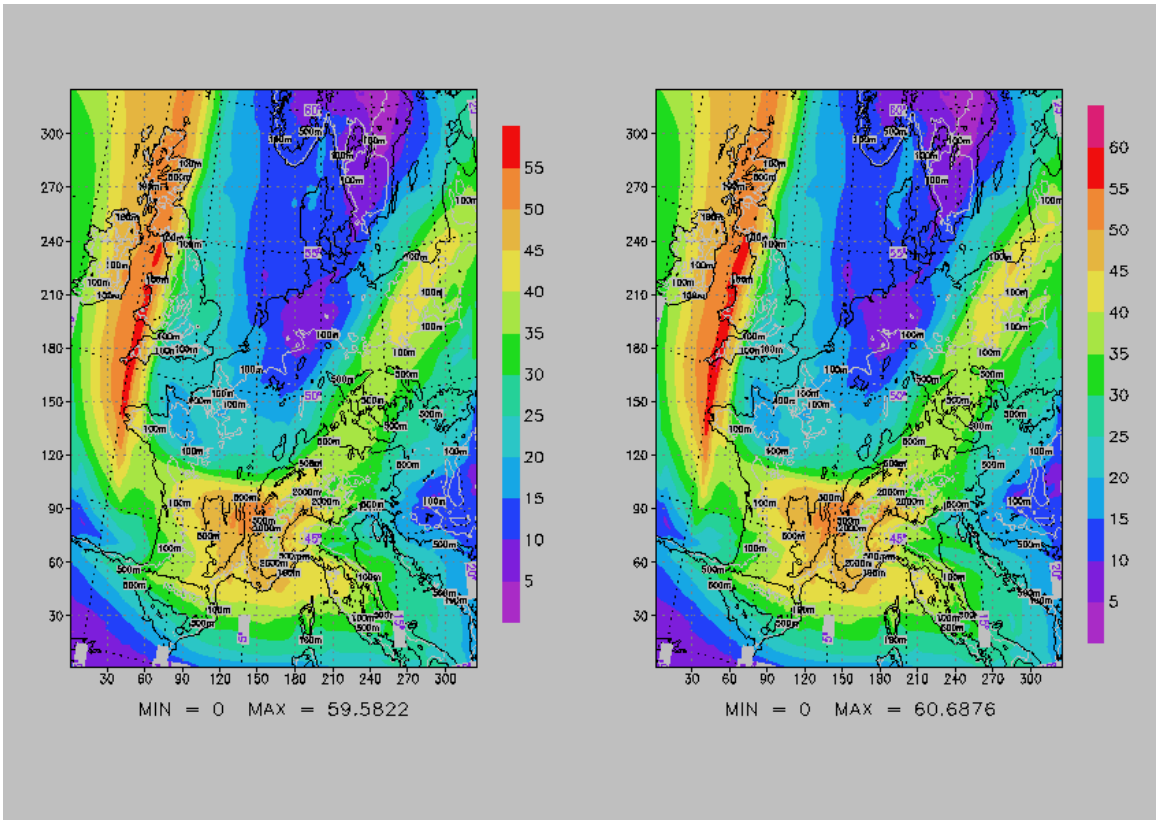

Figure 3: *Wind speed (m/s) at a height of about 10 km for a LM simulation of 22 July 1999 00 UTC + 12 h. Left: old turbulence scheme. Right: new turbulence scheme.*

Fig. 4 shows cross sections for horizontal wind speed, potential temperature and TKE at a constant model row index of 150, which is at about 48° geographical latitude see the y-axis of Fig. 3). The wind speed chart shows two jet maxima corresponding to the western and eastern flanks of the trough. The lower part of Fig. 4 shows the related TKE fields for both LM versions. Results with the new turbulence scheme are plotted at the left hand side and results with the old turbulence scheme at the right hand side. Due to the stable stratification (see upper right picture of Fig. 4), over most of the higher troposphere, the old scheme gives just the background value for TKE. Only at some discrete areas, where the Richardson number is less than its critical value, TKE values are calculated being different from the background value.

But the new scheme is able to simulate some realistic structure of the TKE field even in the higher troposphere. There are two local TKE maxima belonging to the upper and lower edge of each of both jet maxima, where strong vertical gradients of horizontal velocity occur. But at the western jet maximum, especially the upper region of large vertical velocity gradients corresponds to the region of strong stable stratification, damping the shear production of TKE. Thus the corresponding TKE maximum has a rather low magnitude and is shifted towards regions with weaker thermal stability in the west of the jet.

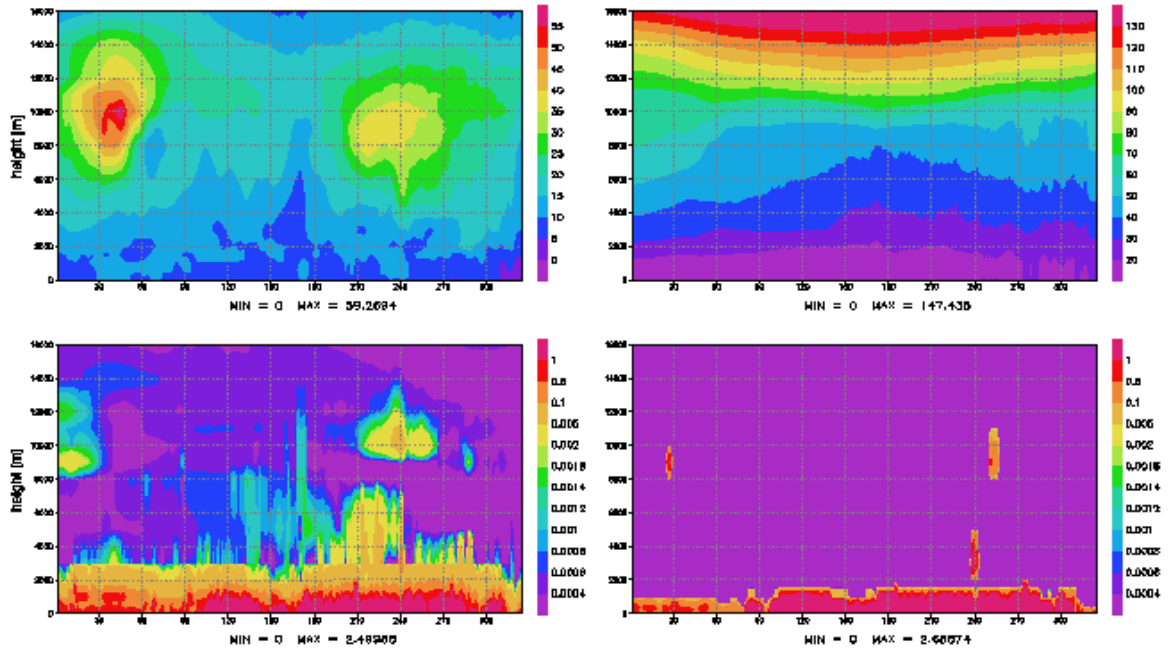

Figure 4: *Vertical cross section from west to east along the model row index 150, which is about 48 deg.N. (for 22 July 1999 00 UTC + 12 h).*
Top left: horizontal wind speed (m/s), new turbulence scheme.
Top right: Potential temperature (C), new turbulence scheme.
Bottom left: Turbulent kinetic energy (m^2/s^2), new turbulence scheme.
Bottom right: Turbulent kinetic energy (m^2/s^2), old turbulence scheme.

Fig. 4 shows cross sections for horizontal wind speed, potential temperature and TKE at a constant model row index of 150, which is at about 48° geographical latitude see the y-axis of Fig. 3). The wind speed chart shows two jet maxima corresponding to the western and eastern flanks of the trough. The lower part of Fig. 4 shows the related TKE fields for both LM versions. Furthermore, above the mixed boundary layer, which has a height of about 1500 m, the new scheme produces an considerable entrainment zone. The sharp upper borders of the boundary layer in both versions are due to the coarse vertical model resolution in comparison with the strong vertical TKE-gradients in this regions.

6 References

Mellor, G.L. and T. Yamada. 1982: Development of a turbulence closure model for geophysical flow problems. *Rev. Geophys. and Space Phys.*, **20**, 831-875.

Raupach, M.R. and R.H. Shaw. 1981: Averaging procedures for flow within vegetation canopies. *Bound. Layer Meteo.*, **22**, 79-90.

Sommeria, G. and J.W. Deardorff. 1976: Subgrid-scale condensation in models of non-precipitating clouds. *J. Atmos. Sci.*, **34**, 344-355.

9.4 A Version of the Nonhydrostatic Model LM in Z - Coordinates

J.Steppeler (DWD) and H.W. Bitzer (AWGeophys
Deutscher Wetterdienst (DWD)
P.O. Box 100465, D-63004 Offenbach, Germany
juergen.steppeler@dwd.de

A version of the nonhydrostatic model LM in z - coordinates is developed. This version is considered essential for model applications using resolutions of about 3 km, which are planned for LM in the near future. For such fine scale operational applications it seems important to avoid the forcing by numerical errors, which is present in models using terrain following coordinates with second order differencing. While the flow near the mountain will be improved, the representation of hydrostatic gravitational waves may cause problems with step mountain orography (Gallus and Klemp, 2000).

The z-coordinate version of LM does not use the step mountains, but rather a representation based on the shaved elements. This approach uses a representation of mountains by bilinear splines on a rectangular grid. Some of the grid cells are cut by the orography. There are three classes of grid cells:

- Cells which are entirely in the atmosphere
- Cells which are entirely under the orography
- Cells which are cut by the orography ("Shaved Cells")

While the two first classes can be treated in an obvious way, the treatment of the third class requires attention, and is normally done using the finite volume method. Direct application of the finite volume method may lead to rather stringent CFL-conditions, as the cells may be rather small. The z-coordinate version of LM uses the thin wall approximation, known from oceanography (Bonaventura, 2000). This approximation assumes a representation of the orography by vertical walls, which are then used to obtain weights for the computation of the divergence term.

In view of the derivation of the thin wall approximation from the finite volume method, it is required to introduce also horizontal walls, and as a consequence there are also flux limiters in the vertical direction. The z-coordinate LM uses horizontal walls as well as vertical ones.

The z-coordinate LM is tested using gravitational waves induced by a mountain. According to Gallus and Klemp (2000) the hydrostatic case is of particular interest. The results of tests for small mountains with the terrain following LM are given by Saito et. al (1998) and compared with the analytical solution. Models using the terrain following coordinate have normally no difficulties in producing the correct result. Therefore it will be necessary that the z-coordinate version reproduces the solution of the terrain following version for this particular test.

Figure 1 shows vertical velocities and streamlines of a two dimensional solution of the z-coordinate LM using a mountain of the shape h(x) = h0/(1 + (x/a)**2) with a = 10 km, dx=2 km, h0 = 1847 m. This mountain is rather high and therefore represents a rather difficult test. The vertical velocity field has approximately the shape as known from small mountains (Saito et al, 1998). The streamlines have much more structure, as compared to

the linear solution, obtained with a small mountain. This is an indication of the presence of nonlinear effects. The double maxima and minima in the vertical velocity field ("peanut structure") are also caused by nonlinear effects. The deficiencies observed by Gallus and Klemp (2000) are not present in the solution shown in Fig. 1. In particular the system of gravitational waves is well developed and a strong foehn effect exists.

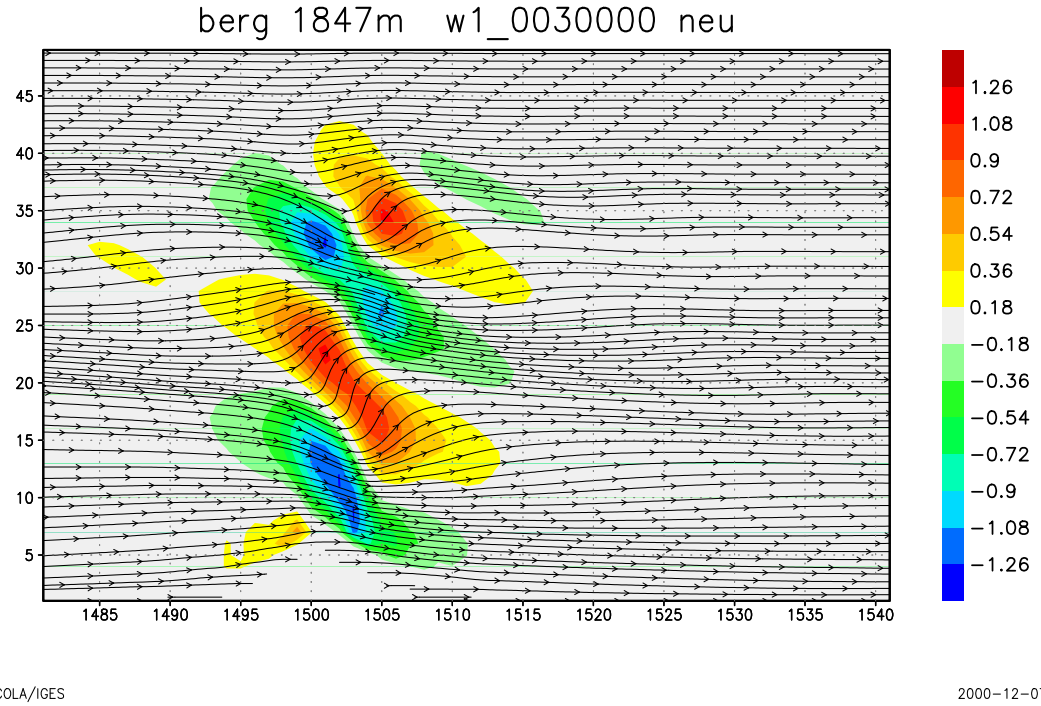

Figure 1: *Solution of the z-coordinate version of LM for a flow over a bell-shaped mountain*

References

Gallus, W., and J. Klemp, 2000: Behavior of Flow over Step Orography. *Mon. Wea. Rev*, **128**, 1153-1164.

Saito, K., G. Doms, U. Schättler and J. Steppeler, 1998: 3-D Mountain Waves by the Lokal-Modell of DWD and the MRI Mesoscale Nonhydrostatic Model. *Papers in Meteorology and Geophysics*, **49**, 7-19.

Bonaventura, L., 2000: A Semi-implicit Semi Lagrangian Scheme Using the Height Coordinate for a Nonhydrostatic and Fully Elastic Model of Atmospheric Flows. *J. Comp. Phys.*, **158**, 1-28.

10 Collaboration and External Users of LM

All national weather services of COSMO are members of EUMETNET, the network of meteorological services within Europe. EUMETNET provides a framework to organize co-operative programmes between the Members in the various fields of basic meteorological activities such as observing systems, data processing, basic forecasting products, research and development, training (*www.eumetnet.eu.org*). COSMO's activities are embedded in this network and are especially related to EUMETNET programmes such as MAP-NWS (Mesoscale Alpine Programme - National Weather Services) and EUCOS (EUMETNET Composite Observing System).

Since the 1st of January 2000, EUMETNET provides a Coordinator for the SRNWP (Short Range Numerical Weather Prediction) Group. Representatives of the NWP branches of European National Meteorological Services meet in this group on a yearly basis to organize co-operative activities in development of numerical atmospheric models. The present SRNWP-coordinator is J. Quiby from MeteoSwiss. Within the SRNWP Group, Lead Centres have been selected for different topics. The Lead Centres have the responsibility to organize intercomparisons, workshops and to ensure the flow of information between participants. DWD has taken the role as the Lead Centre for Nonhydrostatic Modelling (responsible for this LC is Jürgen Steppeler from DWD). For more information on SRNWP and its Lead Centres see *http://srnwp.sma.ch*.

All COSMO partners are also members of EWGLAM (European Working Group on Limited Area Modelling). This group meets once a year to exchange information on the current status and on recent developments in high-resolution numerical weather prediction.

Another type of collaboration with other European meteorological services is via COST, an intergovernmental framework for European *Co-operation in the field of Scientific and Technical Research*, allowing the co-ordination of nationally funded research on an European level (for more information about COST see *www.netmaniacs.com/cost*).

10.1 International Projects

This section lists the current participation of COSMO partners in international research projects which are related to LM. This list will be updated in the forthcoming issues.

- **EFFS** *An European Flood Forecasting System.*
  Type: EU-project with funding.
  DWD contribution: *Hindcasting of flood events, input to flood forecasting models, analysis of precipitation (24-h totals) based on rain gauge data and radar estimates.*
  Information: http://effs.wldelft.nl

- **CLIWA-NET** *Cloud Liquid Water Network.*
  Type: EU-project with funding.
  DWD contribution: *Supply of special LM-output for intercomparison with observations and other models.*
  Information: www.knmi.nl/samenw/cliwa-net (with online results from LM)

- **SEAROUTES**
  Type: EU-project with funding.
  DWD contribution: *Supply of LM-data over the Baltic Sea for the development of a high-resolution sea wave model at GKSS (Geesthacht)*
  Information: no homepage yet

- **EUROGRID** *Application Testbed for European GRID Computing.*
  Type: EU-project with funding.
  DWD contribution: *Implementation of a relocatable LM using the EUROGRID environment*
  Information: no homepage yet

- **COST 717** *Use of Radar Observations in Hydrological and NWP models.*
  Type: COST concerted research action
  MeteoSwiss contribution: *Chairmanship (A. Rossa).*
  DWD contribution: *Validation of LM by using radar information.*
  MeteoSwiss contribution: *Assimilation of three-dimensional radar reflectivities into a nonhydrostatic NWP model.*
  Information: www.smhi.se/cost717

- **COST 716** *Exploitation of ground-based GPS for climate and numerical weather prediction applications.*
  Type: COST concerted research action
  DWD contribution: *Validation of integrated water vapour from ground-based GPS observations and their assimilation in the LM of DWD.*
  Information: www.oso.chalmers.se/geo/cost716.html

- **EUCOS** *EUMETNET Composite Observing System*
  Type: EUMETNET Programme
  MeteoSwiss contribution: *Observing system experiments on the impact of aircraft data and frequent radiosonde data.*
  Information: www.eumetnet.eu.org

Furthermore, a lot of activities of COSMO members are related to the *Mesoscale Alpine Project* (MAP). For more information, see the MAP homepage at *www.map.ethz.ch.*

10.2 National Projects and Collaboration

This section lists LM-related projects and collaboration of COSMO members on a national level. At present, the list is by no means complete. Please inform the editors on such activities, especially those with national funding, in order to get a more complete list in the next COSMO newsletter.

- **DWD/University of Bonn** *Use of Radar Information for Initialization of LM*
  Type: bilateral project, funded by DWD.

- **DWD/University of Bonn** *Special Investigations in Statistical Model Interpretation*
  Type: bilateral project, funded by DWD.

- **DWD/University of Trento** *Development of a Z-coordinate Version of the LM*
  Type: bilateral collaboration, no funding.

10.3 External Users of LM

The source code of the LM-package is available free of charge for scientific and educational purposes to third parties outside COSMO. Such external users, however, must register and sign a special agreement with DWD. For questions about the request and the agreement, please contact D. Frühwald from the COSMO Steering Committee (dieter.fruehwald@dwd.de).

Meanwhile, a number of universities and research institutes have received the model software. Once a year, there is a *User Workshop on Scientific Applications of the LM* organized by J. Steppeler at DWD (contact: juergen.steppeler@dwd.de, see also Section 7.4). There is, however, not always a feedback on the activities or on results and problems. Table 1 lists the current registered users of the LM (outside the COSMO group).

Table 1: ***Registered Scientific Users of LM outside COSMO***

Institution	**Research Activities**	**since**
Meteorological Research Institute, Japan	Model comparison	1997
Academy of Science, Institute for Physics of the Atmosphere, Czech Republic	Clouds and precipitation	1999
University of Ljubljana, Slovenia	Latent heat nudging	1999
Meteorological Research Institute, Korea	unknown	1997
National Center for Atmospheric Research Scientific Computing Division, USA	Semi-implicit time scheme	1998
University of Trento (I)	Numerics, shaved elements	1999
University of Frankfurt (D)	Numerics and cloud physics	1996
University of Hamburg (D)	unknown	1997
University of Hannover (D)	Studies on atmosphere-surface interaction	2001
University of Karlsruhe (D)	Soil modelling, case studies	1996
University of Cologne (D)	unknown	2000
University of Leipzig (D)	Cloud physics, hydrology	2000
University of Bonn (D)	Physical initialization Statistical postprocessing Step mountain coordinate Regional evaporation and land use Greenland katabatic winds Water resource managment	1997
University of Munich (D)	Model comparison, case studies	2000
Konrad-Zuse Institut, Berlin (D)	Scientific visualization	1997
Alfred Wegener Institut, Bremerhaven (D)	Cloud physics	2000
Potsdam Institute for Climate Impact Research (PIK), Potsdam (D)	Regional climate studies Low Mach-number dynamics	1999
GKSS Research Centre Geesthacht (D),	GEWEX cloud system studies, regional climate simulations	2000
Institute for Research in the Troposphere (IFT), Leipzig, (D)	Turbulence studies	1998
German Aerospace Centre, Institute of Atmospheric Physics, Oberpfaffenhofen, (D)	Turbulence studies	2000

References

Doms, G., U. Schättler. 1999: The Nonhydrostatic Limited-Area Model LM (Lokal-Modell) of DWD. Part I: Scientific Documentation. Deutscher Wetterdienst (DWD), Offenbach. January 1999.

Hess, R. 2000: Variational Soil Moisture Analysis with First Operational Results. Quarterly Report of the Operational NWP-Models of the Deutscher Wetterdienst, **22**, 8-15.

Jacobsen, I. and E. Heise. 1982: A new economic method for the computation of the surface temperature in numerical models. *Contr. Atmos. Phys.*, **55**, 128-141.

Louis, J.-F. 1979: A parametric model of vertical eddy fluxes in the atmosphere. *Bound. Layer Meteor.*, **17**, 187-202.

Lynch. P., Girard D. and V. Ivanovici. 1997: Improving the efficiency of a digital filtering scheme. *Mon. Wea. Rev.*, **125**, 1976-1982.

Majewski, D. 1998: The new global icosahedral-hexagonal grid point model GME of the Deutscher Wetterdienst. *ECMWF Seminar on Numerical Methods in Atmospheric Models*, 1998.

Raymond, W.H. 1988: High-order low-pass implicit tangent filters for use in finite area calculations. *Mon. Wea. Rev.*, **116**, 2132-2141.

Ritter, B. and J. F. Geleyn. 1992: A comprehensive radiation scheme for numerical weather prediction models with potential applications in climate simulations. *Mon. Wea. Rev.*, **120**, 303-325.

Schraff, C. 1996: Data assimilation and mesoscale weather prediction: A study with a forecast model for the Alpine region. Publication No. 56, Swiss Meteorological Institute.

Schraff, C. 1997: Mesoscale data assimilation and prediction of low stratus in the Alpine region. *Meteorol. Atmos. Phys.*, **64**, 21-50.

Skamarock, W. C. and J. B. Klemp. 1992: The stability of time-split numerical methods for the hydrostatic and the nonhydrostatic elastic equations. *Mon. Wea. Rev.*, **120**, 2109-2127.

Thomas, S., C. Girard, G. Doms and U. Schättler. 2000: Semi-implicit scheme for the DWD Lokal-Modell. *Meteorol. Atmos. Phys.*, **75**, 105-125.

Tiedtke, M. 1989: A comprehensive mass flux scheme for cumulus parameterization in large-scale models. *Mon. Wea. Rev.*,**117**, 1779-1799.

Wicker, L. and W. Skamarock. 1998: A time-splitting scheme for the elastic equations incorporating second-order Runge-Kutta time differencing. *Mon. Wea. Rev.*, **126**, 1992-1999.

Appendix A: The GRIB Binary Data Format used for LM I/O

All input and output arrays of the LM and of the preprocessor programs providing interpolated initial conditions and the boundary values are stored in a compressed binary data format called GRIB-code. GRIB means "gridded binary" and is designed for the international exchange of processed data in the form of grid-point values expressed in binary form.

The GRIB-code is part of the FM-system of binary codes of the World Meteorological Organization (WMO). Currently, we use Edition 1 of the GRIB-code with number FM 92-VIII. For coding details, see the *Manual on Codes, International Codes, Volume 1.2* of WMO (WMO Publication No. 306, 1995). In this section, we describe only the basic features of the GRIB code which are relevant for the I/O of the LM-system.

A.1 Code Form

Each GRIB-coded record (analysis or forecast field) consists of a continuous bit-stream which is made up of a sequence of octets (1 octet = 8 bits). The representation of data by means of series of bits is independent of any particular machine representation. The octets of a GRIB messsage are grouped in sections (see Table 1, where the length of the record and the length of the sections are expressed in octets. Section 0 has a fixed length of 4 octets and section 5 has a fixed length of 4 octets. Sections 1, 2, 3 and 4 have a variable length which is included in the first three octets of each section.

Table 1: *Form of GRIB-code*

Section number	**Name**	**Contents**
0	Indicator Section	"GRIB"; length of record; GRIB edition number
1	Product Definition Section	Length of section; identification of the coded analysis/forecast field
2	Grid Description Section (optional)	Length of section; grid geometry, as necessary
3	Bit-map Section (optional)	Length of section; the bit per grid-point, placed in suitable sequence
4	Binary Data Section	Length of section; data values
5	End Section	7777

Octets are numbered 1, 2, 3, etc., starting at the beginning of each section. Bit positions within octets are referred to as bit 1 to 8, where bit 1 is the most significant bit and bit 8 is the least significant bit. Thus, an octet with only bit 8 set to 1 would have the integer value 1.

A.2 Indicator and End Section

The Indicator Section has a fixed length of 8 octets. The first four octets shall always be character coded as "GRIB" (according to the CCITT International Alphabet No.5). The remainder of the section shall contain the length of the entire GRIB-record (including the Indicator Section) expressed in binary form over the left-most 3 octets (i.e. 24 bits in octet 5-7), followed by the GRIB edition number (currently 1), in binary, in the remaining octet 8.

The End Section has a fixed length of 4 octets. These octets are character coded as '7777' according to the International Alphabet No.5.

Thus, the beginning and the end of a GRIB-record can be identified by the character coded words "GRIB" and "7777". All other octets included in the code represent data in binary form. Each input or output array defined on the rotated lat/lon grid of the LM (e.g the surface pressure or the temperature at a specified model level) is coded as a GRIB-record. Various such records can be combined in a single GRIB-file.

A.3 Product Definition Section

The Product Definition Section (PDS) contains the necessary information to identify the binary coded field contained in the GRIB-record. The most important octet in this section is the indicator of the meteorological parameter. The indicator relates a specific meteorological element to an integer number. This indicator number is also referred to as GRIB-number or element-number and is defined in a separate code table. More than one indicator code tables may be used in GRIB-code. Thus, one can have the same element-number but different code table numbers for various fields. The element-numbers and code tables used by LM are described below.

The program `grbin1` of the supplementary GRIB-library `griblib` of the LM-system can be used to decode GRIB binary code. Besides the decoded data set, this program does also retrieve the contents of the octets of the PDS in an integer array `ipds`. To illustrate the structure of the PDS, Table 2 shows the contents of the product definition section of a binary coded LM output array, the total cloud cover (CLCT). The GRIB-record for this field is valid for 28.10.1998 00 UTC + 11 h and was created at 28.10.1998 7.04 UTC by an LM forecast.

Octet 4 (ipds(2)) assigns a table number to the parameter indicator number given in octet 9. Currently, we use 3 additional code tables besides the WMO-table (see Table 3). A full list of variables defined by these tables is available from DWD.

Octet 6 (ipds(4)) indicates the process identification number which is allocated by the originating centre. Currently, we use only two different process numbers for forecasts or analyses (see Table 4).

The level or layer for which the data are included in the GRIB-record is coded in octets 10 - 12 (ipds(8) - ipds(9)), where octet 10 indicates the type of level and octets 11 and 12 indicate the value of this level. Table 5 shows the code figures used for LM. For reserved values, or if not defined, octets 11 and 12 shall contain zero.

All 3-D variables of LM except the vertical velocity are defined on terrain-following main levels. In GRIB, these main levels are coded as level-type 110: hybrid layers between two adjacent hybrid levels - which are the LM half levels, i.e the layer interfaces. In this case, octet 11 contains the level index of the upper half level and octet 12 contains the level index of the lower half level. The vertical velocity and the height of the half levels are coded as level type 109: hybrid levels, i.e. the LM half levels. In this case, octet 11 contains zero and octet 12 contains the level index of the model half level. Pressure levels (ipds(8) = 100) and height levels (ipds(8) = 105) are used when the interpolation from model to specified p- or z-surfaces is switched on for model output.

Table 2: ***Contents of the Product Definition Section***

array ipds(i)	Octet number	Contents of PDS Value	Remarks
1	1-3	54	Length of the PDS (in octets)
2	4	2	Version number of the GRIB indicator table (see Table 3)
3	5	78	Identification of originating/generating centre (DWD has WMO number 78)
4	6	132	Generating process identification number (allocated by originating centre, see Table 4)
5	7	255	Number of grid used - from catalogue defined by the originating centre. Octet 7 set to 255 indicates a non-cataloged grid, in which case the grid is defined in the grid description section.
6	8	128	Block-flag; the value 128 indicates that the grid description section is included.
7	9	71	Indicator of parameter (element number) from GRIB-table in ipds(2); see Section 3.7
8	10	1	Indicator of type of level, see Table 5
9-10	11-12	0	Value of level (height, pressure, etc.) for which the data are included (see Table 5)
11	13	98	Year (start time of forecast; analysis time)
12	14	10	Month (start time of forecast; analysis time)
13	15	28	Day (start time of forecast; analysis time)
14	16	0	Hour (start time of forecast; analysis time)
15	17	0	Minute (start time of forecast; analysis time)
16	18	1	Indicator of unit of time range (see Table 6)
17	19	11	P1 - period of time (number of time units);
			time units given by octet 18 (ipds(16))
18	20	0	P2 - period of time (number of time units);
			time units given by octet 18 (ipds(16))
19	21	0	time range indicator (see Table 7)
20	22-23	0	Number of forecasts included in average, when octet 21 (ipds(19)) indicates an average or accumulation of forecasts (or analyses); otherwise set to zero.
21	24	0	Number of forecasts missing from averages or accumulations.
22	25	20	Century of reference time of data given by octets 13- 17
23	26	255	Sub-centre identification, national use
24	27-28	0	Units decimal scale factor (D)
25-36	29-40	0	Reserved: need not to be present
37	41	254	Octets 41-54 are reserved for the originating centre. The integer value 254 indicates that additional data follow. We use this part as follows:
38	42	0	not used
39	43-45	0	not used
40	46	0	not used
41	47	0	Additional indicator for a GRIB element number
42	48	98	Year of production of GRIB-record
43	49	98	Month of production of GRIB-record
44	50	11	Day of production of GRIB-record
45	51	2	Hour of production of GRIB-record
46	52	0	Minute of production of GRIB-record
47	53-54	1	Version number, currently 1 for LM

Table 3: *GRIB-tables for parameter (element) indicator number*

Version number of GRIB-table; ipds(2)	**Comment**
2	WMO-table of indicator parameters
201	national table of DWD for internal use
202	national table of DWD for internal use
203	national table of DWD for internal use

Table 4: *Process identification numbers*

process id-number; ipds(4)	**Comment**
131	LM-analyses from data assimilation cycle
132	LM-forecasts and initialized analyses

Table 5: *Types of fixed levels or layers used by LM*

level type ipds(8)	**Meaning**	**ipds(9)**	**ipds(10)**
1	Ground or water surface	0	0
2	Cloud base level	0	0
3	Level of cloud tops	0	0
4	Level of $0°C$ isotherm	0	0
8	Top of atmosphere	0	0
100	Pressure (isobaric) level	0	Pressure in hPa
102	Mean sea level	0	0
103	Specified height above mean sea level	0	Height in m
105	Specified height level above ground	0	Height in m
109	Hybrid level (half levels)	0	Level number (k)
110	Hybrid layer (main level) between two hybrid levels	Level number of top (k)	Level number of bottom (k+1)
111	Depth below land surface	0	Depth in cm
112	Layer between two depths below land surface	Depth of upper surface in cm	Depth of lower surface in cm

Octets 13-17 contain the reference time of the data: the start of a forecast, the time for which an analysis is valid or the start of an averaging or accumulation period. The year of the century is coded in octet 13 and the century (100 years) in octet 25. For a reference time within the year 2000, octet 13 will contain the integer value 100 and octet 25 will contain the integer value 20.

The time or time interval for which the data are valid with respect to the reference time is coded in octets 18-21 (ipds(16)-ipds(19)). Octets 19 and 20 contain two periods of time, P1 and P2. The units of the values of P1 and P2 are defined in octet 18. Currently, we use hours as the time unit, but other values may be more appropriate for special applications of the model as the maximum integer number in an octet is 256. Thus, for long-term climate runs or short-term cloud simulations, other time units must be chosen. The WMO code-table for the unit of time in P1 and P2 is given in Table 6.

Table 6: *Code table for unit of time*

ipds(16)	Meaning	ipds(16)	Meaning	ipds(16)	Meaning
0	Minute	5	Decade	11	6 hours
1	Hour	6	Normal	12	12 hours
2	Day	7	Century	13-253	Reserved
3	Month	8-9	Reserved	254	Second
4	Year	10	3 hours		

The meaning of the time period P1 in octet 19 (ipds(17)) and of the time period P2 in octet 20 (ipds(18)) - given in the units coded in octet 18 - depends on the time-range indicator, which is contained in octet 21 (ipds(19)). The WMO code-table allows for a large number of indicators including averages and accumulation over a number of forecasts and analyses. For the LM-system, we use only a few standard indicators as shown in Table 7.

Table 7: *Time range indicators used by LM*

ipds(19)	Meaning
0	Forecast product valid for reference time + P1 (if P1 > 0) or uninitialized analysis product valid for reference time (P1 = 0)
1	initialized analysis product valid for reference time (P1 = 0)
2	Product with a valid time ranging between reference time + P1 and reference time + P2
3	Average from reference time + P1 to reference time + P2
4	Accumulation from reference time + P1 to reference time + P2; product valid for reference time + P2

A.4. Grid Description Section

Section 2 of a GRIB-record, the grid description section GDS, contains all information about the geometry of the grid on which the data are defined. For all input and output files of the LM, this section is coded completely for every field contained in the file. The program `grbin1` of the supplementary GRIB-library `griblib` retrieves the contents of the GDS in an integer array `igds`.

The contents of the grid description section of an LM GRIB-record is illustrated in Table 8 for the model domain used operationally at DWD. The octets corresponding to the integer array `igds` are numbered relative to this section.

Table 8: ***Contents of the Grid Description Section***

array igds(i)	Octet number	Contents of GDS Value	Meaning
1	1-3	202	Length of GDS (in octets) including the vertical coordinate parameters. (here for $ke = 35$ layers, i.e. $ke + 1 = 36$ half levels)
2	4	40	NV: Number of vertical coordinate parameters (four base state parameters + $(ke + 1)$ values of the vertical coordinates of the half levels)
3	5	43	PV: Location (octet number) of the list of vertical coordinate parameters
4	6	10	Data representation type according to WMO code-table 6; '10' assigns a rotated latitude/longitude grid
5	7-8	325	Number of gridpoints in 'zonal' direction
6	9-10	325	Number of gridpoints in 'meridional' direction
7	11-13	-17000	Rotated latitude of the first gridpoint in millidegrees
8	14-16	-12500	Rotated longitude of the first gridpoint in millidegrees
9	17	0	Resolution flag according to WMO code-table 7; '0' means that the grid spacing is not given
10	18-20	3250	Rotated latitude of the last gridpoint in millidegrees
11	21-23	7750	Rotated longitude of the last gridpoint in millidegrees
12	24-25	0	Longitudinal direction increment (grid spacing in λ-direction, not given)
13	26-27	0	Meridional direction increment (grid spacing in ϕ-direction, not given)
14	28	64	Scanning mode flag according to WMO code-table 8 '64' means that points scan in +i and +j direction and adjacent points in i-direction are consecutive
15-19	29-32	0	Reserved (set to zero)
20	33-35	-32500	Geographical latitude of rotated southern pole in millidegrees
21	36-38	10000	Geographical longitude of rotated southern pole in millidegrees
22	39-42	0	Angle of rotation
26-65	43-202	.....	List of vertical coordinate parameters, each packed on 4 octets (length = 4 x NV octets). first the three parameters defining the base state: `igds(26)=p0sl`, `igds(27)=t0sl`, `igds(28)=dt0lp`; then the parameter `igds(29)=vcflat` of the hybrid coordinate system; and finally the $ke + 1$ values of the vertical coordinate $\eta(k)$ of the model half levels for $k = 1, \ldots, ke + 1$ in `igds(30)`,..., `igds(65)`.

Appendix B: Available LM Output Fields

This appendix summarizes the GRIB parameter indicators (element numbers), the table numbers and the dimensions of the direct model output variables. Any changes will be updated in the next COSMO Newsletter.

B.1 General Remarks

For direct model output, we distinguish between so-called *multi-level fields* which are defined on model layers or levels or on fixed pressure or height levels, and *single level fields* which are defined at the surface or on another fixed level.

The fields contained in the model output GRIB-files can be freely chosen by the user: The names of the model variables to be written out have to be specified on the following NAMELIST input character arrays:

- `yvarml` for output on the model grid and for single level data,
- `yvarpl` for output on constant pressure levels
- `yvarzl` for output on constant height levels.

If latter two variables are empty, the model-internal interpolation to pressure and height levels is omitted. If they are set, the values of the corresponding pressure and height levels can be specified by the NAMELIST input arrays `plev` and `zlev`. By default, some multi-level variable are interpolated to 10 pressure levels and 4 height levels:

- p-levles: 1000, 950, 850, 700, 600, 500, 400, 300, 250, 200 hPa.
- z-levles: 1000, 2000, 3000, 5000 m (above sea level).

B.2 Element and Table Numbers used by LM

The name of an input/output field is specified as a CHARACTER variable (in capital letters, names must be 8 characters long, filled with blanks) in NAMELIST input. The model then relates this name internally to a corresponding GRIB element number and table number as well as the corresponding global model variable (which has usually the same name but with small letters). However, some names of output variables are not related to a globally defined model variable. In these cases, the output array is calculated locally only at the output time step.

Table 1 shows the GRIB-element numbers (ee) and table numbers (tab) for the multi-level fields available for LM output files. The level-types (lty) and the corresponding values in octet 11 (lvt) and octet 12 (lv) as well as the physical units (unit) are also included. For variables with level-types 109 and 110, the integer level numbers denoted by k (and k+1) are stored in octets 11 and 12. For pressure levels the constant pressure value in hPa is stored in octet 12 (denoted by pres), and for height levels the constant height level in m above sea level (denoted by z) is stored in octet 12.

Some of the multi-level fields in Table 1 can only be put on the output list if certain parameterization schemes are switched on. These variables are denoted as optional fields. All variables on the list for constant pressure and constant height levels are in the default output list.

Table 1: ***Multi-level fields of LM GRIB-output***

Name	Meteorological Element	ee	tab	lty	lvt	lv	unit
Multi-level fields on model layers/levels k							
U	Zonal wind component (rotated grid)	33	2	110	k	k+1	m/s
V	Meridional wind component (rotated grid)	34	2	110	k	k+1	m/s
W	Vertical wind component	40	2	109	-	k	m/s
P	Pressure	1	2	110	k	k+1	Pa
PP	Pressure perturbation	139	201	110	k	k+1	Pa
T	Temperature	11	2	110	k	k+1	K
QV	Specific humidity	51	2	110	k	k+1	kg/kg
QC	Specific cloud water content	31	201	110	k	k+1	kg/kg
CLC	Fractional cloud cover	29	201	110	k	k+1	%
HHL	Height of half levels (i.e. layer interfaces) constant with time, written only at t=0	8	2	109	-	k	m
Optional multi-level fields on model layers/levels k							
QI	Specific cloud ice content	33	201	110	k	k+1	kg/kg
TKE	Specific turbulent kinetic energy	152	201	109	-	k	m^2/s^2
TKVM	Turbulent diffusion coefficient for vertical momentum transport	153	201	109	-	k	m^2/s
TKVH	Turbulent diffusion coefficient for vertical heat transport	154	201	109	-	k	m^2/s
Multi-level fields interpolated on pressure levels pres (in hPa)							
U	Zonal wind component (rotated grid)	33	2	100	-	pres	m/s
V	Meridional wind component (rotated grid)	34	2	100	-	pres	m/s
OMEGA	Vertical motion	39	2	100	-	pres	Pa/s
T	Temperature	11	2	100	-	pres	K
RELHUM	Relative humidity	52	2	100	-	pres	%
GPH	Geopotential	6	2	100	-	pres	m^2/s^2
Multi-level fields interpolated on height levels z (in m)							
U	Zonal wind component (rotated grid)	33	2	103	-	z	m/s
V	Meridional wind component (rotated grid)	34	2	103	-	z	m/s
W	Vertical wind component	40	2	103	-	z	m/s
T	Temperature	11	2	103	-	z	K
P	Pressure	1	2	103	-	z	Pa
RELHUM	Relative humidity	52	2	103	-	z	%

Table 2 shows the GRIB-element numbers (ee) and table numbers (tab) for the single-level forecast fields available for LM output files. As in the previous table, the level-types (lty) and the corresponding values in octet 11 (lvt) and octet 12 (lv) as well as the physical units (unit) of the fields are also included. See Table 5 in Appendix A for the units of the numbers stored in lvt and lv for the corresponding level-type.

Table 2: ***Single-level fields of LM GRIB-output***

Name	Meteorological Element	ee	tab	lty	lvt	lv	unit
Single-level fields: valid at output time							
PS	Surface pressure	1	2	1	-	-	Pa
PMSL	Mean sea level pressure	2	2	102	-	-	Pa
U_10M	Zonal 10m-wind	33	2	105	-	10	m/s
V_10M	Meridional 10m-wind	34	2	105	-	10	m/s
T_2M	2m-temperature	11	2	105	-	2	K
TD_2M	2m-dewpoint temperature	17	2	105	-	2	K
T_G	Temperature at the interface surface-atmosphere	11	2	1	-	-	K
T_SNOW	Temperature of snow surface (surface temperature if no snow)	203	201	1	-	-	K
T_S	Temperature below snow (surface temperature if no snow	85	2	111	-	0	K
T_M	Temperature at the bottom of first soil layer	85	2	111	-	9	K
QV_S	Specific humidity at the surface	51	2	1	-	-	kg/kg
W_SNOW	Water content of snow	65	2	1	-	-	kg/m^2
W_I	Water content of interception store	200	201	1	-	-	kg/m^2
W_G1	Water content of upper soil layer	86	2	112	0	10	kg/m^2
W_G2	Water content of middle soil layer	86	2	112	10	100	kg/m^2
TCM	Turbulent transfer coefficient for momentum at the surface	170	201	1	-	-	-
TCH	Turbulent transfer coefficient for heat and moisture at the surface	171	201	1	-	-	-
Z0	Roughness length (land and water)	83	2	1	-	-	m
ALB	Surface albedo for shortwave radiation	84	2	1	-	-	%
CLCT	Total cloud cover	71	2	1	-	-	%
CLCH	High cloud cover (0 - 400 hPa)	75	2	1	-	-	%
CLCM	Middle cloud cover (400-800 hPa)	74	2	1	-	-	%
CLCL	Low cloud cover (800hPa-surface)	73	2	1	-	-	%
CLCT_MOD	Total cloud cover (modified for graphics)	204	203	1	-	-	-
CLDEPTH	Normalized cloud depth (modified for graphics)	203	203	1	-	-	-
HTOP_DC	Top height of dry convection (height above mean sea level)	82	201	1	-	-	m
HZEROCL	Height of $0°C$ isotherm (above mean sea level)	84	201	1	-	-	m
MFLX_CON	Massflux at convective cloud base	240	201	1	-	-	kg/m^2s
CAPE_CON	Convective available potential energy	241	201	1	-	-	J/kg
QCVG_CON	Moisture convergence below convective cloud base	242	201	1	-	-	1/s
TKE_CON	Convective turbulent kinetic energy	243	201	1	-	-	J/kg
IWATER	Vertically integrated total water	41	201	1	-	-	kg/m^2
IWV	Vertically integrated water vapour	54	2	1	-	-	kg/m^2

Name	Meteorological Element	ee	tab	lty	lvt	lv	unit
Single-level fields: Accumulated since start of the forecast							
RAIN_GSP	Amount of grid-scale rain	102	201	1	-	-	kg/m^2
SNOW_GSP	Amount of grid-scale snow	79	2	1	-	-	kg/m^2
RAIN_CON	Amount of convective rain	113	201	1	-	-	kg/m^2
SNOW_CON	Amount of convective snow	78	2	1	-	-	kg/m^2
TOT_PREC	Total precipitation amount	61	2	1	-	-	kg/m^2
RUNOFF_S	Surface water run-off	90	2	112	0	10	kg/m^2
RUNOFF_G	Ground water run-off	90	2	112	10	100	kg/m^2
IDIV_HUM	Vertically integrated divergence of specific humidity	42	201	1	-	-	kg/m^2
AEVAP_S	Accumulated flux of surface moisture	57	2	1	-	-	kg/m^2
Single-level fields: Averaged over the forecast period							
AUMFL_S	Surface u-momentum flux	124	2	1	-	-	N/m^2
AVMFL_S	Surface v-momentum flux	125	2	1	-	-	N/m^2
ASHFL_S	Surface sensible heat flux	122	2	1	-	-	W/m^2
ALHFL_S	Surface latent heat flux	121	2	1	-	-	W/m^2
ASOB_S	Solar radiation budget at the earth surface	111	2	1	-	-	W/m^2
ASOB_T	Solar radiation budget at the top of the atmosphere	113	2	8	-	-	W/m^2
ATHB_S	Thermal radiation budget at the earth surface	112	2	1	-	-	W/m^2
ATHB_T	Thermal radiation budget at the top of the atmosphere	114	2	8	-	-	W/m^2
APAB_S	Budget of photosynthetic active radiation at the earth surface	5	201	1	-	-	W/m^2
Single-level fields: Extreme values over certain time intervals							
TMIN_2M	Minimum of 2m-temperature	16	2	105	-	2	K
TMAX_2M	Maximum of 2m-temperature	15	2	105	-	2	K
VMAX_10M	Maximum of 10m-wind speed	187	201	105	-	10	m/s
HTOP_CON	Top height of convective clouds (above mean sea level)	69	201	3	-	-	m
HBAS_CON	Base height of convective clouds (above mean sea level)	68	201	2	-	-	m
TOP_CON	Main-level index of convective cloud top	73	201	1	-	-	-
BAS_CON	Half-level index of convective cloud base	72	201	1	-	-	-
Single-level fields: Constant and climatological fields							
FIS	Geopotential of earth surface	6	2	1	-	-	m^2/s^2
HSURF	Geometrical height of surface	8	2	1	-	-	m
FR_LAND	Land fraction of a grid area	81	2	1	-	-	-
SOILTYP	Soil texture for land fraction (key number 1-8, over water =9)	57	202	1	-	-	-
PHI	Geographical latitude	114	202	1	-	-	° N
RLA	Geographical longitude	115	202	1	-	-	° E
PLCOV	Fractional plant cover	87	2	1	-	-	-
LAI	Leaf area index of vegetation	61	2	1	-	-	-

Name	Meteorological Element	ee	tab	lty	lvt	lv	unit
ROOTDP	Root depth of vegetation	62	202	1	-	-	m
FC	Coriolis parameter	113	202	1	-	-	s^{-1}
T_CL	Temperature of the lowest soil layer (climatological value)	85	2	111	-	36	K
W_CL	Water content of the lowest soil layer (climatological value)	86	2	112	100	190	kg/m^2
VIO3	Vertically integrated ozone	65	202	1	-	-	Pa O3
HMO3	Height of ozone maximum	64	202	1	-	-	Pa

All variables required on the input and boundary data files use also the corresponding GRIB table and element numbers from the above tables. The preprocessor programs to interpolate initial and/or boundary conditions to the LM-grid require the GRIB-files containing the external parameter data sets. The table and element numbers of the external parameter fields are shown in table 3.

Table 3: ***Single-level fields in the LM external parameter files***

Name	Meteorological Element	ee	tab	lty	lvt	lv	unit
FIS	Geopotential of earth surface	6	2	1	-	-	m^2/s^2
HSURF	Geometrical height of surface	8	2	1	-	-	m
FR_LAND	Land fraction of a grid area	81	2	1	-	-	-
Z0	Roughness length (land and water)	83	2	1	-	-	m
SOILTYP	Soil texture for land fraction (key number 1-8, over water =9)	57	202	1	-	-	-
PHI	Geographical latitude	114	202	1	-	-	° N
RLA	Geographical longitude	115	202	1	-	-	° E
PLCOV_V	Plant cover, vegetation period	67	202	1	-	-	%
PLCOV_V	Plant cover, rest period	68	202	1	-	-	%
LAI_V	Leaf area index, vegetation period	69	202	1	-	-	-
LAI_R	Leaf area index, rest period	70	202	1	-	-	-
ROOTDP	Root depth of vegetation	62	202	1	-	-	m